

**EVALUATION OF THE HALOGEN BOND AND THE SALT BRIDGE
INTERACTIONS USING THE MOLECULAR TORSION BALANCE**

by

Sandra K. Keyser

B.S., The College of New Jersey, 2005

Submitted to the Graduate Faculty of
Arts and Sciences in partial fulfillment
of the requirements for the degree of
Doctor of Philosophy

University of Pittsburgh

2010

UNIVERSITY OF PITTSBURGH
SCHOOL OF ARTS AND SCIENCES

This dissertation was presented

by

Sandra K. Keyser

It was defended on

August 13, 2010

and approved by

Dr. Scott G. Nelson, Professor, Chemistry

Dr. Joseph J. Grabowski, Professor, Chemistry

Dr. Linda Jen-Jacobson, Professor, Biology

Dissertation Advisor: Dr. Craig S. Wilcox, Professor, Chemistry

Copyright © by Sandra K. Keyser

2010

EVALUATION OF THE HALOGEN BOND AND THE SALT BRIDGE INTERACTIONS USING THE MOLECULAR TORSION BALANCE

Sandra K. Keyser, Ph. D.

University of Pittsburgh, 2010

A molecular torsion balance was synthesized to study the halogen bond in nonpolar and polar solvents. The folding energies were found to be between -0.2 and -0.3 kcal/mol in deuteriochloroform. The strength of the halogen bond decreased in the following order: Cl ~ Br > I, which is contrary to the computationally predicted order, I > Br > Cl. This reversed trend may be due to the gauche effect and/or simultaneous steric effects specific to our model system.

Three different functionalities, an alcohol, a carbamate, and an amide, were used as the halogen bond acceptors. The amide gave among the highest folding ratios, indicative of the strength of the halogen bond with bromide or chloride. Solvent studies were performed on the brominated torsion balance as well as a hydroxy analog to compare the hydrogen and halogen bonding interactions. Based on the solvent data, it takes more water to obstruct a halogen bond compared to a hydrogen bond. The folding energies were also compared to several solvent parameters.

A molecular torsion balance was also successfully synthesized to study the solvent exposed salt bridge interaction in water and in several buffer solutions. We found that the folding energies varied between -0.3 to -0.5 kcal/mol for the ammonium-carboxylate and guanidinium-carboxylate interaction when exposed to solvent; unequivocally, salt bridges that are exposed to solvent are stabilizing. Temperature is negligible whereas ionic strength has a weak but experimentally significant effect on the strength of the salt bridge interaction. The only measurable change in the folding ratios came from adjusting the pD of the buffer solutions.

TABLE OF CONTENTS

1.0	TRÖGER'S BASE AND THE MOLECULAR TORSION BALANCE.....	1
1.1	MEASURING THE EDGE-TO-FACE INTERACTION USING THE FIRST GENERATION MOLECULAR TORSION BALANCE.....	2
1.2	MEASURING THE ATTRACTION BETWEEN ORGANIC FLUORINE AND AN AMIDE GROUP	5
1.3	MEASURING HYDROPHOBIC AND CH-II EFFECTS IN WATER WITH THE SECOND GENERATION TORSION BALANCE.....	6
2.0	THE HALOGEN BOND	8
3.0	EVALUATION OF THE HALOGEN BOND.....	12
3.1	SYNTHESIS OF THE HALOGEN BONDING TORSION BALANCES... 	13
3.2	¹H NMR ANALYSIS AND FOLDING ENERGIES OF THE TORSION BALANCES IN DEUTERATED CHLOROFORM.....	17
3.3	THE OBSERVED TREND FOR THE STRENGTH OF THE HALOGEN BOND	25
3.4	FOLDING ENERGIES IN NONPOLAR AND POLAR SOLVENTS.....	27
3.5	CONCLUSIONS	32
4.0	THE STRENGTH OF SALT BRIDGES AND THEIR CONTRIBUTION TO PROTEIN STABILIZATION	35

4.1	EVALUATION OF METHODS TO MEASURE THE SALT BRIDGE.....	41
5.0	EVALUATION OF THE SALT BRIDGE USING THE MOLECULAR TORSION BALANCE.....	44
5.1	SYNTHESIS OF SALT BRIDGE TORSION BALANCES.....	45
5.2	¹ H NMR SPECTRA OF SALT BRIDGING TORSION BALANCES.....	50
5.3	THE STRENGTH OF THE SALT BRIDGE INTERACTION.....	55
5.4	THE EFFECTS OF IONIC STRENGTH ON SALT BRIDGE INTERACTIONS.....	61
5.5	CONCLUSIONS.....	64
6.0	EXPERIMENTAL.....	67
6.1	SYNTHESIS.....	68
6.2	PREPARATION OF BUFFER SOLUTIONS.....	110
6.3	ERROR ANALYSIS.....	112
7.0	BIBLIOGRAPHY.....	116

LIST OF TABLES

Table 1. Experimental folding energies for esters 1a-i and 2a-c in CDCl ₃ at 25 °C.....	3
Table 2. Folding energies for methyl (3), isopropyl (4), and phenyl esters (5) in CDCl ₃ at 25 °C.	4
Table 3. Folding energies for esters 11a-f at 25 °C.....	7
Table 4. Synthesis of torsion balances 26-28	16
Table 5. Folding energies for torsion balances 26-29 in CDCl ₃	22
Table 6. Solvent effects on folding data for torsion balances 28a and 28c	28
Table 7. Folding data at 15 °C compared to solvent parameters.	30
Table 8. Folding ratios and energies at varying pD.....	57
Table 9. Folding data for control 51	61
Table 10. Ionic strength effect on folding energies.	63

LIST OF FIGURES

Figure 1. Tröger's base.....	1
Figure 2. The first generation torsion balance (folded on left and unfolded on right).	2
Figure 3. Structures of a benzene dimer.	2
Figure 4. Torsion balances for the tilted-T edge-to-face interaction.	3
Figure 5. Methyl, isopropyl, and phenyl esters.....	4
Figure 6. Torsion balances to measure the C-F \cdots amide interaction.....	5
Figure 7. Torsion balances to measure hydrophobic effects.....	6
Figure 8. Schematic of a halogen bond interaction.....	8
Figure 9. Representative chemical structures for the folded and unfolded conformers.	12
Figure 10. ^1H NMR spectrum of 26a at -5 °C.	18
Figure 11. ^1H NMR spectra of 26a at -5 °C, 5 °C, 15 °C, and 25 °C.	19
Figure 12. Simulations of bromoethyl (middle spectrum) and propyl (top spectrum) esters of 26a at -5 °C (bottom spectrum) using iNMR.	20
Figure 13. Torsion balances used in solvent studies.....	28
Figure 14. Experimental folding data of 28a at 15 °C (log K_{eq}) against solvent parameters.	31
Figure 15. Representative chemical structures for the folded and unfolded conformers.	44
Figure 16. ^1H NMR spectrum of 47a at 15 °C in D_2O	51
Figure 17. The ^1H NMR spectrum for 47c at 5 °C in D_2O	52

Figure 18. ^1H NMR spectra at 5 (purple), 15 (green), and 25 °C (orange) for 47c in D_2O	53
Figure 19. Simulations of the NMR signals of the carboxyethyl (middle spectrum) and methyl (top spectrum) esters of 47a at 5 °C (bottom spectrum).....	54
Figure 20. Lowest energy conformer for 47b	58
Figure 21. Lowest energy conformer for 48b	59
Figure 22. The lowest energy conformer of solvated 48b (front and side views).....	60
Figure 23. A simulation of the bromoethyl protons (blue) overlaid with the experimental spectrum (red) of 26a at -5 °C.	113
Figure 24. A simulation of the bromoethyl group with a 1.5% reduction in the folding ratio. ..	113
Figure 25. A simulation of the bromoethyl group with a 1.5% increase in the folding ratio.	114
Figure 26. Relative error in folding energies versus folding ratios for a $\pm 1.5\%$ error in folding ratios.....	115

LIST OF SCHEMES

Scheme 1. Modification of isophthalates.....	14
Scheme 2. Synthesis of <i>tert</i> -butyl carbamate.....	14
Scheme 3. Synthesis of the primary alcohol.....	15
Scheme 4. Synthesis of the dimethylamide.	15
Scheme 5. Iodination of dimethylamide.	16
Scheme 6. Methylation of carbamate.....	17
Scheme 7. Retrosynthetic analysis.....	45
Scheme 8. Mitsunobu reaction.....	46
Scheme 9. Synthesis of isophthalate 37	47
Scheme 10. Synthesis of isophthalate 40	47
Scheme 11. Synthesis of isophthalate 42	47
Scheme 12. Synthesis of isophthalate 44	48
Scheme 13. Synthesis of amines 47	49
Scheme 14. Synthesis of guanidines 48	49
Scheme 15. Synthesis of the control.	50

1.0 TRÖGER'S BASE AND THE MOLECULAR TORSION BALANCE

Tröger's base [2,8-dimethyl-6H,12H-5,11-methanodibenzo[*b,f*][1,5]diazocine] (Figure 1) was first described in 1887,¹ though the structure was not elucidated until 1935.² The dibenzodiazocine derivative is a concave, V-shaped molecule with angle of 89-104° between the two aryl rings^{3,4} and owes its chirality to the two configurationally stable amines. Its relative rigidity, unique cleft-shape, and potential to direct functionalities towards the cleft through substitution at C-2 and C-8 make Tröger's base analogs ideal frameworks for biomimetic systems. The dibenzodiazocine scaffold has been used in cyclophanes as receptors^{3,4} for benzenoid substrates and in diacids as hydrogen bonding hosts.⁵⁻⁸

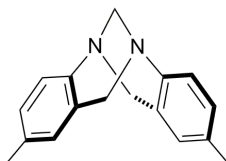


Figure 1. Tröger's base.

The molecular torsion balance was first introduced in 1994⁹ as a tool to measure non-covalent interactions (Figure 2). Rotation of the asymmetric aryl ring atop a Tröger's base analog is gently restricted with an estimated barrier to rotation of approximately 14 kcal/mol, low enough to surmount at room temperature but high enough to monitor the populations of the two conformations by ¹H NMR. The dibenzodiazocine hinge is flexible enough to optimize distance requirements for non-covalent interactions. The top ring has two possible orientations;

any deviation from a 1:1 ratio between the two states is indicative of an intramolecular force. The torsion balance has been used to evaluate the benzene dimer edge-to-face, aryl- and alkyl-CH- π interactions, and the hydrophobic effect.

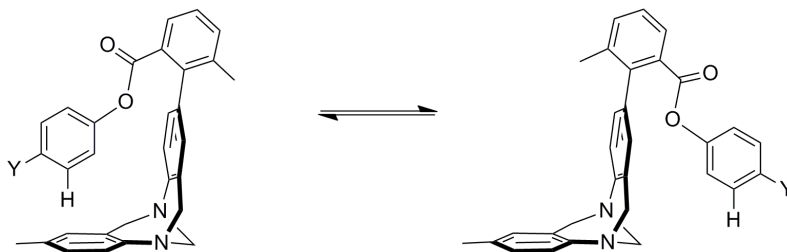


Figure 2. The first generation torsion balance (folded on left and unfolded on right).

1.1 MEASURING THE EDGE-TO-FACE INTERACTION USING THE FIRST GENERATION MOLECULAR TORSION BALANCE

Aromatic rings have been found to adopt an edge-to-face (EF, Figure 3) configuration in the solid state for benzene¹⁰ and in protein crystal structures.¹¹⁻¹³ The arrangement brings the partially positive protons of the edge ring in close proximity to the partially negative center of the face ring. The approach is perpendicular with centroid separations of 3.4-6.5 Å. Monte Carlo simulations¹⁴ and ab initio calculations¹⁵ determined separately that the tilted-T edge-to-face interaction (TT, Figure 3) with a centroid distance of 5.0-5.5 Å was favored for benzene.

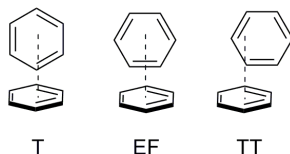


Figure 3. Structures of a benzene dimer.

The first set of torsion balances synthesized were used to measure the stability of the tilted-T edge-to-face interaction and the effects of substitution (Figure 4, Table 1).⁹ The electron withdrawing substituents of **1d** and **1e** perturb the folding ratio by increasing electron deficiency of the edge ring, though the iodoester **1f** shows the same stabilization of folding. Surprisingly, the *tert*-butyl **2c** shows greater folding than its aryl counterparts, indicating that the *tert*-butyl-aryl interaction is as significant as the edge-to-face interaction.

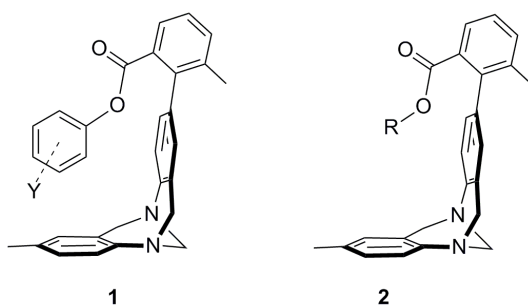


Figure 4. Torsion balances for the tilted-T edge-to-face interaction.

Table 1. Experimental folding energies for esters 1a-i and 2a-c in CDCl₃ at 25 °C.

<i>Ester</i>	<i>Y</i>	<i>R</i>	$-\Delta G^{ca,b}$
1a	H	–	0.24
1b	<i>p</i> -CH ₃	–	0.37
1c	<i>p</i> -OCH ₃	–	0.24
1d	<i>p</i> -CN	–	0.65
1e	<i>p</i> -NO ₂	–	0.65
1f	<i>p</i> -I	–	0.65
1g	<i>m</i> -CH ₃	–	0.00
1h	<i>m</i> -CN	–	0.24
1i	3,5-dimethyl	–	-0.37
2a	–	CH ₃	0.00
2b	–	cyclohexyl	0.37
2c	–	<i>tert</i> -butyl	0.82

a) \pm 10% error. b) kcal/mol.

A series of phenyl, methyl, and isopropyl esters were then analyzed by ¹H NMR to determine the relationship between the electrostatic potential of the aromatic face ring and the strength of edge-to-face and CH- π interactions (Table 2, Figure 5).¹⁶ The isopropyl ester is

preferentially folded, and the free energy of folding is about -0.5 kcal/mol at room temperature, whereas the phenyl ester, despite its relative electron deficiency in the edge ring, exhibited a less favorable free energy of folding of -0.3 kcal/mol.¹⁶ The substituents have little to no effect on folding, which belies the significance of electrostatic potential and is consistent with London dispersion forces as the major driving force in edge-to-face interactions.

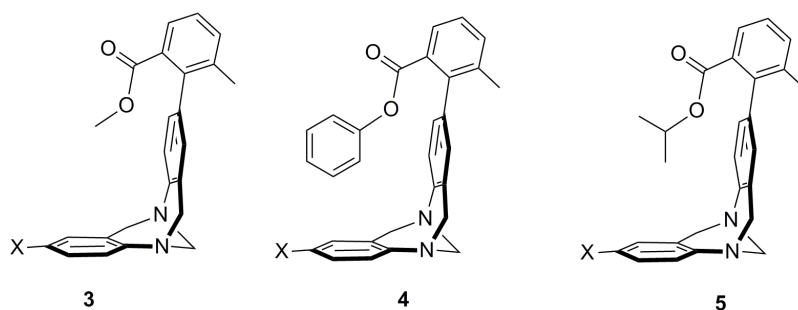


Figure 5. Methyl, isopropyl, and phenyl esters.

Table 2. Folding energies for methyl (3), isopropyl (4), and phenyl esters (5) in CDCl₃ at 25 °C.

X	$-\Delta G^{\text{oa,b}}$ (3)	$-\Delta G^{\text{oa,b}}$ (4)	$-\Delta G^{\text{oa,b}}$ (5)
NO ₂	-0.11	0.21	0.51
CN	-0.06	0.30	0.64
I	0.06	0.23	0.46
Br	-0.02	0.26	0.54
OCH ₃	0.04	0.27	0.44
OH	0.03	0.23	0.47
NH ₂	0.06	0.18	0.34

a) $\pm 10\%$ error. b) kcal/mol.

1.2 MEASURING THE ATTRACTION BETWEEN ORGANIC FLUORINE AND AN AMIDE GROUP

In medicinal chemistry, fluorine, which has been exchanged for hydrogen due to steric similarity, enhances metabolic stability, pharmacokinetic and toxicological properties, and binding efficacy and selectivity.^{17,18} Yet fluorine differs considerably from hydrogen in terms of electronegativity, and reasons for improved efficacy have not been fully addressed. Diederich *et al.* noticed a characteristic geometry of an organic fluorine orthogonal to a carbonyl in a fluorinated inhibitor-thrombin complex and in other examples from the Cambridge Structural Database (CSD) and RCSB Protein Data Bank.¹⁹

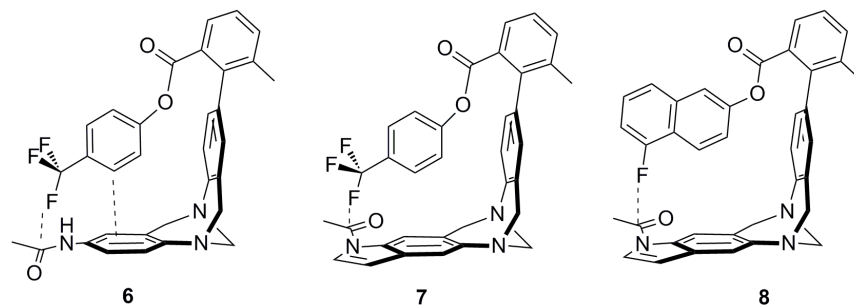


Figure 6. Torsion balances to measure the C-F...amide interaction.

The Diederich group has applied the torsion balance²⁰ to measure the C-F...amide interaction in combination with the double mutant cycle approach,²¹ using trifluorophenyl **6** (Figure 6). The C-F...amide coupling energy was -0.25 kcal/mol in CDCl₃, -0.20 kcal/mol in C₆D₆, and negligible in CD₃OD.²⁰ However, several uncertainties regarding these data called for a subsequent study in which an indole was appended to the Tröger's base scaffold (**7**, Figure 6). The interaction was strongest in nonpolar solvents: -0.19 kcal/mol in C₆D₆ versus -0.07 kcal/mol in CDCl₃ and -0.10 in CD₃OD. To reduce perturbations upon acetylation of indole, naphthyl **8**

was designed, obtaining values of -0.29 kcal/mol in C₆D₆ and -0.14 kcal/mol in CDCl₃.²² These data support the attractive orthogonal dipolar C_{sp3}F^{δ-}amide and C_{sp2}F^{δ+}amide interactions.

1.3 MEASURING HYDROPHOBIC AND CH-II EFFECTS IN WATER WITH THE SECOND GENERATION TORSION BALANCE

In the first generation torsion balances, an aryl or alkyl ester was opposite a methyl group; these two groups differ in dipole moment and with solvation, which can affect the conformer ratio. To improve the symmetry of the molecule and address the above issue, an ester was set against another ester. A major purpose of the second generation torsion balances was to measure noncovalent interactions *in water*, and therefore, hydrophilic groups were added to improve solubility. Because these groups are located on the axis of rotation and will not experience changes in environment due to rotation, they cannot contribute to the energy change observed during folding (Figure 7, **11**).²³

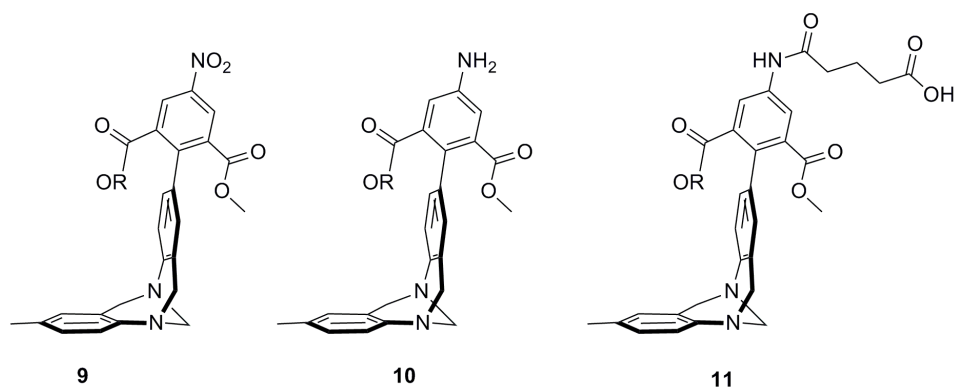


Figure 7. Torsion balances to measure hydrophobic effects.

The hydrophobic contribution to folding in water was defined as the difference between the folding energies of the torsion balance in water and in nonpolar solvents, the value of which

grew with increasing alkyl group size. The hydrophobic contribution for an isopropyl ester was -0.22 kcal/mol and for an adamantyl ester -0.35 kcal/mol (Table 3),²³ demonstrating the influence of water on the conformation of small molecules.

Table 3. Folding energies for esters 11a-f at 25 °C.

Ester	R	$-\Delta G_{\text{fold}} [\text{CDCl}_3]^{\text{a,b}}$	$-\Delta G_{\text{fold}} [\text{D}_2\text{O}]^{\text{a,b}}$
11a	(CH ₃) ₂ HC-	0.50	0.72
11b	(CH ₃) ₃ C-	0.65	0.92
11c	cyclohexyl	0.36	0.67
11d	1-adamantyl	0.36	0.68
11e	2-adamantyl	0.55	0.90
11f	H ₃ C-	0.00	0.00

a) $\pm 10\%$ error. b) kcal/mol.

2.0 THE HALOGEN BOND

The halogen bond is a noncovalent interaction between a halogen such as iodine, bromine or chlorine but not fluorine, and a Lewis base, which can include but is not limited to oxygen, nitrogen and sulfur. The interaction has a strong directional preference with an angle, θ , (Figure 8) typically between 160° and 180° . In a CSD survey of 40,000 structures containing C-X bonds²⁴ and an analysis of PBD crystal structures,²⁵ nucleophiles of oxygen or nitrogen approached preferentially at an θ of approximately 160 - 165° , regardless of the substitution pattern of the carbon (primary, secondary, tertiary or sp^2 hybridized), whereas gas phase studies²⁶ and other CSD surveys^{27,28} suggest linearity in θ . The angle corresponds to angular orientation of the σ^* antibonding orbital of the C—X bond. Charge transfer between the HOMO of the Lewis base and the LUMO of the halogen dictate this angle.^{27,28}

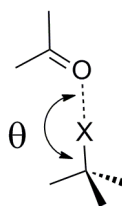


Figure 8. Schematic of a halogen bond interaction.

The stabilizing potential energy of the halogen bond has been estimated from 1 kcal/mol to slightly greater than that of the average hydrogen bond.²⁹ On the lower end of the spectrum, the strength of $N\cdots Cl$ interactions of gas phase cyanuric chlorides are estimated to be -1.2 kcal/mol by ab initio calculations,³⁰ and the energy gain for a chloro-cyanoacetylene dimer is

-2.4 kcal/mol (half that of a hydrogen bond) based on IMPT calculations.²⁸ The interaction energy is -5.8 kcal/mol for $\text{CF}_3\text{I}\cdots\text{NH}_3$ according to MP2 quantum chemical calculations³¹ and -7.4 kcal/mol for 2,2,6,6-tetramethylpiperidine and 1-iodoperfluorohexane as measured by an adiabatic accelerating calorimeter.³² The halogen bond interaction can be as strong as -18.9 kcal/mol, which is calculated for the interaction between ammonia and BrF using density functional theory and atoms in molecular theory.³³

The halogen bond is attributed to electrostatics, dispersion, and charge transfer^{24,28} as well as the anisotropy of halogen electron density.^{34,35} This polar flattening²⁸ refers to the emergence of an electropositive crown²⁵ or sigma hole³⁶ along the C-X axis that increases with the polarizability of the halogen. This implies that halogen bonding would be strongest with iodine but would not occur with fluorine. According to CSD surveys²⁸ and computational studies,^{25,37} the tendency to form halogen bonds among the halogens is as follows: $\text{I} > \text{Br} > \text{Cl} \gg \text{F}$. Surveys have also suggested propensity for halogen bonding occurs in terms of electronegativity; sp^1 hybridized nucleophiles show the strongest preference to form the interaction compared to sp^3 , which shows the weakest, and oxygen forms the interactions at a higher percentage than nitrogen and even more so than sulfur.²⁸ Computational studies have suggested Lewis bases in the following order for the strength of interaction: $\text{N} > \text{S} > \text{O}$.^{33,38}

Halogen bonding was proposed more than a century ago in the synthesis of NH_3I_2 ,³⁹ but was not verified until Odd Hassel's crystallographic studies of molecular bromine and p-dioxane in 1954,⁴⁰ which elucidated a $\text{Br}\cdots\text{O}$ distance of 2.71 Å (the sum of the van der Waals radii for singly bonded bromine and oxygen is 3.35 Å) and a C—Br \cdots O angle of 180°. Since then halogen bonding has been reviewed,^{29,41,42} used extensively in crystal engineering,²⁹ and gained recognition in biological systems.

Halogen bonding has only recently captured the attention of the biological community. The enzyme aldose reductase (AR) complexes to halogenated inhibitor, IDD594, and NADP⁺, forming a short Br···O contact of 3.0 Å between the bromine of the inhibitor and a threonine oxygen of the enzyme.⁴³ Bromination decreases the IC₅₀ value of the inhibitor by a factor of 2.3 compared to that of chlorination.⁴⁴ In 2003, two biomolecular single-crystal structures were isolated which exhibited halogen bonding. Ho and coworkers found that of two analogous DNA sequences, d(CCAGTACTGG) and d(CCAGTACbr⁵UGG),⁴⁵ differing mainly by a methyl group versus a bromine, only the brominated version forms a four-way Holliday junction.⁴⁶ The junction draws the bromine into a halogen bond with an oxygen of a backbone phosphate group.²⁵ To directly compare hydrogen and halogen bonding, four-stranded DNA constructs, capable of conformational isomerization at their Holliday junction, were synthesized in a crystallographic assay. Of the structurally similar and isoenergetic isomers, which differed only by hydrogen or halogen bond stabilization, a preference was shown for the latter; the halogen bond was estimated to be 2 kcal/mol more stable than the hydrogen bond.⁴⁷ However, this value was based on two assumptions: 1) there is no entropic difference between the two isomers and 2) the crystals formed reflect a preestablished equilibrium in solution.

Parallels have been drawn between hydrogen and halogen bonding. Simple complexes in the gas phase between Lewis bases and hydrogen or halogen bonding acceptors demonstrated similar angular geometries and binding strengths,²⁶ indicating that the origins of the interactions derive from comparable sources. Attempts to cooperatively incorporate both interactions were moderately successful in cocrystallization reactions,⁴⁸⁻⁵⁰ but replacement of hydrogen for halogen bonding in biomolecules has had limited success.^{51,52} The two interactions were in

direct competition in few experiments, including the Holliday junction study,⁴⁷ but halogen bonding has shown it can compete⁵³ and even prevail over hydrogen bonding.^{32,54,55}

While there is an abundance of data for hydrogen bonding interactions in solution,⁵⁶ there is little information measuring the strength of the halogen bond in solution. To date, association constants for halogen-bonding interactions have been determined in only a few cases,⁵⁷⁻⁶¹ and most information regarding the strength of the interaction is computational. However, computational studies will fail to accurately represent halogen bonding unless based on experimental evidence. Rational drug design depends upon a comprehensive knowledge of weak intermolecular interactions; the significant impact of halogen bonding brings to attention the need for a more thorough understanding of the effects of halogenation and halogen bonding in solution. Our objective in this project is to provide quantitative experimental data concerning the halogen bond by using the molecular torsion balance.

3.0 EVALUATION OF THE HALOGEN BOND

Our first objective was to address the deficiency in quantitative measurements of the halogen bond in solution and to examine the effects of solvent polarity on the halogen bond. The second generation torsion balance was modified to have two isosteric esters, one functionalized with a bromine and the other with an alkyl group (Figure 9). The torsion balance adopts two conformational states, folded and unfolded, separated by a barrier of 14 kcal/mol and easily discernable by ^1H NMR.

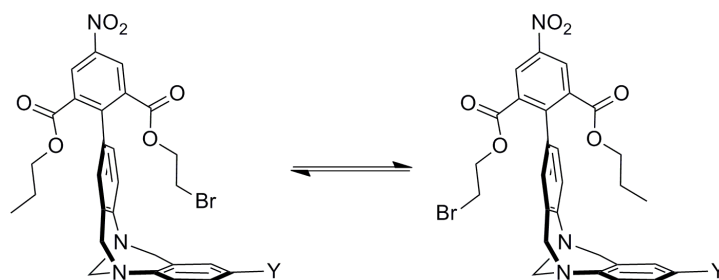


Figure 9. Representative chemical structures for the folded and unfolded conformers.

The top ring of the torsion balance has always featured a methyl group, either attached directly to the aryl ring in place of or as an ester. The reason for this choice was twofold: 1) interactions with the lower half of the dibenzodiazocine cleft would be minimized, and 2) the methyl group with its unfolded and folded signals is relatively easy to examine by line shape analysis. However, a balance of a haloalkyl ester versus a propyl ester would be more appropriate. If the project had assumed its original course, the torsion balances would have been analyzed in water. A methyl ester, as the smaller group, would preferentially fold out due to

hydrophobic effects. It would be difficult to discern halogen bonding stabilization from hydrophobic effects in the resulting folding energies. The rotation of the pseudo-symmetric diester ring exchanges a methyl group for a bromine; any deviation from a 1:1 ratio between the two states is indicative of a halogen bond.

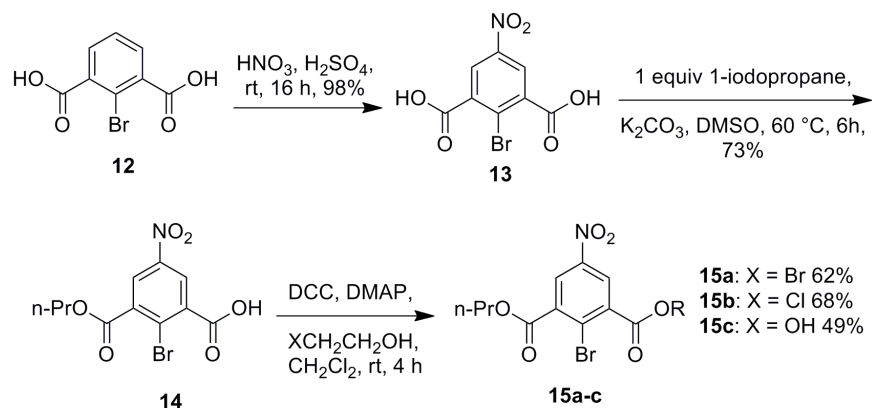
3.1 SYNTHESIS OF THE HALOGEN BONDING TORSION BALANCES

Three different sets of torsion balances were synthesized to measure the strength of the halogen bonding interaction, each featuring an asymmetric diester. To provide this common fragment, diacid, **12**, prepared from commercially available 2-bromo-*m*-xylene,⁶² was treated with nitric and sulfuric acid and subsequently alkylated⁶³ to provide hemiester, **14** (Scheme 1). Esterification with dicyclohexylcarbodiimide (DCC) and 4-dimethylaminopyridine (DMAP) afforded the desired diesters, **15a-c**.⁶⁴ In torsion balances prepared from **15a-b**, a Lewis basic moiety is positioned to interact with an alkyl halide side chain that incorporates a bromine or chlorine. It would be illuminating to compare the halogen bond interaction with a hydrogen bonding interaction. With this in mind, hydroxyethylester **15c** was synthesized.

We planned to use Suzuki coupling to synthesize the desired torsion balances, but the presence of an alkyl bromide and chloride could lead to competitive side reactions. The oxidative addition of palladium(0) to alkyl halides is generally slower than that of aryl halides.⁶⁵ However, the rates between the alkyl and aryl halides can be competitive in certain situations; alkyl iodides have been shown to couple under mild conditions⁶⁶ and specific electron rich phosphine ligands (P(*i*-Pr)₃ and PCy₃) can induce Pd catalyzed coupling of alkyl bromides.⁶⁷ Therefore, we expected that a Suzuki-type coupling reaction using substrates **15a-15c** would

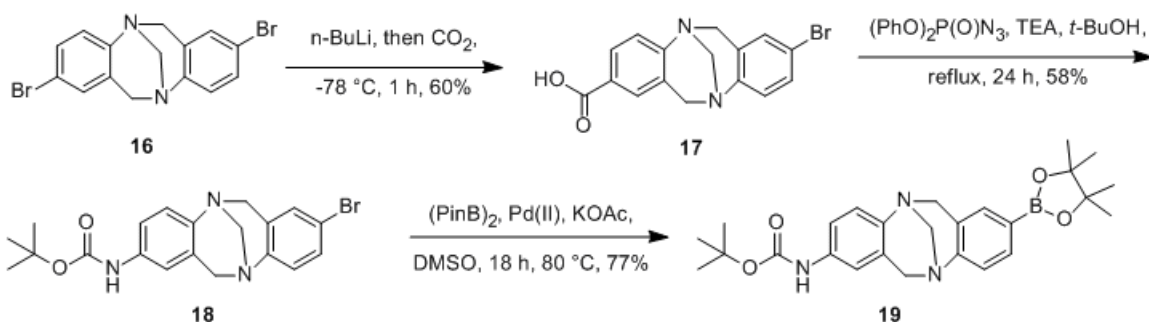
yield *predominantly* the desired torsion balances but expected that the iodo ester would be better synthesized by a substitution reaction after the Suzuki coupling.

Scheme 1. Modification of isophthalates.



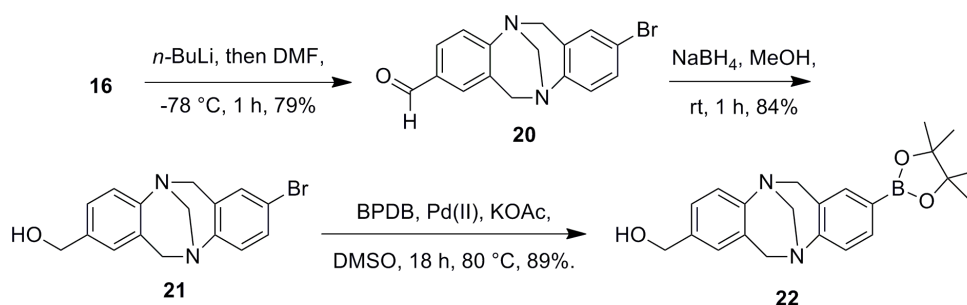
According to the method of Wärnmark, 4-bromoaniline and paraformaldehyde were converted to 2,8-dibromo-6*H*,12*H*-5,11-methanodibenzo[*b,f*][1,5]diazocine **16**,⁶⁸ which was then selectively transformed into different functional groups via the bromine-lithium exchange.⁶⁹ As shown in Scheme 2, bromide **16** was converted to carboxylic acid **17**, which underwent Curtius rearrangement of the isocyanate using diphenyl phosphoryl azide ((PhO)₂P(O)N₃) in *tert*-butanol to give carbamate **18**.⁷⁰ Subsequent treatment with dichlorobis[methylenebis(diphenylphosphine)]-dipalladium-dichloromethane adduct⁷¹ (Pd(II)) as the catalyst and bis(pinacolato)diboron (PinB₂) gave **19**.⁷²

Scheme 2. Synthesis of *tert*-butyl carbamate.

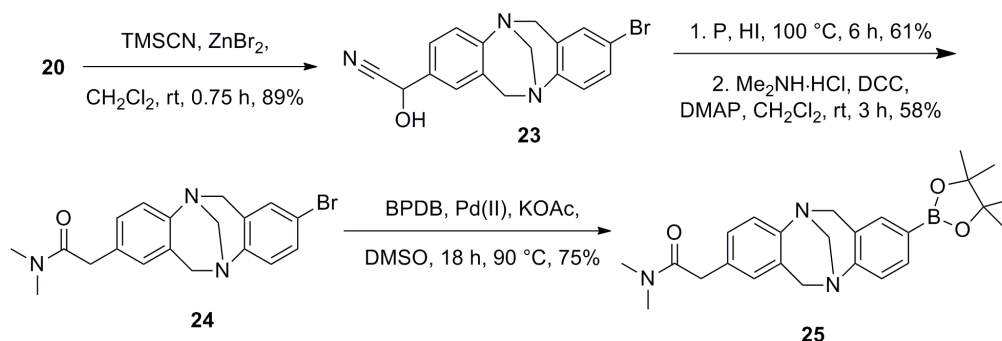


Treatment of **16** with *n*-butyllithium and then DMF, reduction of the resulting aldehyde with sodium borohydride to provide alcohol **21**, and subsequent borylation gave the boronate, **22** (Scheme 3). The last Tröger's base analog, dimethylamide **25**, (Scheme 4) was obtained by starting with the aldehyde **20**, which was treated with trimethylsilyl cyanide and zinc bromide to give **23**.⁷³ Reduction and hydrolysis⁷⁴ provided the carboxylic acid, and subsequent amidation⁷⁵ provided **24**. Borylation of the aryl bromide furnished boronic ester, **25**.

Scheme 3. Synthesis of the primary alcohol.



Scheme 4. Synthesis of the dimethylamide.

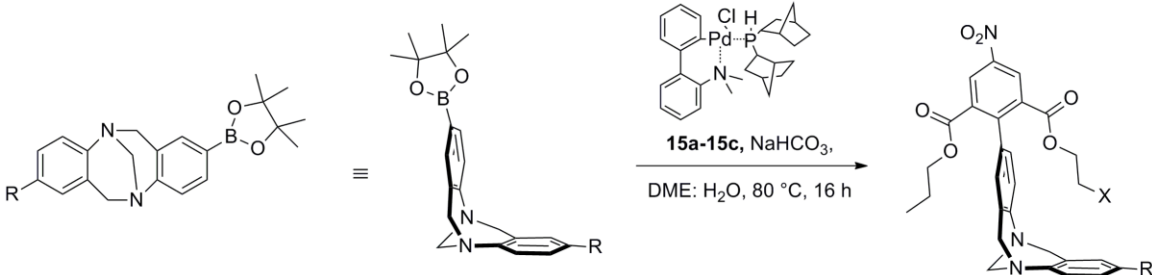


Formation of the torsion balances proved to be difficult under traditional Suzuki conditions. The Suzuki coupling of the isophthalates and **19** with tetrakis(triphenylphosphine) palladium in xylenes at 90 °C for 16 hours returned starting material. The solvent polarity was increased and the palladium catalyst was substituted. Each of the boronic esters were treated with Blaser's catalyst⁷⁶ and heated overnight in a 1:1 solution of dimethoxyethane and water in

the presence of isophthlates **15a-c** and sodium bicarbonate⁷⁷ to give the desired torsion balances.

The yields for each conversion are summarized in Table 4.

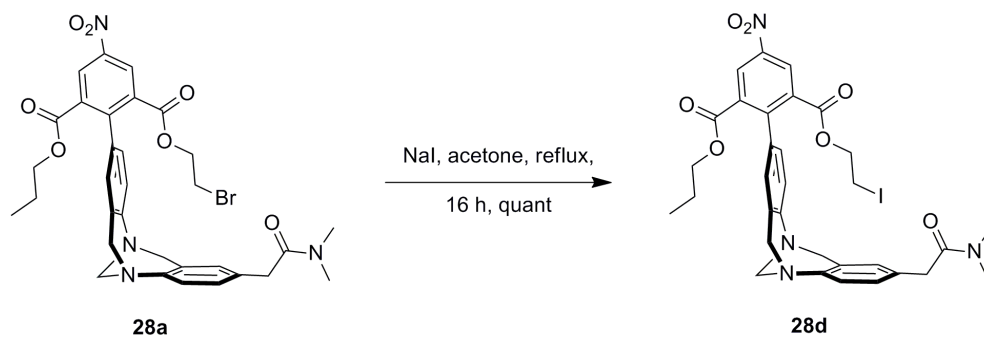
Table 4. Synthesis of torsion balances 26-28.



R	X	Yield (%)
BocNH (26a)	Br	44
BocNH (26b)	Cl	44
BocNH (26c)	OH	40
HOCH ₂ (27a)	Br	28
HOCH ₂ (27b)	Cl	63
HOCH ₂ (27c)	OH	45
Me ₂ NOCCH ₂ (28a)	Br	42
Me ₂ NOCCH ₂ (28b)	Cl	68
Me ₂ NOCCH ₂ (28c)	OH	69

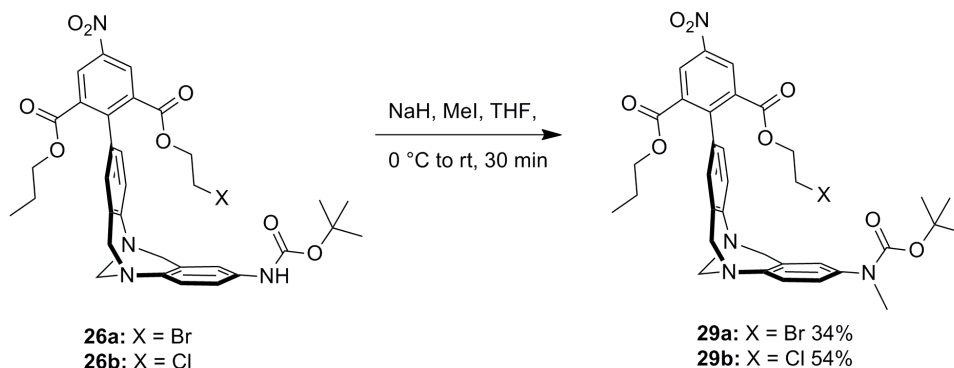
We were interested in obtaining the folding energies of an iodide compared to bromide and chloride analogs. Therefore, an iodoester of the dimethylamide was synthesized from the corresponding bromide. Bromide **28a** was refluxed with sodium iodide in acetone overnight to give the iodide **28d** in quantitative yield (Scheme 5).

Scheme 5. Iodination of dimethylamide.



Molecular modeling suggested that the carbamate functionality of torsion balances **26a-c** preferentially lies in the same plane as the adjacent aromatic ring, which increases the distance between the Lewis base and the halogen and decreases the strength of the halogen bond. To form a halogen bond would require rotation about the C_{aryl}—N bond, which would need to be offset by the stabilization of the interaction. The energetic penalty of this rotation could be reduced by increasing the substitution of the carbamates, thereby destabilizing the planar configuration.^{78,79} Therefore, the torsion balances **26a** and **26b** were methylated to give tertiary carbamates **29a** and **29b** (Scheme 6).

Scheme 6. Methylation of carbamate.



3.2 ¹H NMR ANALYSIS AND FOLDING ENERGIES OF THE TORSION BALANCES IN DEUTERATED CHLOROFORM

The ¹H NMR spectra of the torsion balances exhibited two sets of signals, one for each of the two slowly interconverting conformers available to these biaryl esters. When the haloethyl ester is inside the cleft and in a position where it may potentially contact both dibenzodiazocine aromatic rings and their substituents, it will be referred to as the ‘folded’ conformer. The

conformers where the halogenated alkyl ester is outside the cleft, and is able to contact only one of the dibenzodiazocine rings, will be identified as ‘unfolded.’

Esters **26-29** gave useful ^1H NMR spectra, although they were somewhat complicated due to the diastereotopicity of the geminal methylene protons in the side chains and their partial overlap with the dibenzodiazocine bridging methylene groups. The ^1H NMR spectra for torsion balance **26a** in CDCl_3 at $-5\text{ }^\circ\text{C}$ provides a good example of the data obtained for all the esters.

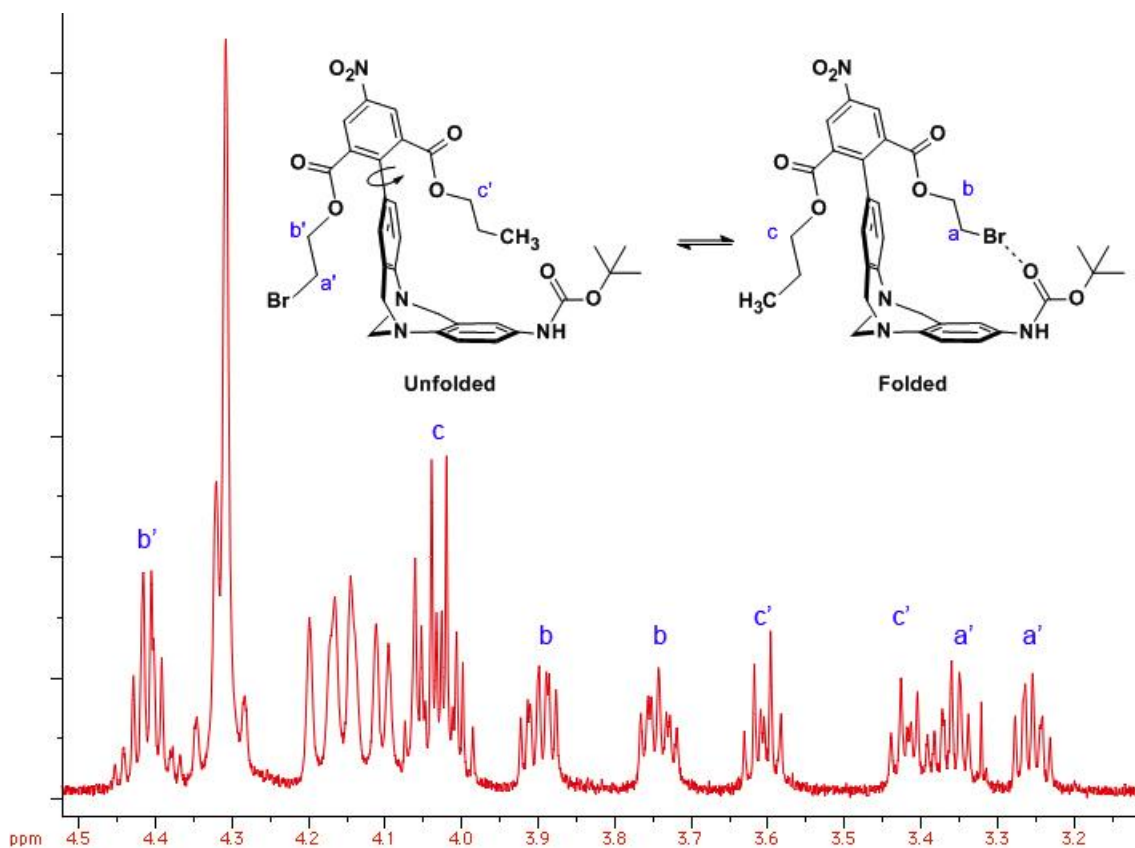


Figure 10. ^1H NMR spectrum of **26a** at $-5\text{ }^\circ\text{C}$.

Folding ratios were found to be concentration independent in the 1-10 mM range in CDCl_3 . Isophthalate **15a** exhibits a triplet at 4.39 ppm for the inner methylene of the propyl ester. After Suzuki coupling, the two methylene protons are diastereotopic and exhibit unique signals in the unfolded and folded states; in the latter, two doublet of triplets partially overlap at 4.03 ppm (c, Figure 10), while the shielded signals in the unfolded state appear at 3.61 and 3.41

ppm (c', Figure 10). Parallel changes also occur for the bromoethyl ester. The inner methylene of isophthalate **15a** appears as a triplet at 4.68 ppm. After coupling, this signal moves to 3.90 and 3.74 ppm in the folded (b) and 4.41 ppm (b') in the unfolded state of the torsion balance. The distal methylene of **15a** appears as a triplet at 3.67 ppm. This moves upfield to 3.36 and 3.26 ppm in the unfolded (a') and 2.34 and 2.26 ppm in the folded state (a, not shown in Figure 10). Upon Suzuki coupling, the alkyl side chains of the isophthalate are in close proximity to the dibenzodiazocine. The chemical shift difference of more than 1 ppm between the isophthalate **15a** and the folded signals (a, not shown in Figure 10) of the bromoethyl's distal methylene are a result of its proximity to both upper and lower rings of the dibenzodiazocine.

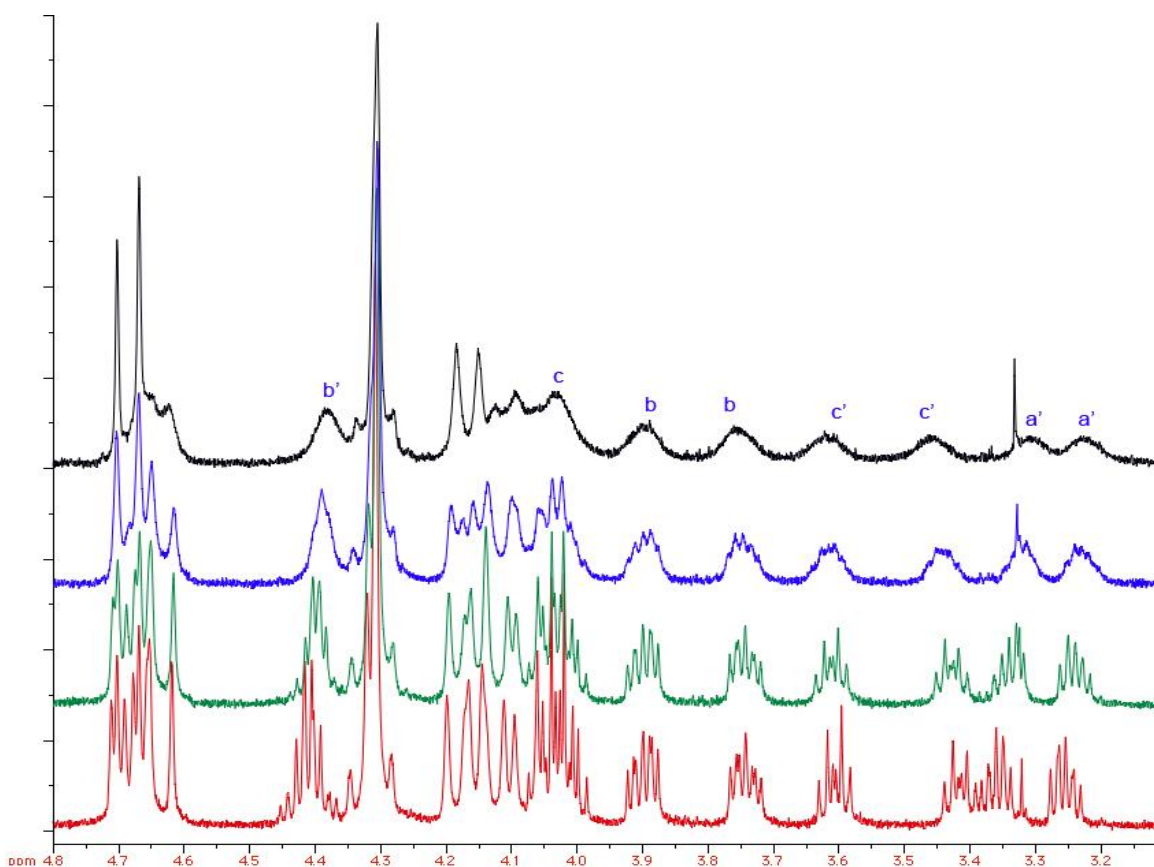


Figure 11. ^1H NMR spectra of **26a** at $-5\text{ }^\circ\text{C}$, $5\text{ }^\circ\text{C}$, $15\text{ }^\circ\text{C}$, and $25\text{ }^\circ\text{C}$.

^1H NMR spectra were acquired at temperatures ranging from $-5\text{ }^\circ\text{C}$ to $25\text{ }^\circ\text{C}$ by ten degree increments. All samples were 1 mM in CDCl_3 , a concentration at which no aggregation was observed. Torsion balance **26a** again represents the other esters in the ^1H NMR spectra at varying temperatures (Figure 11), which change considerably in appearance over the $30\text{ }^\circ\text{C}$ range. The splitting patterns of the geminal methylene protons are difficult to discern at $15\text{ }^\circ\text{C}$, significant broadening of the peaks occur at room temperature, and the signals begin coalescing (e.g. c' clearly moves downfield and a' upfield from -5 to $25\text{ }^\circ\text{C}$).

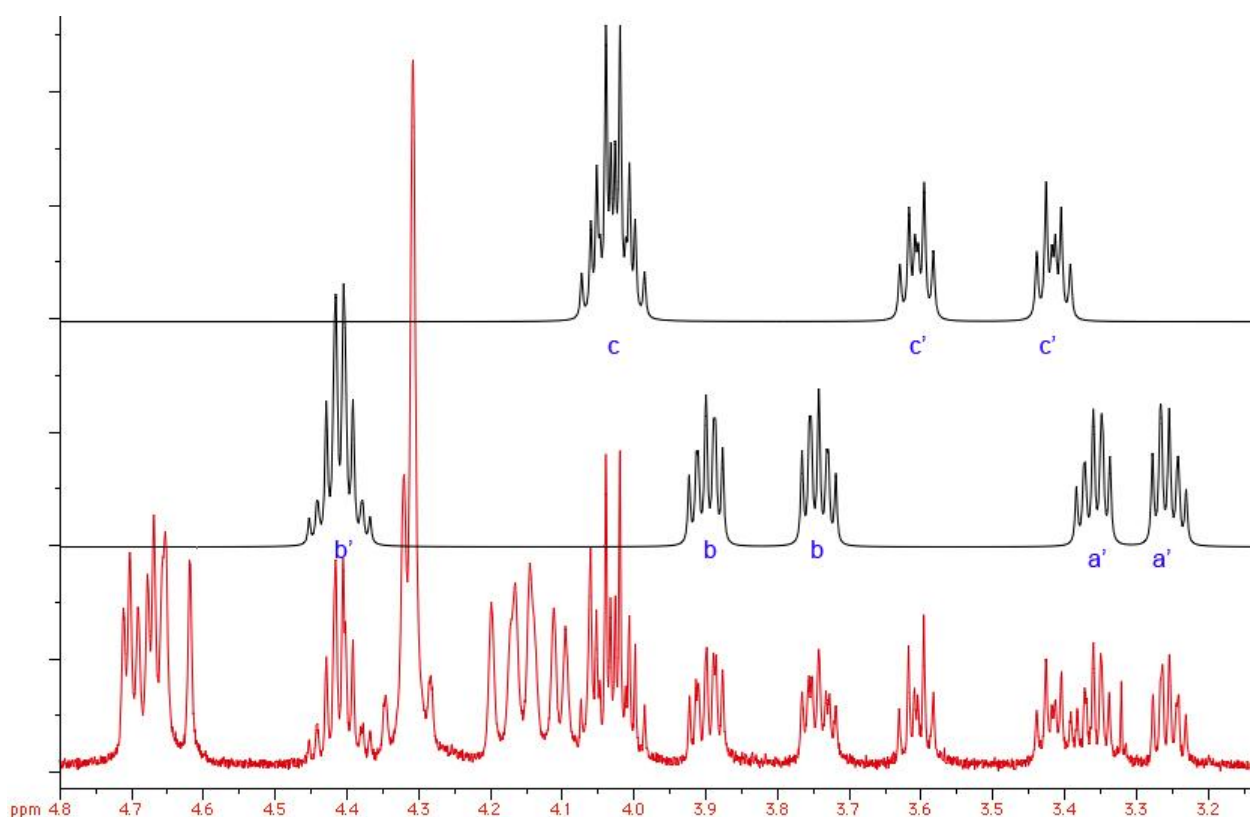


Figure 12. Simulations of bromoethyl (middle spectrum) and propyl (top spectrum) esters of 26a at $-5\text{ }^\circ\text{C}$ (bottom spectrum) using iNMR.

The population of the folded to unfolded conformers were determined for temperatures -5 to $15\text{ }^\circ\text{C}$ using dynamic NMR line shape fitting assisted with the program iNMR.⁸⁰ NMR spectra taken at room temperature or above were too difficult to analyze due to significant signal broadening and poor signal to noise ratio.

Spin system simulations become prohibitively slow when the total number of protons in the system exceed six. Therefore, NMR simulations were conducted on three sets of protons: the inner methylene, and outer methyl of the propyl group, and the bromoethyl group. In Figure 12, the simulations of the inner methylene (top) and a portion of the bromoethyl group (middle) are shown compared to the experimental spectrum (bottom). The simulated spectrum was similar to the experimental spectrum and was sensitive to changes in the folding ratio. Changes as little as 1.5% to the overall folding percent lead to distinct discrepancies between observed and calculated spectra. Therefore, the error in amount of folded conformer was estimated to be $\pm 1.5\%$. Error analysis is discussed further in Section 6.3.

The free energy of folding is defined by the following equations:

$$K_{\text{eq}} = \frac{k_1}{k_{-1}} = \frac{[\textit{folded}]}{[\textit{unfolded}]} \quad (\text{Equation 1})$$

$$\Delta G^\circ = -RT \ln K_{\text{eq}} \quad (\text{Equation 2})$$

in which R is the universal gas constant (1.9875 cal / K mol), T is the temperature in Kelvin, and K_{eq} represents the equilibrium constant or the ratio of the concentrations of the folded state to the unfolded state. Three sets of line shape analyses were performed to obtain three ratios of folded and unfolded states, which were averaged to provide experimental folding energies for torsion balances **26-29**. The results are shown in Table 5.

We conclude that the folding energies of torsion balances are not affected (within the limits of the uncertainty of our experiments) by temperature in the range of temperatures between -5 °C and 15 °C. These data imply small enthalpy changes in our limited range of temperatures. In general, the folding energies for the torsion balances are modest: the values for **26a**, **26b**, **27a**, and **27b** are all approximately -0.2 kcal/mol. We attribute these folding energies to a halogen bonding interaction. The results may be interpreted to suggest the carbamate and

the hydroxymethyl functionalities have similar halogen bond acceptor abilities. However, the generally accepted order of strength for the hybridization of the halogen bond acceptor is $sp > sp^2 > sp^3$,²⁸ even though the carbamate oxygen is sp^2 hybridized and the hydroxymethyl

Table 5. Folding energies for torsion balances 26-29 in $CDCl_3$.

	R	X	T (°C)	% Folded ^{a,b}	$-\Delta G^\circ$ c,d
26a	BocNH	Br	-5	57	0.15
			5	58	0.18
26b	BocNH	Cl	-5	58	0.18
			5	59	0.20
			15	57	0.17
26c	BocNH	OH	-5	66	0.36
			5	66	0.37
			15	66	0.38
27a	HOCH ₂	Br	-5	61	0.23
			5	60	0.21
			15	60	0.23
27b	HOCH ₂	Cl	-5	59	0.19
			5	58	0.18
			15	59	0.20
27c	HOCH ₂	OH	-5	71	0.47
			5	70	0.48
			15	69	0.46
28a	Me ₂ NOCCH ₂	Br	-5	60	0.20
			5	61	0.25
			15	63	0.30
28b	Me ₂ NOCCH ₂	Cl	-5	61	0.24
			5	62	0.26
			15	61	0.25
28c	Me ₂ NOCCH ₂	OH	-5	79	0.70
			5	78	0.71
			15	74	0.60
28d	Me ₂ NOCCH ₂	I	-5	56	0.14
			5	56	0.13
			15	57	0.16
29a	BocNMe	Br	-5	64	0.32
			5	66	0.36
			15	66	0.37
29b	BocNMe	Cl	-5	64	0.31
			5	66	0.37
			15	62	0.29

a) The percentages folded were determined from line shape analyses of the ¹H NMR spectra, acquired on a 500 MHz NMR. b) ±1.5% error. c) ±15% error for the free energy. d) kcal/mol.

oxygen is sp^3 hybridized. This similarity of the two functional groups could be an accident due to unequal geometry requirements for the two groups.

As noted earlier, the preferred geometry of the aryl-carbamate is one in which the group is planar with the adjacent aryl ring, though the halogen bond would require orthogonality between the carbamate and the benzene ring. The barrier to rotation about the N—C_{carbonyl} bond of a carbamate is reported to be 12.3 kcal/mol at -23 °C.^{78,81} Rotation about the N—C_{aryl} bond is less hindered compared to that of the amide bond. The barrier to rotation for the N—C_{aryl} bond of *N*-methylaniline is calculated to be 6.3 kcal/mol at -135 °C.⁸² For *N,N*-dimethylaniline, the barrier is calculated to be 5.1 kcal/mol at -140 °C.⁸³ The barrier for an *N*-phenylcarbamate derivative is likely to be lower than found in these aniline systems.

Tertiary carbamates, **29a** and **29b**, were designed to increase the propensity for orthogonality and improve a halogen bonding interaction. In general, anilides, which bear some resemblance to *N*-phenylcarbamates, adopt a *trans* configuration. Based on *ab initio* molecular orbital (MO) calculations,⁷⁹ the *trans* structure places the phenyl ring preferentially coplanar to the acetamido group. This preference for the *trans* orientation reverses upon methylation of acetanilide, but in both the lowest energy *cis* and *trans* conformers, the phenyl group is perpendicular to the amide group.⁷⁹ The perpendicularity is observed both in the solid state^{84,85} and in solution.⁸⁴

The folding energies observed for the secondary and tertiary carbamates differed only by 0.1 kcal/mol. If the tertiary carbamate mimicked the amide conformational changes by adopting a *cis* conformation, halogen bond could no longer form and the folding energy of the tertiary carbamate would be significantly different from that of the secondary carbamates. The 0.1 kcal/mol difference suggests that methylation of the secondary carbamates destabilizes the

coplanar geometry without altering the *trans* configuration. The tertiary phenylcarbamates, **29a** and **29b**, gave some of the highest folding ratios for all the torsion balances synthesized.

A carbamate functionality was not originally intended for use in this halogen bond project, but in the synthetic route to access the dimethylamidomethyl torsion balances **28a-d**, carbamates **26a-c** were easily accessible. As a result, lower folding ratios were almost to be expected. The alcohols **27a-c** had greater flexibility and did not have the geometric constraints in the same way as the carbamates, but the nature of the halogen bond acceptor, an sp^3 hybridized oxygen, is in theory poor compared to the sp^2 hybridized oxygen of a dimethylamide.²⁸ The less favorable folding energies of -0.2 kcal/mol calculated for **27a-b** were reasonable.

We expected more favorable folding for the dimethylamides **28a-d** compared to the hydroxymethyl and Boc-protected aminomethyl torsion balances, **26a-c** and **27a-c**, because of the hybridization of the oxygen in the dimethylamide and molecular modeling. To our delight, the strength of the halogen bond increased between bromine or chlorine and the carbonyl oxygen of the amide to approximately -0.3 kcal/mol. Notably, among the dimethylamidomethyl analogs **28a-d**, iodide **28d** has the least favorable folding energy of -0.15 kcal/mol. Contrary to the prediction that the strength of the halogen bond will decrease in the order of $I > Br > Cl > F$,^{28,29} the results indicate that the iodinated species has the weakest interaction with the carbonyl oxygen of the dimethylamide moiety among the halogens studied, and that there is no statistically verifiable difference in folding between bromine and chlorine. Therefore, based on these data, the strength of the interaction follows the order, $Cl \approx Br > I$.

The folding energies observed for the halogen bonding torsion balances in chloroform are small compared to that of the hydrogen bonding molecules. The folding energies for the

carbamate **26c**, hydroxymethyl **27c**, and dimethylamidomethyl **28c** are approximately -0.4, -0.5 and -0.7 kcal/mol respectively. In each case, the folding of the hydroxylated analog is favored by a factor of two compared to that of the brominated or chlorinated form. The geometric requirements for halogen and hydrogen bond formation are quite similar. Therefore, these results reveal that the hydrogen bond is stronger than the halogen bond in chloroform.

The results may be summarized as follows: the strength of interaction measured by our torsion balance follows the order, $\text{Cl} \approx \text{Br} > \text{I}$, which does not follow the conventional order of $\text{I} > \text{Br} > \text{Cl} > \text{F}$ for a halogen bond. The tertiary Boc-protected aminomethyl and the dimethylamidomethyl torsion balances **29a-b** and **28a-c** formed stronger interactions in the folded state compared to the alcohols and secondary carbamates **27a-c** and **26a-c**. And finally, the strength of the hydrogen bond is stronger than that of the halogen bond in chloroform.

3.3 THE OBSERVED TREND FOR THE STRENGTH OF THE HALOGEN BOND

The folding of the torsion balance increased in the following order: $\text{Cl} \sim \text{Br} > \text{I}$. This observed trend is contrary to the calculated halogen bond, $\text{I} > \text{Br} > \text{Cl}$. The halogen bond is attributed to electrostatics, dispersion, charge transfer,^{24,28} and most especially the anisotropy of halogen electron density.^{34,35} These properties however support the established trend, not the experimental observed results. Therefore, another factor must be occurring to alter the propensity for halogen bond formation.

This reversed trend may be due to the gauche effect and/or simultaneous steric effects specific to our model system. Typically, the anti conformation for a 1,2-disubstituted ethane is preferred, but the substitution of certain electronegative atoms in the ethane will cause a

preference for the gauche configuration over the anti, the quintessential example of which is 1,2-difluoroethane. The arrangement is primarily attributed to bent bonds and a stabilizing $\sigma_{\text{CH}} \rightarrow \sigma_{\text{CF}}^*$ hyperconjugative effect in molecules such as 1-fluoropropane,⁸⁶ though other factors may contribute or outweigh hyperconjugation.⁸⁷ 2-chloro-,⁸⁸ 2-bromo-^{89,90} and 2-iodoethanol⁸⁹ show evidence for a gauche-gauche preference (concerning the dihedral angle of the C—C and C—O bonds), due to the gauche effect as well as internal hydrogen bonding.

The energy difference between the anti and gauche conformations increases as the size of the halogen increases. The preference for the gauche effect decreases in the 1,2-dihaloethanes in the following order: $\text{F} > \text{Cl} > \text{Br} > \text{I}$.⁹¹ Of the four halogens, iodine prefers the anti over the gauche by a considerable energetic difference. The spatial requirements for halogen bond formation require the haloethylester to adopt an anti conformation; as the population of gauche haloethylesters increased, we would see a reduction in the folding ratio of the torsion balances.

If the gauche effect is prevalent in the synthesized torsion balances and reduces the folding ratios of the torsion balances, compounds containing the 2-haloethoxycarbonyl functionality should also exhibit this conformational preference. A search through the Cambridge Structural Database for the haloethylester ($\text{XCH}_2\text{CH}_2\text{O}_2\text{C}-$) yielded a limited number of results. The iodoethylester did not return any matching results, whereas seven unique crystal structures were acquired for the bromoethylester and three for the chloroethylesters. The latter crystals were exclusively in the gauche conformation,⁹²⁻⁹⁴ and only one⁹⁵ of the seven^{92,94-98} bromides were isolated in the anti configuration. Overwhelmingly, the gauche conformer was favored in the solid state.

The relationship between the crystals and the compounds in solution is tentative. Solvent polarity is known to affect conformational equilibria, and it has been reported that the energetic

difference between the trans and gauche configurations reduces with greater solvent polarity experimentally and computationally.⁹⁹⁻¹⁰²

Chlorine is more likely than bromine and iodine to adopt a gauche conformation and yet the chlorinated torsion balance has one of the highest folding ratios, comparable to that of the brominated torsion balance. The smaller folding energies of the iodide **28d** may be due to the gauche effect and/or simultaneous steric effects specific to our model system. Iodine has a van der Waals radius of 1.97 Å.¹⁰³ Charton suggests that the van der Waals radius for a methyl group ranges from 1.72 Å to 2.23 Å;¹⁰⁴ Bondi proposes 2.0 Å.¹⁰³ According to these data, a methyl group is the same size as iodine. However, the reduction in folding ratios for iodide **28d** compared to the bromide and chloride **28a** and **28b** suggest that the proposed van der Waals radii for a methyl group are not accurate and that an iodine is in fact larger than the methyl group. Measurement of a van der Waals radius is context dependent, and 2.0 Å is an overestimation for the radius of a methyl group. The iodine may prefer the gauche conformation to alleviate steric strain, which is paid in part by stabilization from the halogen bond.

3.4 FOLDING ENERGIES IN NONPOLAR AND POLAR SOLVENTS

The dimethylamidomethyl torsion balances **28a** and **28c** (Figure 13) were examined in additional deuterated solvents, methanol, acetone, dimethylformamide, and a 1:1 methanol: water solution, to ascertain the role of solvent in folding and to compare these folding ratios to common empirical solvent parameters.

Though designed for intramolecular interactions between two functionalities, the torsion balances interact with solvent. Solvent interactions stabilize the unfolded state of the torsion

balance, thereby diminishing the folding energy. The results indicate that the solvent competes effectively as an alternative hydrogen or halogen bond acceptor (Table 6). The highest folding ratios and most favorable energies for hydroxyethylester **28c** were found in chloroform, which is a weak hydrogen bond donor, whereas **28c** shows little to no preference for the folded state in deuterated methanol and dimethylformamide, one of which will form strong hydrogen bonds to the carbonyl group and the other capable of hydrogen bonding with the hydroxyl group. Both solvents inhibit hydrogen bond formation.

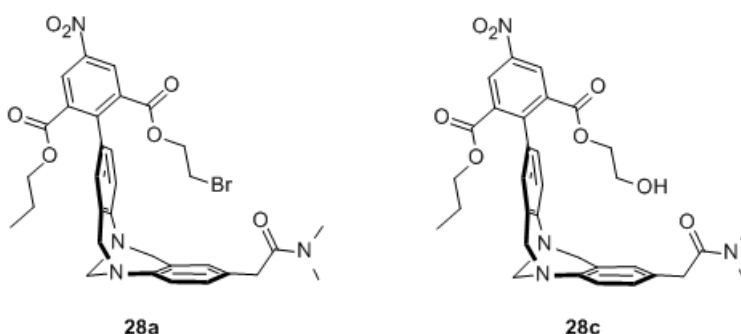


Figure 13. Torsion balances used in solvent studies.

Table 6. Solvent effects on folding data for torsion balances 28a and 28c.

	T (°C)	CDCl ₃	CD ₃ OD	Acetone- <i>d</i> ₆	DMF- <i>d</i> ₇	1:1 CD ₃ OD:D ₂ O
		% Folded ^{a,b}				
28a (Br)	-5	60	59	54	49	53
	5	61	62	54	52	51
	15	63	59	55	56	
28c (OH)	-5	79	50	54	50	45
	5	76	50	59	49	44
	15	74	50	61	48	42
	T (°C)	-ΔG° ^{c,d}				
28a (Br)	-5	0.22	0.20	0.09	-0.02	0.06
	5	0.25	0.27	0.09	0.04	0.01
	15	0.30	0.20	0.11	0.13	
28c (OH)	-5	0.71	0.00	0.09	0.00	-0.11
	5	0.70	-0.02	0.20	-0.02	-0.14
	15	0.60	-0.02	0.24	-0.04	-0.18

a) The percentages folded were determined from line shape analyses of the ¹H NMR spectra, acquired on a 500 MHz NMR. b) ±1.5% error in folding ratios. c) ±15% error for the free energies. d) kcal/mol.

The folding ratios of bromoethylester **28a** are lower than that of hydroxyethylester **28c** in chloroform. In deuterated methanol, the percent folded of **28a** is higher than that of **28c**. Chloroform may be a competitor for the intramolecular halogen bonding interaction in **28a**. Its abilities at hydrogen bond donation on the other hand are considered weak, and the solvent is not as able at competing with the intramolecular interaction in **28c**. Methanol stabilizes the unfolded state of **28a** through strong hydrogen bonding such that there are equal populations of the two conformers, but is a poor competitor for halogen bonding.

It is interesting to note that in the equimolar solution of water and methanol, **28c** favors the unfolded conformer by 0.1-0.2 kcal/mol. This propensity to place the alcohol outside the cleft indicates the strength of the hydrogen bonding stabilization in the (albeit diluted) presence of water. The desolvation of the amide and alcohol is so costly as to make folding unfavorable. Meanwhile, the folding energies of **28a** in chloroform are similar to that in methanol, although chloroform is considered weakly polar. The halogen bonding interaction only slightly favors the folded state over the unfolded state in dimethylformamide, and only the introduction of water obliterates the folding event in the presence of the halogen bond.

Several conclusions can be drawn from the data in Table 6. Methanol is capable of blocking the hydrogen bonding interaction and inhibiting the folding event in balance **28c** but cannot impede the halogen bonding interaction as effectively in torsion balance **28a**. Equimolar amounts of water and methanol favor the unfolded state for **28c**, but equally favor the folded and unfolded states for **28a**. Based on the solvent data, it takes a significant amount of water to obstruct the halogen bond.

To evaluate solvent effects on folding energies, the data were compared to common solvent parameters (Table 7). Dielectric constants (ϵ), Taft and Kamlet's π^* scale¹⁰⁵ and

Reichardt's normalized parameters, E_T^N ,¹⁰⁶ are measures of solvent polarity, while Taft and Kamlet's β scale¹⁰⁵ measures the ability of solvent to donate an electron pair in a solute-to-solvent hydrogen bond.

Table 7. Folding data at 15 °C compared to solvent parameters.

Solvent	% Folded ^a		log K_{eq}		ϵ^b	E_T^N ^c	β^d	π^{*d}
	28a	28c	28a	28c				
CDCl ₃	63	74	0.23	0.45	4.81	0.259	0	0.58
CD ₃ OD	59	49	0.16	-0.02	32.7	0.762	0.62	0.60
acetone- <i>d</i> ₆	59	61	0.16	0.19	20.7	0.355	0.48	0.71
DMF- <i>d</i> ₇	56	48	0.10	-0.03	36.7	0.386	0.69	0.88

a) $\pm 1.5\%$ error in folding ratios. b) dielectric constant. c) Reichardt's normalized values.¹⁰⁶ d) Taft and Kamlet's basicity, β , and polarity, π^* , scales.¹⁰⁵

For **28a**, log K_{eq} was derived from the folding ratios and graphed against empirical solvent scales. The resulting graphs are presented in Figure 14. A strong correlation between log K_{eq} and each of the solvent parameters was found ($R^2 \geq 96\%$), but only when linear regression excluded methanol. As shown in Figure 14 methanol is a clear outlier in all cases, indicating its ability to compete with the folding of the balances as a strong hydrogen bond donor. The data suggest that halogen bonding is strongly affected by polarity and basicity of solvents, but loses predictability of its strength in the presence of strong hydrogen bond donors like methanol.

These results differ from those obtained recently from Taylor and coworkers.⁶¹ The log of association constants for a iodoperfluorooctane-triethylamine complex varied very slightly relative to solvent polarity except in *t*-butanol, *i*-propanol and chloroform, which significantly weakened binding by competing through hydrogen bonding. In our dataset, we consider chloroform to be a weak competitor and it corresponded well with the trendlines. This difference may be attributable to the systems studied: titration and complexation of triethylamine with

iodides are more sensitive to bulk solvent properties compared to the intramolecular interactions of torsion balances.

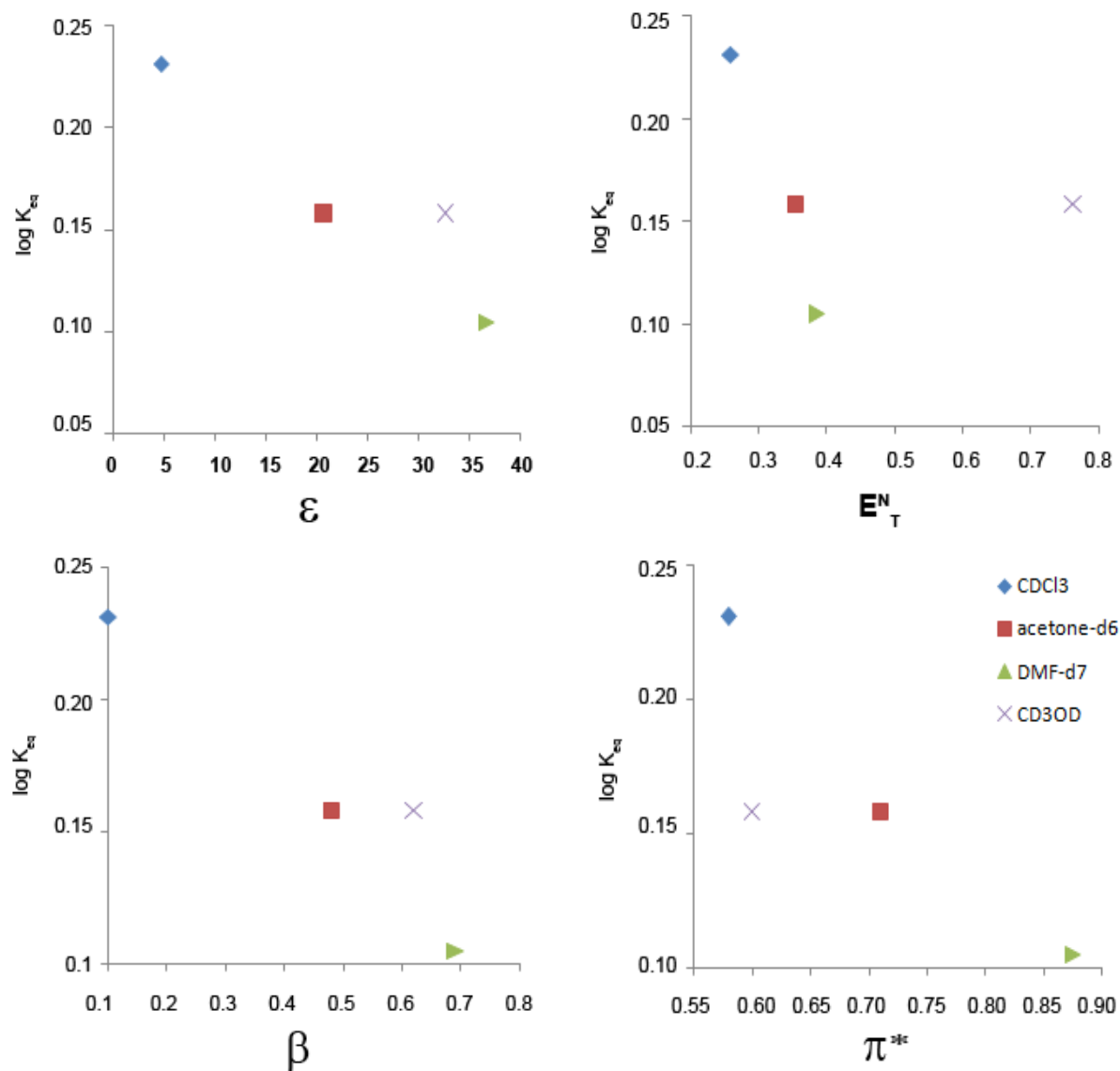


Figure 14. Experimental folding data of 28a at 15 °C ($\log K_{eq}$) against solvent parameters.

There are two points to consider regarding these folding data compared to solvent parameters: 1) the highest temperature at which folding ratios were obtained was 15 °C and not room temperature, the temperature at which many of these parameters were calculated and measured, and 2) the torsion balances were analyzed in deuterated solvents, but the solvent

parameters are measured specifically for the protonated versions. Although attempts were made to obtain folding ratios at 25 °C, low signal-to-noise ratios made line shape analysis of the ^1H NMR spectra challenging. However, folding ratios did not change greatly from -5 to 15 °C (see Table 5), so one can assume that the equilibrium constants of 15 and 25 °C would be similar at room temperature as well. The second point is difficult to address, as parameters are typically not measured in deuterated solvents. Only the E_T^N value for CDCl_3 is provided as 0.256 versus 0.259 for CHCl_3 .¹⁰⁶ And if the 1% difference between the two chloroforms is of any indication, the variation between protonated and deuterated solvents is negligible.

3.5 CONCLUSIONS

Halogen bonding has been recognized for decades and has been used extensively in the assembly of supramolecular structures. The strength of the halogen bonding interaction in solution is a relatively unknown quantity. Association constants for halogen-bonding interactions have been determined in only a few cases,⁵⁷⁻⁶¹ and most information regarding its strength was determined computationally. However, computational studies will fail to accurately represent halogen bonding unless based on experimental evidence. Rational drug design depends upon a comprehensive knowledge of weak intermolecular interactions; the significant impact of halogen bonding brings to attention the need for a more thorough understanding of the effects of halogenation and halogen bonding in solution. For these reasons, we sought to measure the halogen bond by using the molecular torsion balance.

We found that the strength of the halogen bond as measured by ΔG decreased in the following order: Cl ~ Br > I. This observed trend is contrary to the computationally predicted order, I > Br > Cl. The halogen bonding interaction requires an anti conformation in the haloethylester group to minimize the distance between the acceptor and donor. This reversed trend may be due to the gauche effect and/or simultaneous steric effects specific to our model system. The substitution of certain electronegative atoms in a 1,2-disubstituted ethane will cause a preference for the gauche configuration over the anti. This gauche effect decreases with the size of the halogen, however; iodide **28d**, which featured the lowest folding ratios, should be least prone of the halogens to adopt a gauche configuration. The lower folding preference could also be a result of steric hindrance, in which the iodoethylester is too large to be in an anti conformation. As a result, propensity for folding decreases.

We found that the stabilizing potential energy of the halogen bond was -0.2-0.3 kcal/mol in chloroform. These values are considerably lower than those reported for gas phase studies and computational studies. The interaction between bromobenzene and formaldehyde reduces in strength from -1.15 kcal/mol in vacuum to -0.64 kcal/mol in water, according to ab initio calculations with solvation corrections.³⁷ In addition, the folding energies of torsion balances are not affected by temperature in the range of temperatures between -5 °C and 15 °C.

The hydroxymethyl and carbamate functionalities gave similar folding energies of 0.2 kcal/mol, though this does not necessarily contradict the generally accepted order of strength of $sp^2 > sp^3$,²⁸ instead, this could be an accident due to unequal geometric requirements for the two groups. The secondary carbamates may prefer coplanarity between the carbamate and the adjacent aryl ring, increasing the distance between the halogen bond donor and acceptor and thereby reducing the folding energies. Methylation of the secondary carbamate reduces this

preference for coplanarity. The tertiary carbamates gave modest folding ratios of approximately -0.3 kcal/mol, more than observed for the secondary carbamates.

The dimethylamides **28a-d** had folding energies similar to the tertiary carbamates. The strength of the halogen bond between bromine or chlorine and the carbonyl oxygen of the amide was approximately -0.3 kcal/mol. Our desired dimethylamides served as a model system, providing not only the bromide and chloride **28a-b** but the iodide as well, **28d**. Notably, iodide **28d** had the least favorable folding energy of -0.15 kcal/mol, indicating that among the halogens studied, the iodinated species has the weakest interaction with the dimethylamide moiety.

Our solvent studies provide invaluable data for comparing the strengths of hydrogen and halogen bonding. The halogen bond interaction is weaker in chloroform than hydrogen bonding. Methanol is capable of blocking the hydrogen bonding interaction and inhibiting the folding event in balance **28c** but in **28a**, methanol cannot impede the halogen bonding interaction as effectively. Equimolar amounts of water and methanol favor the unfolded state for **28c**, but equally favor the folded and unfolded states for **28a**. Based on the solvent data, it takes a significant amount of water to obstruct the halogen bond.

The folding energies of the torsion balances were also compared to the solvent parameters, dielectric constant, Taft and Kamlet's π^* and β scales, and Reichardt's normalized parameters. A strong correlation between $\log K_{eq}$ and these solvent parameters were found only when linear regression excluded methanol. Methanol is a clear outlier in all cases, indicating its ability to compete with the folding of the balances as a strong hydrogen bond donor. The data suggest that halogen bonding is strongly affected by polarity and basicity of solvents, but loses predictability of its strength in the presence of strong hydrogen bond donors like methanol.

4.0 THE STRENGTH OF SALT BRIDGES AND THEIR CONTRIBUTION TO PROTEIN STABILIZATION

The tertiary structure of proteins relies on non-covalent interactions for stabilization,¹⁰⁷ among which are London dispersion forces and electrostatic interactions. Electrostatic interactions can be attractive or repulsive and occur over a wide range of distances. The salt bridge interaction is an attraction between two oppositely charged amino acids separated by 3-5 Å;^{108,109} as one or more hydrogen bonds frequently accompany such close functional group arrangements, salt bridges are typically considered a special type of hydrogen bond.¹¹⁰

Ion pairs occur between negatively and positively charged amino acid side chains; negative side chains occur in aspartate and glutamate residues and the common amino acids with positively charged side chains are lysine, arginine, and histidine. According to a survey conducted among 38 proteins with 229 total ion pairs, 38% of ion pairs occurred with arginine, 29% with histidine and 20% with lysine.¹⁰⁸ The potential for monodentate or bidentate interactions and thus a greater flexibility in arginine's¹¹¹ and histidine's binding modes may account for the more frequent participation of these amino acids in salt bridges. In two separate surveys, arginine was preferred as the cationic amino acid in buried salt bridges whereas lysine was favored for surface salt bridges, though no preference was noted for the anionic residues, aspartic and glutamic acids.^{108,109}

Studies on the contribution of salt bridges to protein stability have provided contradictory results – probably because the strength of salt bridges is highly context dependent. The protein, the geometry of the interaction, solvent conditions, nearby chemical groups, and other aspects of the environment of the salt bridge all play important roles in its strength.^{109,112} Evidence from continuum electrostatic calculations of 21 different salt bridges suggest that the replacement of salt bridge residues with hydrophobic isosteres would be favorable,¹¹³ which has also been shown experimentally.¹¹⁴⁻¹¹⁶ The desolvation penalty for the salt bridge residues diminishes with increases in solvent exposure¹¹³ and also temperature.¹¹⁷ On the other hand, it has been suggested that the desolvation costs were overestimated in the continuum electrostatic calculations,^{118,119} and continuum electrostatic calculations by Kumar and Nussinov for 222 salt bridges considered nearly all (86%) the interactions stabilizing by $-3.7(\pm 3.9)$ kcal/mol; they also determined that buried salt bridges were more stabilizing than exposed ones.¹⁰⁹

The general consensus is that salt bridges buried in the interior of a protein are stabilizing; the energetic penalty for the desolvation of charged residues in the unfolded state to form the folded state is offset by the strength of the interaction in an environment with a low dielectric constant.¹¹⁹ Chymotrypsin exists in two conformations, the enzymatically active and inactive forms. The equilibrium between these states was found to be affected by the existence of a buried salt bridge between the amino terminus of Ile16 and the carboxylate of Asp194.¹²⁰ Deprotonation of this salt bridge at a pH greater than 8 contributes to a loss of 2.9 kcal/mol in stabilization energy, a value calculated from equilibrium constants.¹²¹ A site-directed mutation of Arg10 to methionine of the DNA-binding domain of 434 repressor led to a 2 kcal/mol decrease in stability.¹²² Site-directed mutagenesis of two buried salt bridges of barnase, Arg69/Asp93 and Arg83/Asp75, proved to be destabilizing; substitution of the aspartates with

lysines led to 4.11 and 4.80 kcal/mol losses in protein stability and coupling energies of the salt bridges determined by double mutant cycle were -3.34 and -3.53 kcal/mol respectively.¹¹¹

The contribution of salt bridges located at the surface of proteins to the stability of proteins has proven to be a contentious issue. Results suggest that salt bridge contributions to the stability of the protein decrease as exposure to solvent increases, and that this is due to solvent screening and the entropic cost of amino acid immobilization.^{119,123,124} Site-directed mutagenesis of the glutamic and aspartic acids to the corresponding amides of each of the six surface salt bridges on or near the surface of human lysozyme was conducted to determine the salt bridge contribution to stability. The results suggest that salt bridge contributions to stabilization energies would be insignificant when fully exposed to solvent and would be as large as -2.2 kcal/mol when fully buried.¹²⁵

Crystal structures of the B1 domain of protein G reveal consistent formation of three surface salt bridges involving lysines. That these salt bridges *do not* appear in solution is shown by the fact that in 50 mM phosphate buffer, the lysine protons exchange more readily with the solvent than the carboxylate.¹²⁶ The coupling energy of the engineered surface salt bridge between Glu28 and Lys32 of barnase was only -0.2 kcal/mol, measured by double mutant cycle.¹²⁷ The incorporation of salt bridges to the surface of the CGN4 leucine zipper increased its stability by only -0.08 kcal/mol,¹²⁸ while engineered surface salt bridges of T4 lysozyme only added between -0.1 to -0.25 kcal/mol to its stability.¹²⁹ Solvent exposure seems to have a deleterious effect on the strength of the salt bridge.

Solvent screening and the entropic cost of amino acid immobilization are two possible reasons for decreased strength of the salt bridge with greater solvent exposure.^{119,123,124} The analysis of two salt bridges of a rubredoxin variant (PFRD-XC4) support the concept of entropic

penalties for amino acid immobilization. Hyperthermophilic organisms maintain stability at significantly higher temperatures than their mesophilic counterparts with optimum growth temperatures usually between 80 and 100 °C. The resilience of hyperthermophiles is typically ascribed to an increased number of salt bridges and salt bridge networks in their hyperthermophilic proteins. The rubredoxin variant PFRD-XC4 has two important surface salt bridges that potentially contribute to the hyperthermostability, one between the side chains of Lys6 and Glu49 and another between the amino-terminus and Glu14. The Lys6-Glu49 salt bridge was found to have a negligible bonding energy whereas a main chain to side chain salt bridge between the amino-terminus and Glu14 was measured to be -1.5 kcal/mol.¹³⁰ The greater strength of the latter salt bridge may be due to preorganization of the N-terminus, which is immobilized as part of the main chain; fixing the position of only one residue reduces the entropic penalty and increases the interaction energy.

The strength of salt bridging is not always weak or negligible when exposed to solvent. In one study, all the surface arginines of ubiquitin were modified to ureas; little difference in stability between the mutant and the wild type was observed.¹³¹ These results however only account for the electrostatic portion of the salt bridge; the ureas are capable of hydrogen bonding. In another study evaluating the strength of two conserved surface salt bridges in the hyperthermophilic protein Ssh10b, the salt bridges between Glu36 and Lys68 and between Glu54 and Arg57 were measured as -1.4 kcal/mol and -0.60 kcal/mol respectively. Both salt bridges are near the surface of the protein, but the solvent accessible surface areas (ASA) for the residues indicated only partial exposure: Glu54: 5%, Arg57: 28%, Glu36: 40%, Lys68: 58%. The Glu36/Lys68 salt bridge was significantly more exposed to solvent and yet its strength is twice that of its more buried counterpart.¹³² Due to the close proximity of the two residues in the

primary sequence, a Glu54/Arg57 salt bridge may potentially form in the unfolded state, for which the double mutant cycle cannot account. These data may be an example of a faulty double mutant cycle or a contradiction to the norm that solvent exposed salt bridges are weak.

There are further examples in which surface salt bridges lead to increased stability of the protein. Random-mutagenesis of β -glucosidase A gave thermostable mutant, Glu96Lys, which formed a new salt bridge between Lys96 and Asp28. This mutation doubled the half-life for unfolding relative to that of the wild-type β -glucosidase A at 48 °C.¹³³ A double mutant cycle to analyze a partially solvent exposed ion pair between Asp23 and the N-terminus of ribosomal protein L9 gave varying coupling energies from -0.7 to -1.7 kcal/mol.¹³⁴ The coupling energy of the salt bridge between Lys11 and Glu34 of ubiquitin was found to be -0.86 kcal/mol, using a double mutant cycle.¹³⁵ A surface salt bridge formed between Asp70 and His31 of T4 lysozyme had an estimated strength of 3-5 kcal/mol, based on site-directed mutagenesis and thermal unfolding transitions.¹³⁶ A triad of residues, Asp8, Asp12, and Arg110, on the surface of barnase form two salt bridges. Fersht used double and triple mutant cycles to determine coupling energies of -0.98 kcal/mol between Asp8 and Arg110 and -1.25 kcal/mol between Asp12 and Arg110. These interactions were cooperative; absent one salt bridge, the energy of the other was reduced by 0.77 kcal/mol.¹³⁷

As shown above, the relationship between the strength of a salt bridge interaction and its degree of solvation is controversial. Under physiological conditions, ionic strength also affects salt bridge stability, but the correlation between the two is murky. Salt bridges are primarily electrostatic in nature; therefore, as ionic strength of solution increases, the strength of the interaction should become smaller.¹¹³ Experimental results have largely attested to this prediction. In one case, the coupling energy between aspartic acid and arginine decreased from

-0.98 to -0.35 kcal/mol when the ionic strength increased from 0.0 M NaCl to 0.5 M NaCl.¹³⁷ In human lysozyme, mutation studies showed that salt bridges with greater than 50% exposure to solvent did not contribute to the stability of the protein in 0.2 M KCl. The mutations did not eliminate the hydrogen bonding component of the salt bridge.¹²⁵

On the other hand, the strength of the salt bridge between Asp23 and the N-terminus of protein L9 was largely unaffected by the ionic strength increase from 100 mM NaCl to 750 mM NaCl.¹³⁴ A salt bridge of GCN4 leucine zipper monomer, which has been shown to be indispensable for folding of the coiled-coil formation,¹³⁸ and salt bridges in alanine-based model peptides with lysine or histidine interspersed with aspartic or glutamic acid at regular intervals^{139,140} were only partially screened at salt concentrations up to 2.0 M. Finally, an analysis of the pK_a of a histidine in haemoglobin (His HC3(146)β) verified pK_a did not alter considerably (8.0-8.1) regardless of ionic strength and demonstrated the independence of the strength of surface salt bridges from external salt concentrations in solution.¹⁴¹ Salt bridges may be immune to changes in ionic strength if the interaction acts more like a hydrogen bond than a Coulombic or electrostatic interaction.^{134,142} Even clearly electrostatic interactions can show insensitivity to ionic strength.^{139,143}

In a survey conducted on 28 proteins, maximum accessible contact surface areas (ϕ -areas) were calculated for the 134 salt bridges to determine degree of solvent exposure. 24% were considered buried (ϕ -areas of 0-15% of the maximum), 37% were partially buried (ϕ -areas of 15%-50%) and the remaining 39% were deemed exposed or surface salt bridges.¹⁰⁸ A similar survey of 36 proteins determined that 30% of the total 222 salt bridges were buried ($\phi \leq 20\%$).¹⁰⁹ It is, for the most part, accepted that buried salt bridges stabilize the protein, but a significant number of salt bridges are not buried, and occur on the surface or are partially solvent exposed.

Unfortunately, research has not reached a consistent conclusion on whether or not these solvent exposed interactions are stabilizing. If solvent exposed salt bridges are destabilizing to the protein, why would nature preserve this interaction? One possible explanation, that salt bridges reduce the number of stable conformations adopted by the protein and lend specificity to folding,^{111,113,144} does not justify the frequency with which salt bridges are used.

It is apparent from the data obtained in the past decades that the contribution of salt bridges to the stabilization of proteins is highly context dependent, but many questions are still unanswered. What is the contribution of solvent exposed salt bridges to the stability of proteins? What is the strength of the interaction? How do the factors of ionic strength and temperature affect the strength of the interaction? Our research delves into these questions outside the context and complexity of proteins, using the molecular torsion balance.

4.1 EVALUATION OF METHODS TO MEASURE THE SALT BRIDGE

One must break a salt bridge to measure its strength, and there are two common methods to do so: by mutation effects or by pK_a studies. In the first method, the salt bridge is broken upon protonation of the acidic residue or deprotonation of the basic amino acid, and changes in pK_a are measured to obtain a *relative* stability contribution. Although this method does not require structural modification of the residues and is considered non-invasive, residual electrostatic interactions between the neutralized and charged amino acids can still occur.¹⁴⁵

The second method requires modification of one or both charged residues to uncharged surrogates, usually aliphatic amino acids. Site-directed mutagenesis of a salt-bridge participant and measurement of the resulting destabilization is a popular method to determine the strength of

a salt bridge,^{122,125,129,133,136,142} although the correlation between the strength of the salt bridge and its contribution to the stability of a protein is difficult to establish.¹¹³ The relationship is at best tenuous due to new interactions or solvation differences between the folded and unfolded states.¹¹¹ For example, the coupling energy derived from a double mutant cycle of the Asp166-Arg119 salt bridge in T4 lysozyme is a mere 0.10 kcal/mol, while the lysozyme loses 0.51 kcal/mol in stability when either of the residues are modified. The strength of the salt bridge of Arg6-Glu53 in protein GB1 is predicted by double mutant cycle to be 0.60 kcal/mol, but the stability of the protein is unaffected by the loss of the salt bridge.¹³⁵ Arg31, Glu36 and Arg40 form a buried salt bridge triad in Arc repressor. The coupling energies of Arg31/Glu36 and Glu36/Arg40 are -1.7 and -4.7 kcal/mol respectively, yet the interactions are not considered major contributors to the overall stability of the protein.¹¹⁴ Changes to the stability of the protein do not directly correlate to the strength of the salt bridge, because the relationship is tempered by local context.¹⁴⁵

The double mutant cycle approach solves these problems in part by attempting to isolate one specific noncovalent interaction by cancelling out background interactions. It requires the syntheses of one double and two single mutants, and the system must fulfill several assumptions: 1) no significant structural rearrangements occur in the mutants relative to the wild-type, 2) no interactions occur between the substituted residues in the area of interest, and 3) no changes to the unfolded state transpire.^{134,135} To confirm that the assumptions have been met, more than one double mutant cycle should be carried out and these should yield similar coupling energies.¹⁴⁵ Most research groups however only perform one double mutant cycle, while others have obtained dissimilar results from multiple mutant cycles.¹³⁴ Only one group has conducted a multiple double mutant cycles to obtain the similar strengths for the two salt bridges studied.¹³²

All data regarding the salt bridge have been derived from peptides or proteins. The intricacy of these systems complicates and obscures the accurate measurement of a single interaction. Although the double mutant cycle can alleviate some of these issues, several assumptions must be met for the data to be valid. By subjecting the torsion balances to different conditions, we can obtain accurate, quantitative data for the coupling energy of the salt bridge.

5.0 EVALUATION OF THE SALT BRIDGE USING THE MOLECULAR TORSION BALANCE

Our objective was to measure this salt bridge interaction in a small molecular framework. We sought to obtain quantitative information regarding the strength of the interaction when exposed to water, without employing a double mutant cycle. To achieve this goal, amino and guanidino groups were appended to the lower arm of the dibenzodiazocine framework of our second generation torsion balance (Figure 15). For the two esters that make up the two competing sides of this torsion balance, an alkyl ester (methyl or isopentyl) was balanced against a carboxyethyl ester. At neutral pH in water, a salt bridge may form between the carboxylate and the amine or guanidine, and we planned to use this tool to measure the effects of a salt bridge on folding.

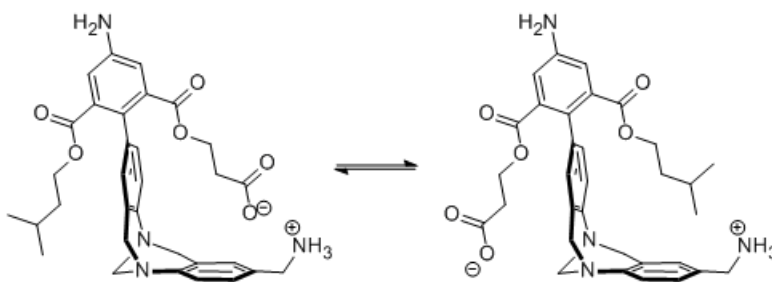
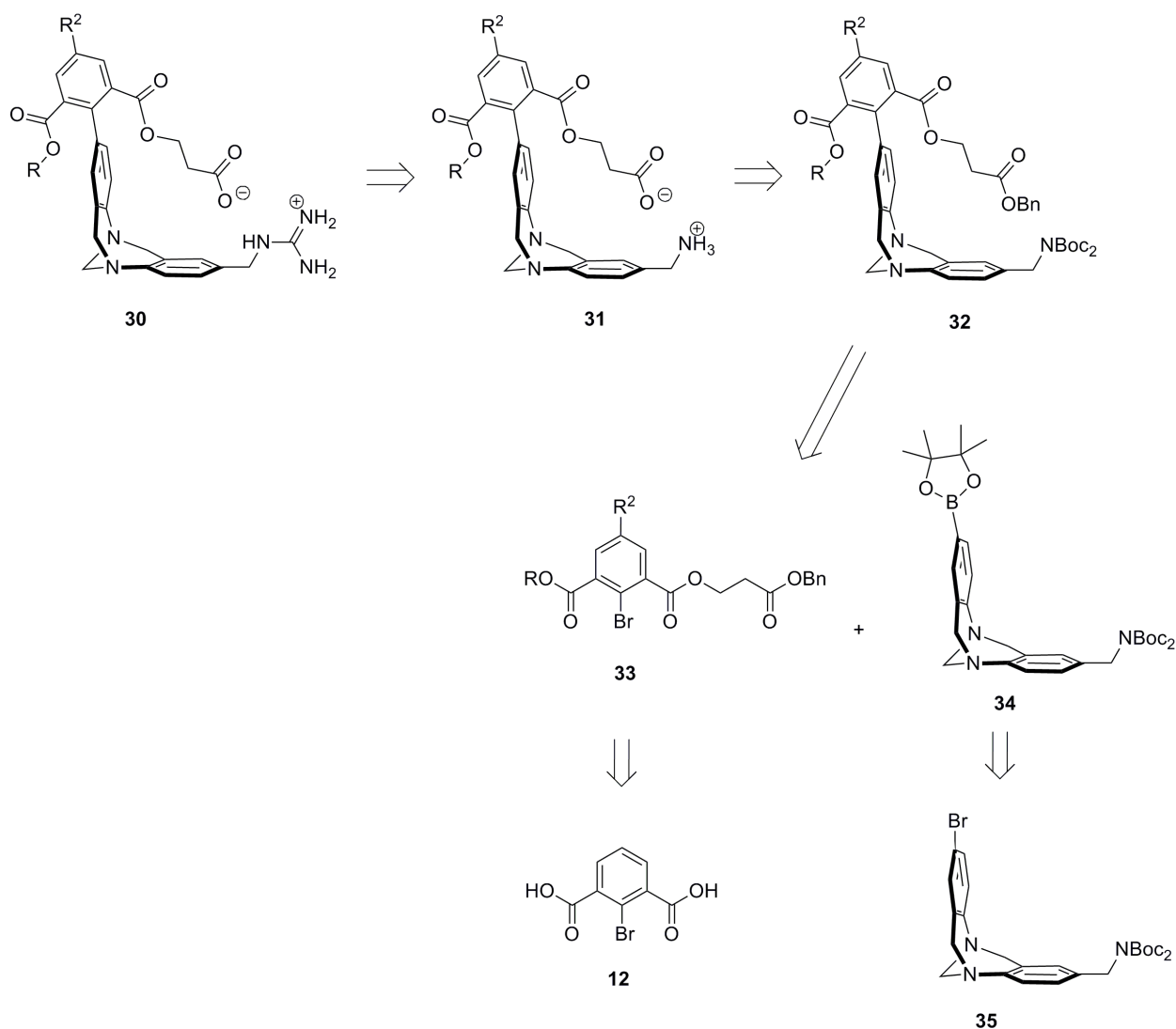


Figure 15. Representative chemical structures for the folded and unfolded conformers.

5.1 SYNTHESIS OF SALT BRIDGE TORSION BALANCES

By observing perturbation in the orientation of the isophthalate moiety, we could use the torsion balance to get a direct comparison of a carboxyethyl and an alkyl group, R (e.g. methyl or isopentyl), as they interact with the interior of the dibenzodiazocine and the amino or guanidino group. The retrosynthetic strategy for the torsion balances is shown in Scheme 7.

Scheme 7. Retrosynthetic analysis.

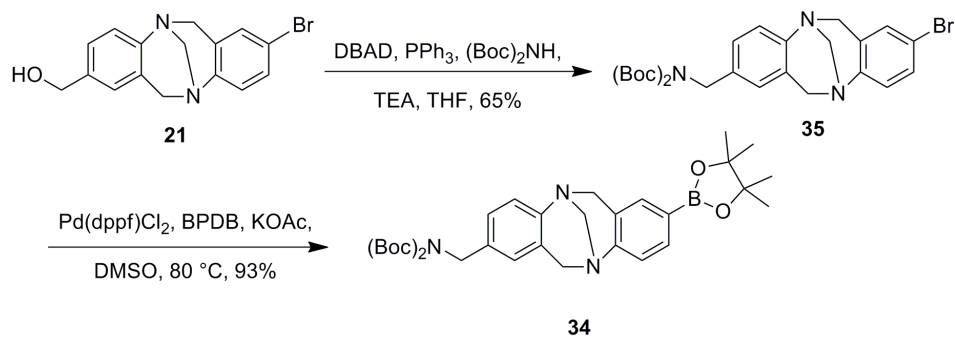


The guanidinium **30** can be accessed from corresponding amine **31**. Protecting groups will be necessary to form the biphenyl bond of the torsion balance through Suzuki coupling between

pinacolatoboronate **34** and bromide **33**. The pinacolatoboronate **34** can be derived from the Tröger's base analog **35**, and the asymmetrical isophthalate was to be synthesized from 2-bromoisophthalic acid **12**.

The pinacolatoboronate **34** was relatively simple to access from the hydroxyalcohol **21**. It is reported that the Mitsunobu reaction works efficiently with acidic nucleophiles with pK_a values lower than 11.^{146,147} Though the pK_a of di-*tert*-butyl iminodicarboxylate (Boc_2NH) should be between 8 and 11, the major product obtained using the usual Mitsunobu conditions formed the new C—N bond between the substrate and the di-*tert*-butyl azodicarboxylate. The addition of triethylamine facilitated the formation of the desired product **35**, which was obtained in 65% yield.¹⁴⁸ Borylation provided **34** in 93% yield.

Scheme 8. Mitsunobu reaction.

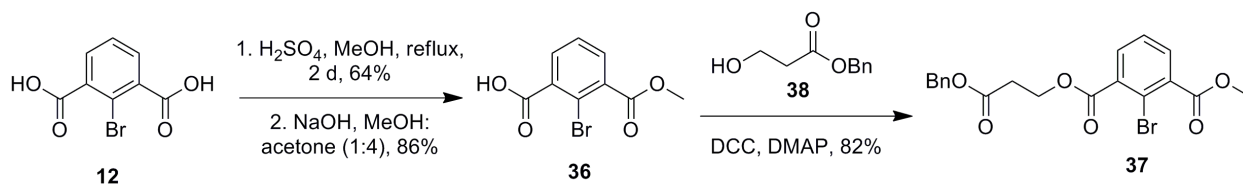


As part of the project on the analysis of hydrophobic effects that was previously carried out in our laboratory, a solubilizing group was appended to the isophthalate moiety of the torsion balance in order to improve solubility of the balance in water.²³ We found that the glutaramide functionality was not necessary to achieve the 1 mM concentration of our desired molecules in water. Although the glutaramide and consequently the nitro group (R^2 , Scheme 7) were not essential, we retained the nitro group in order to have an opportunity to evaluate any effects that changes in this remote position might have on folding.

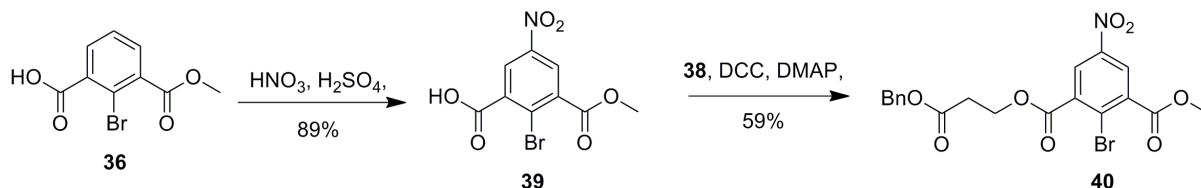
The carboxyethyl group was initially positioned against a methyl group (R, Scheme 7) due to the accessibility of starting materials and the ease of line shape analysis. However, to evaluate steric effects in folding, we also sought to introduce a lipophilic isostere of the carboxyethyl group. Therefore, isopentyl esters (isoamyl, abbreviated as *i*-Am) were also synthesized.

In all, four carboxyethyl isophthalates were generated: **37**, **40**, **42**, and **44**. These included two methyl esters (one bearing the 5-nitro group) and the two isopentyl esters (one with the 5-nitro group). The syntheses of the isophthalates are illustrated in Schemes 9-12. Diacid **12** was esterified and selectively hydrolyzed to give intermediate **36**.¹⁴⁹ Steglich esterification gave the product **37** in 82% yield (Scheme 9). Nitration followed by dicyclohexylcarbodiimide (DCC) coupling provided **40** (Scheme 10). Monoesterification of the diacid **12** furnished hemiester **41**, which underwent DCC coupling to give **42** (Scheme 11).

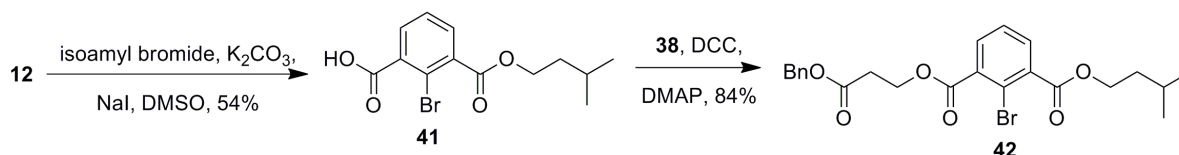
Scheme 9. Synthesis of isophthalate **37**.



Scheme 10. Synthesis of isophthalate **40**.

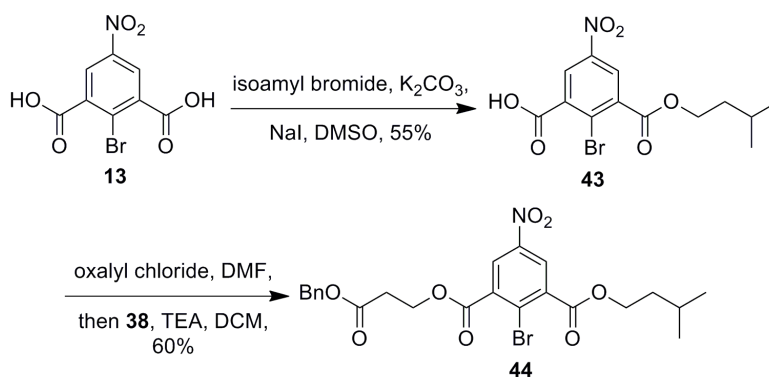


Scheme 11. Synthesis of isophthalate **42**.



For the last needed isophthalate, diacid **13** was esterified with isoamyl bromide to give the monoester **43** (Scheme 12). Although the Steglich esterification of the hemiesters provided **37**, **40**, and **42** in moderate to high yields, these conditions consistently led to poor yields and decomposition for the synthesis of **44**. Therefore, an alternate route via an acid chloride¹⁵⁰ was followed to provide the last ester **44** with moderate yield.

Scheme 12. Synthesis of isophthalate 44.

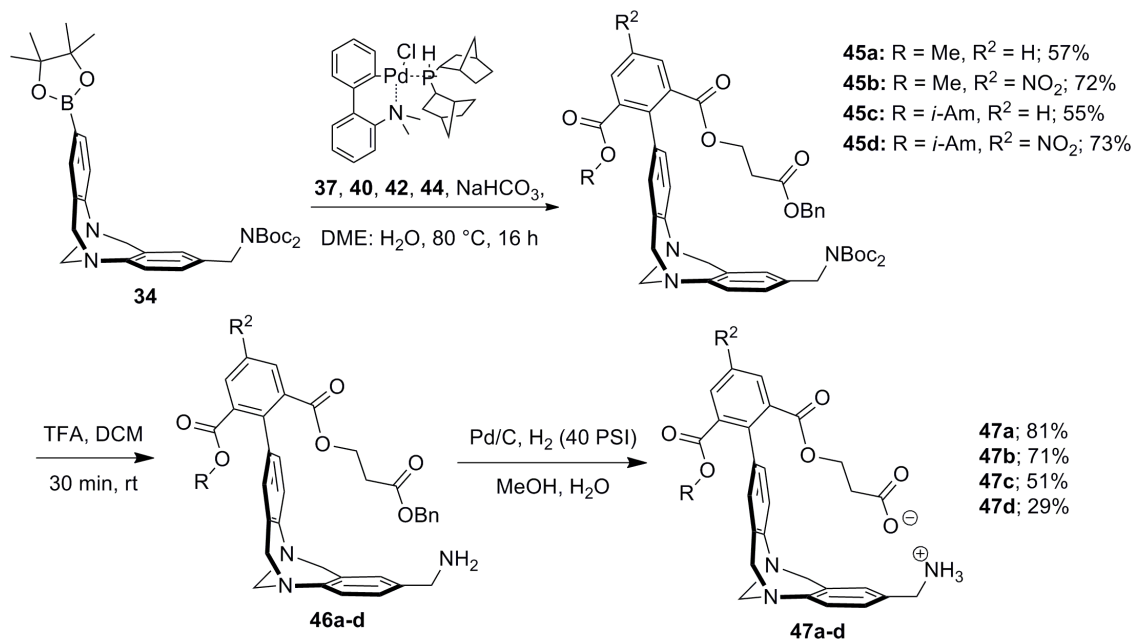


The Suzuki couplings between the four isophthalates and pinacolatoboronate **34** gave the torsion balances in moderate to good yields (Scheme 13), and treatment with trifluoroacetic acid (TFA) deprotected the Boc groups.¹⁵¹ The polarity of the products at this point was high enough that purification through normal phase column chromatography would have been difficult. Fortunately, the crude products of the TFA deprotection did not require purification to move onto the next step. Treatment of **46a-d** with palladium on carbon and hydrogen gas at 40 PSI¹⁵² deprotected the benzyl carboxylates and reduced the nitro groups to give products, **47a-d**. The torsion balances were purified using reverse phase HPLC by applying a linear gradient of water containing 0.1% TFA and acetonitrile containing 0.1% TFA over the course of 20-30 minutes at a flow rate of 15 mL/min.

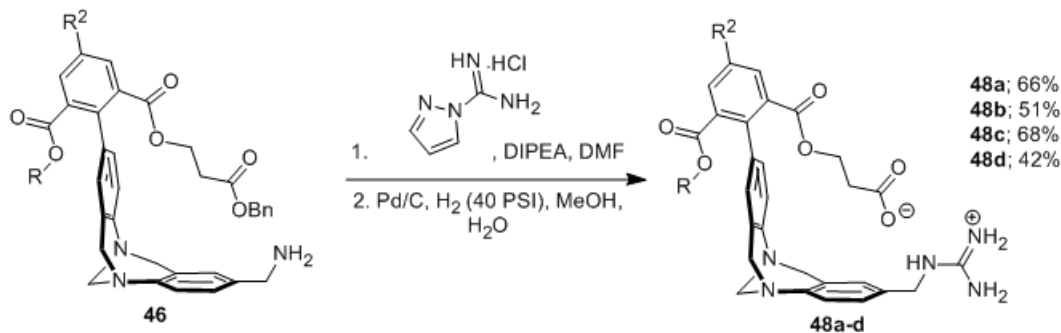
Attempts to directly convert the torsion balances **47a-d** to their corresponding guanidines failed. The best route required treatment of **46a-d** with pyrazole-1-carboxamide in the

presence of Hünig's base in DMF,¹⁵³ followed by debenzoylation and reduction to give the desired guanidines **48a-d** (Scheme 14). The guanidines were less polar compared to their amine analogs and were readily purified by reverse phase HPLC.

Scheme 13. Synthesis of amines **47**.



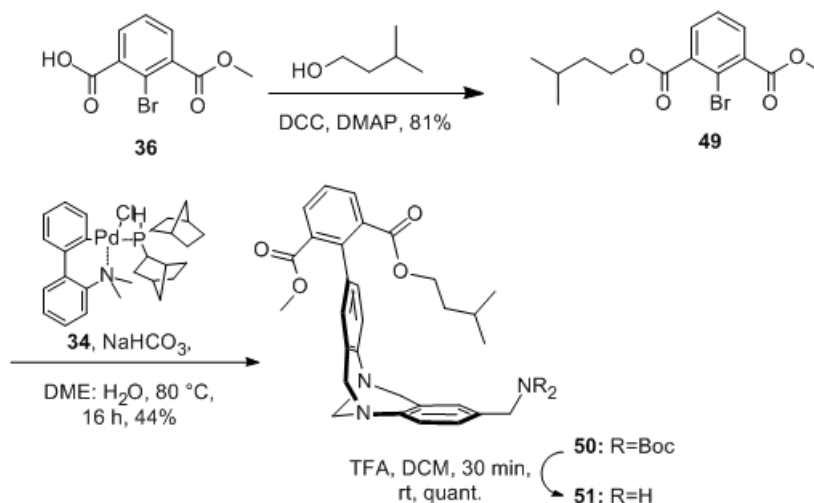
Scheme 14. Synthesis of guanidines **48**.



One last torsion balance was synthesized in order to determine the role of the isopentyl group in the preference for folding (Scheme 15). The diester **49** was obtained through DCC coupling of the hemiester, which was used in a subsequent Suzuki coupling to provide the Boc-

protected torsion balance. Deprotection of the amine gave the desired product **51** in quantitative yield.

Scheme 15. Synthesis of the control.



5.2 ¹H NMR SPECTRA OF SALT BRIDGING TORSION BALANCES

To determine folding ratios, the torsion balances **47a-d** and **48a-d** were analyzed by ¹H NMR at concentrations of 0.5-1.0 mM in D₂O. Changing the concentration used for NMR analysis over a range from 0.1 mM to 2.0 mM did not alter the spectra and the folding ratios determined, signifying a lack of aggregation in water. ¹H NMR spectra were taken at varying temperatures from 5 to 25 °C with ten degree increments on the 700 MHz NMR. Water suppression experiments were tested to improve the resolution of the spectra, but the attenuation of signals within 2 ppm of the water peak made this method impractical for quantitative data acquisition. Torsion balances **47a-d**, containing the ammonium side chain, were very soluble in water, while the corresponding guanidines **48a-d** were decidedly less water soluble. Torsion

balances **47a-d** and **48a-b** were sufficiently soluble in D₂O to obtain 1 mM solutions, but guanidines **48c-d** required more D₂O to be solvated completely; the latter two torsion balances were run at concentrations of 0.5 mM.

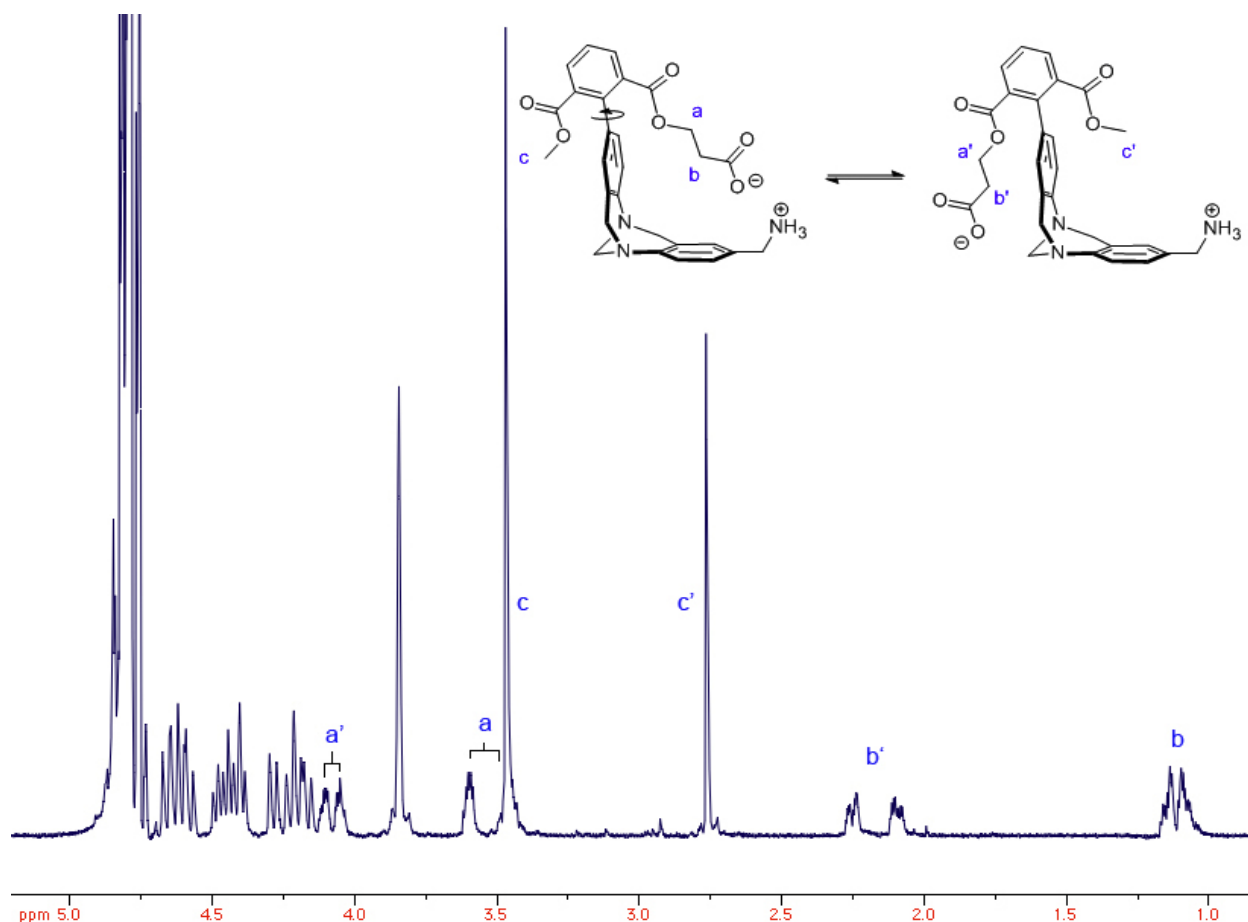


Figure 16. ¹H NMR spectrum of **47a** at 15 °C in D₂O.

The ¹H NMR spectra for compounds **47a** and **47c** serve as suitable models for discussion of the spectra of all the salt bridging torsion balances. The ¹H NMR spectrum of **47a** at 5 °C in D₂O is shown in Figure 16. Assignments of the signals for the two conformers were facilitated by examination of EXSY cross peaks acquired at 5 °C (with a mixing time of 0.5 seconds).

The largest chemical shift difference of the isophthalate before and after the Suzuki coupling occurs at the methylene (b, b') distal from ester. The methylene resonates at 1.11 ppm in the folded state (b) and at 2.15 ppm in the unfolded state (b'), while these protons appear as a

triplet in the model compound bromide **37** at 2.83 ppm; this is a 1.04 ppm difference between the conformers and a 1.73 ppm difference between the folded conformer and the isophthalate before Suzuki coupling. This significant shielding effect induced upon folding is indicative of the close proximity of this group with the lower ring of the dibenzodiazocine in the folded state.

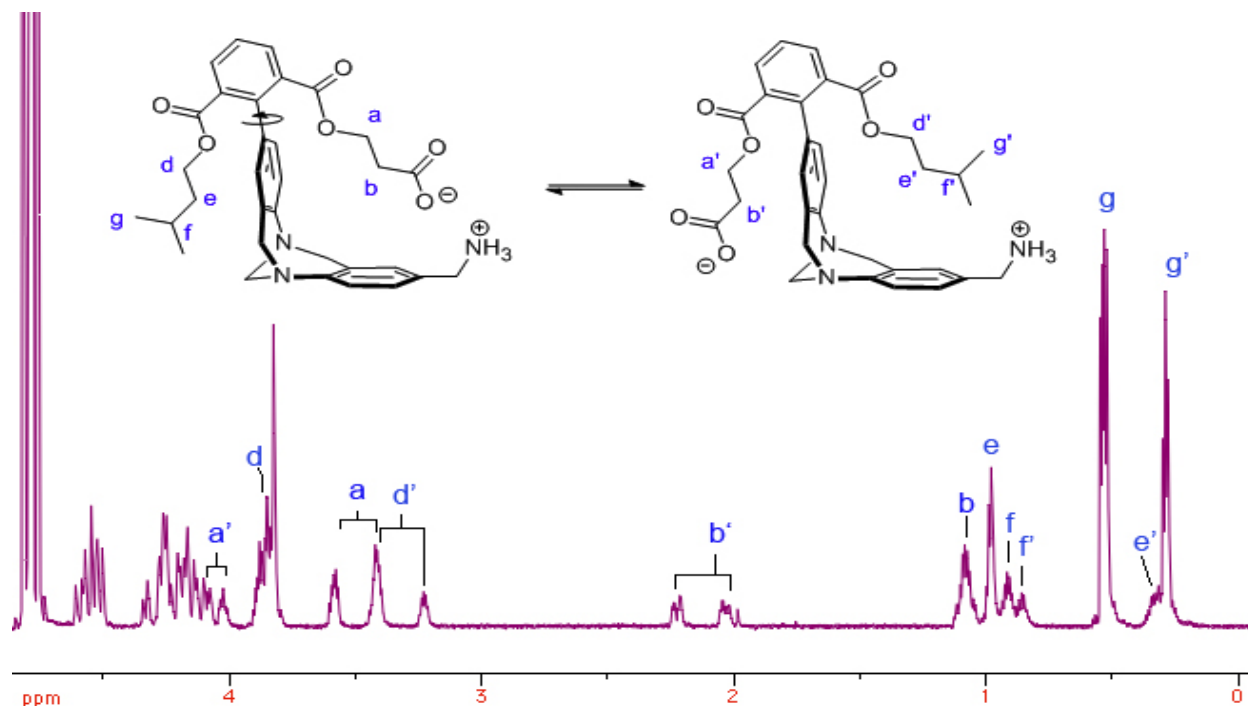


Figure 17. The ^1H NMR spectrum for **47c** at 5 °C in D_2O .

Similar results were observed for other protons, although the difference was not as large. The methyl ester of bromide **37** appears at 3.93 ppm. In **47a**, these protons resonate at 3.47 and 2.76 ppm in the folded (c) and unfolded conformers (c') respectively.

The ^1H NMR spectrum for **47c** is similar to **47a**, but the isoamyl ester group complicates the region from 1.0 to 0.2 ppm (Figure 17). Again, the largest chemical upfield shift induced as a result of Suzuki coupling is that of the distal methylene in the folded state (b) which appears at 1.08 ppm, compared to 2.82 ppm in the starting isophthalate, **42**, a difference of 1.74 ppm. The inner methylene (e'/e) of the isoamyl group experiences comparable changes; the 1.63 ppm signal in **42** moves upfield by 1.3 ppm to 0.33 ppm in the unfolded state (e').

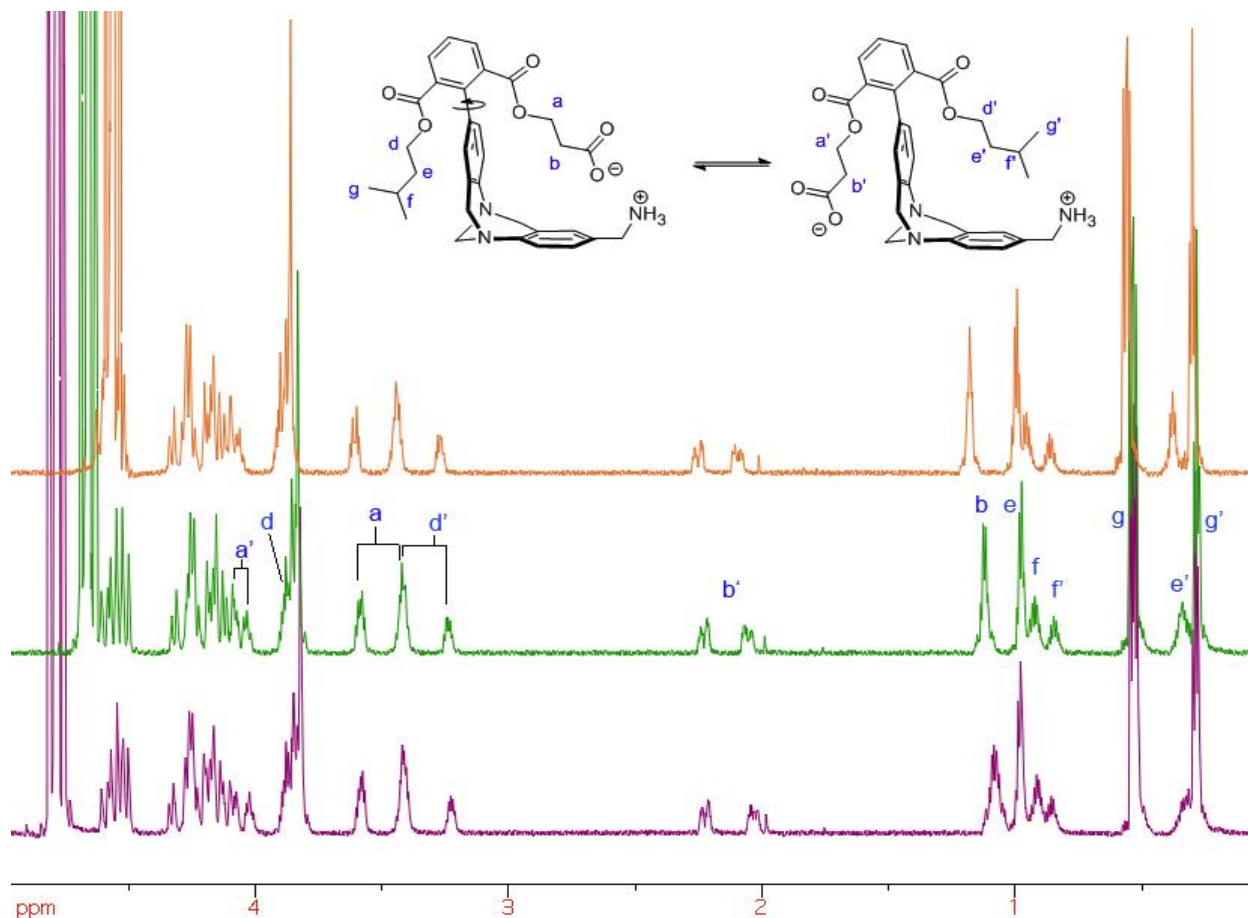


Figure 18. ^1H NMR spectra at 5 (purple), 15 (green), and 25 °C (orange) for 47c in D_2O .

The ^1H NMR spectra do not considerably change over a 20 °C range (Figure 18). The signal attributed to b moves slowly downfield from 1.1 to 1.2 ppm as the temperature increases, while the signal for e' separates from the triplet at 0.3 ppm (g'). The splitting patterns lose definition and broaden as the temperature rises (e.g. b), though the signals are still sharper than the halogen bond torsion balances described in Section 3.2.

The population of the folded to unfolded conformers were determined for temperatures 5 to 25 °C using dynamic NMR line shape fitting assisted with the program iNMR.⁸⁰ NMR spectra taken at 35 °C or above were too difficult to analyze due to significant signal broadening and poor signal to noise ratio.

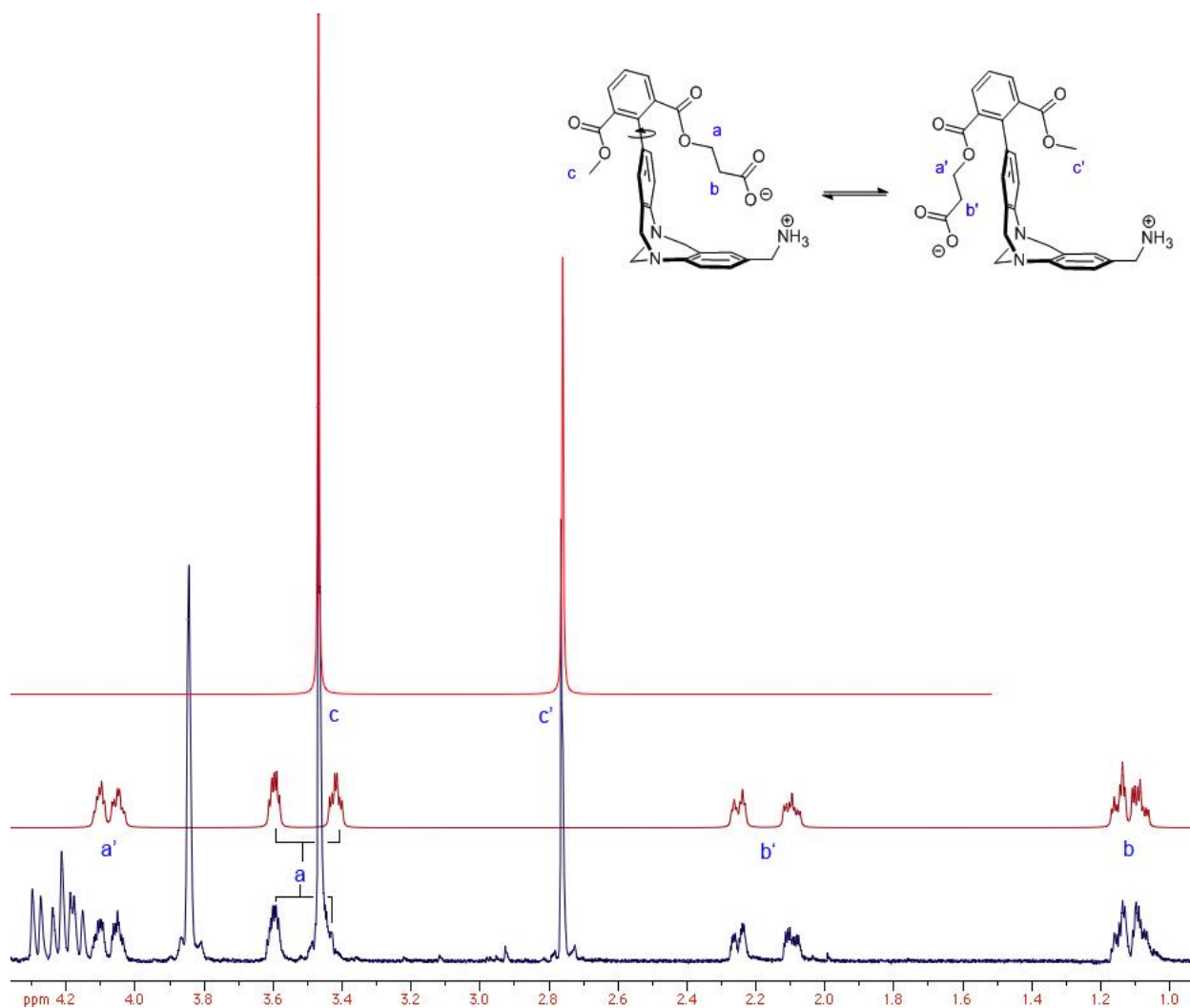


Figure 19. Simulations of the NMR signals of the carboxyethyl (middle spectrum) and methyl (top spectrum) esters of 47a at 5 °C (bottom spectrum).

Two sets of NMR simulations were conducted for **47a**, the methyl ester and the carboxyethyl ester. In Figure 19, the simulations of the methyl (top) and carboxyethyl groups (middle) are shown compared to the experimental spectrum (bottom). Differences between the simulated and experimental spectra for the methyl ester were sensitive to changes of as little as 1.5% to the folding population. Therefore, the error in amount of folded conformer is posited to be $\pm 1.5\%$. Error analysis is discussed further in Section 6.3. The splitting patterns and consequent folding ratios for the carboxyethyl ester portion of these molecules were difficult to

reliably replicate for the torsion balances (and not feasible for the isopentyl esters **47c**, **47d**, **48c**, and **48d** due to signal overlap). For balances **47a**, **47b**, **48a**, and **48b**, the folding ratios reported in Table 8 are derived from the line shape analysis of only the methyl ester signals (*c/c'*, Figure 19). For the isopentyl torsion balances, the terminal methyls of the isopentyls (*g/g'*) were used for the evaluation of folding with an accuracy equal to that of the methyl esters ($\pm 1.5\%$).

5.3 THE STRENGTH OF THE SALT BRIDGE INTERACTION

^1H NMR spectra of torsion balances **47a-d** and **48a-b** at 1 mM and **48c-d** at 0.5 mM concentrations in D_2O and in 50 mM buffer solutions of varying pD. Because few buffer mixtures can cover the entire pH or in this case pD range without exhibiting interfering ^1H NMR signals, several different buffers solutions were made. The buffers used at pD 3.1 and 5.5 were prepared from potassium deuterium phthalate, which displayed two signals in the aromatic region but did not interfere with our analysis. A phosphate buffer was used at pD 7.2, a borate buffer at pD 10.0, and two buffers were used at pD 12, carbonate and phosphate buffers. However, the torsion balances decomposed at pD 12 in both these buffers. Therefore, the pD 12 data are not included in Table 8 below.

The free energy of folding is defined by the following equations:

$$K_{\text{eq}} = \frac{k_1}{k_{-1}} = \frac{[\textit{folded}]}{[\textit{unfolded}]} \quad (\text{Equation 1})$$

$$\Delta G^\circ = -RT \ln K_{\text{eq}} \quad (\text{Equation 2})$$

in which *R* is the universal gas constant (1.9875 cal / K mol), *T* is the temperature in Kelvin, and K_{eq} represents the equilibrium constant or the ratio of the concentrations of the folded state to the

unfolded state. Line shape analysis was performed to obtain ratios of folded and unfolded states, which were used to calculate the experimental folding energies for torsion balances **47a-d** and **48a-d**. The results are shown in Table 8.

The preference for folding was strongest for **47** between pD of 5.5 and 10.0. This is supportive of a salt bridge interaction between the protonated amine and the deprotonated carboxylate for **47**. The range of folding energies varied within this pD range between -0.39 kcal/mol for **47a** at 5 °C and -0.66 kcal/mol for **47c** at 5 and 15 °C. Therefore, the strength of the ammonium-carboxylate interaction is considerable at -0.7 kcal/mol when exposed to solvent. We observed diminished folding at pD 3.1, which correlates to the protonation of the carboxylate and the “breaking” of the salt bridge interaction. The folding energies are still as stabilizing as -0.1 – -0.2 kcal/mol for torsion balances **47a-d** at the pD 3.1. This is indicative of the strength of residual electrostatic interactions that can still occur between a charged and a neutral group.¹⁴⁵

The folding energies of torsion balances **48a-d** vary between -0.39 to -0.59 kcal/mol in the pD range of 5.5 to 10.0, similar to the stabilization obtained for **47a-d**. Ester **48a-d** forms a salt bridge in the folded state between a guanidinium and a carboxylate, while **47a-d** forms one between ammonium and carboxylate. In proteins, ion pairs form more frequently with arginine as the positively charged residue than with lysine. This has been attributed to the ability of the guanidinium ion to bind in a variety of modes.¹¹¹ We found that a salt bridge between a carboxylate and a guanidinium group or an ammonium had similar strengths in the context of these torsion balances.

Table 8. Folding ratios and energies at varying pD.

	T	D2O		pD 3.1		pD 5.5		pD 7.2		pD 10.0	
		%F ^{a,b}	-ΔG ^{oc,d}	%F ^{a,b}	-ΔG ^{oc,d}	%F ^{a,b}	-ΔG ^{oc,d}	%F ^{a,b}	-ΔG ^{oc,d}	%F ^{a,b}	-ΔG ^{oc,d}
47a	5	57	0.16	56	0.13	67	0.39	69	0.43	68	0.43
	15	57	0.16	57	0.16	69	0.44	69	0.47	69	0.46
	25	57	0.16	56	0.15	70	0.49	71	0.54	70	0.50
47b	5	62	0.28	57	0.16	72	0.52	68	0.41	70	0.47
	15	61	0.24	57	0.17	69	0.45	69	0.45	71	0.52
	25	60	0.23	58	0.19	69	0.47	71	0.54	71	0.54
47c	5	63	0.28	58	0.19	77	0.66	75	0.60	74	0.57
	15	61	0.25	57	0.16	76	0.66	73	0.55	73	0.57
	25	59	0.21	56	0.15	73	0.59	73	0.59	72	0.54
47d	5	61	0.25	58	0.18	70	0.48	73	0.56	72	0.52
	15	61	0.26	58	0.17	71	0.52	73	0.56	73	0.56
	25	61	0.26	58	0.18	73	0.57	75	0.63	73	0.59
48a	5	60	0.22	59	0.20	67	0.39	68	0.42	70	0.46
	15	60	0.24	59	0.20	67	0.40	69	0.45	71	0.52
	25	61	0.26	59	0.22	67	0.41	70	0.50	71	0.52
48b	5	59	0.21	59	0.19	66	0.37	68	0.40	70	0.48
	15	61	0.25	59	0.20	66	0.39	68	0.44	70	0.48
	25	60	0.25	59	0.22	68	0.44	70	0.50	70	0.51
48c	5	61	0.24	55	0.11	67	0.39	67	0.40	68	0.41
	15	58	0.19	54	0.10	67	0.40	67	0.41	70	0.48
	25	58	0.18	53	0.07	66	0.39	72	0.57	73	0.59
48d	5	58	0.17	57	0.15	67	0.39	68	0.41	71	0.49
	15	61	0.26	55	0.11	69	0.46	70	0.47	74	0.59
	25	60	0.24	53	0.06	69	0.47	70	0.49	71	0.53

a) %F^a represents percent folded, which were determined from line shape analyses of the ¹H NMR spectra acquired on a 700 MHz NMR. b) ±1.5% error in folding ratios. c) ±15% error for the free energy. d) kcal/mol.

We used molecular modeling to evaluate the possible conformations of torsion balances **47b** and **48b**. The MMFF94s forcefield^{154,155} was applied in systematic conformational searches to locate the lowest energy conformations, shown below in Figures 20 and 21 respectively. The distances measured between the ammonium and the two oxygens of the carboxylate group of **47b** were 2.37 and 2.38 Å, indicative of a strong ionic pairing. The lowest energy conformer in Figure 21 for **48b** features a bidentate interaction with distances of 2.33 and 2.32 Å between the

two oxygens of the carboxylate and two nitrogens of the guanidinium. This indicates that the torsion balance is geometrically capable of forming a bidentate salt bridge.

The forcefield MMFF94s is parameterized for gas phase small organic molecules. As indicated by the modeling, the bidentate interaction is certainly possible, but we were curious as to how the mode of binding may be affected by solvation. To evaluate the effects of solvation on the guanidinium **48b**, energy minimization was applied to the lowest energy conformer shown in Figure 21, using the MMFF94s forcefield in conjunction with the generalized Born implicit solvent model and including several water molecules around the guanidinium and carboxylate functionalities (Figure 22). Water molecules are shown in light blue. The carboxylate group no longer forms a bidentate interaction with the guanidinium, instead approaching in a nearly perpendicular fashion from one side.

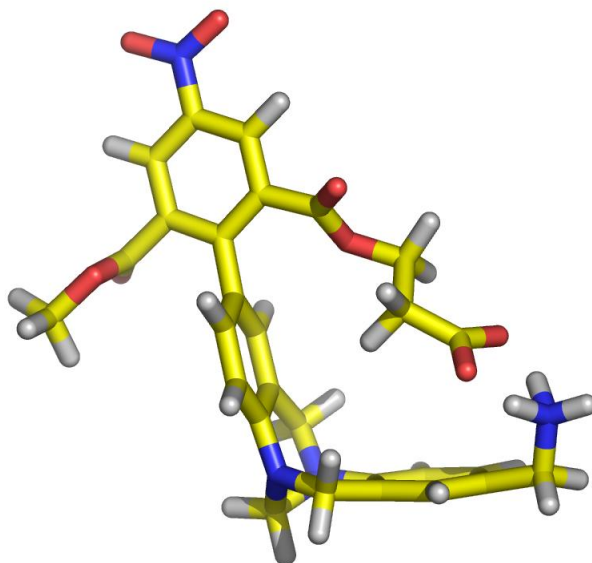


Figure 20. Lowest energy conformer for 47b.

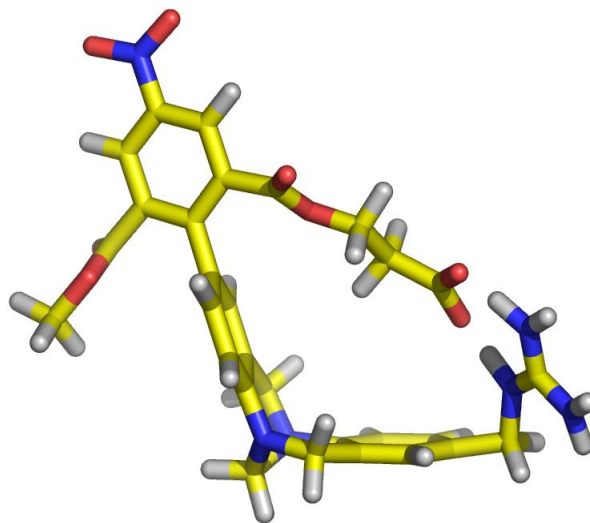


Figure 21. Lowest energy conformer for 48b.

While the distance between oxygen and nitrogen for **47b** were calculated to be as low as 2.3 Å, the distances measured for the conformer in Figure 22 were close to or slightly greater than the sum of the van der Waals radii of oxygen and nitrogen; the distances between the β -nitrogen and the two oxygens were 3.08 and 3.67 Å, and the distances between the δ -nitrogen and the carboxylate oxygens were 3.41 and 4.47 Å. Both the β - and δ -nitrogens of the guanidinium are relatively close to the carboxylate, but as a result of aqueous solvation, the salt bridge features longer distances between the carboxylate and the guanidinium ions.

The substituent at the *meta* position (R^2 , Scheme 7), whether proton or amine, makes no experimentally significant difference to the folding ratios of the torsion balances. This is consistent with the observations made in our studies of hydrophobic interactions,¹⁵⁶ in which substitution of a nitro, amine or glutaramide group did not affect folding energies, though interestingly, changes to the rates of rotation were seen.

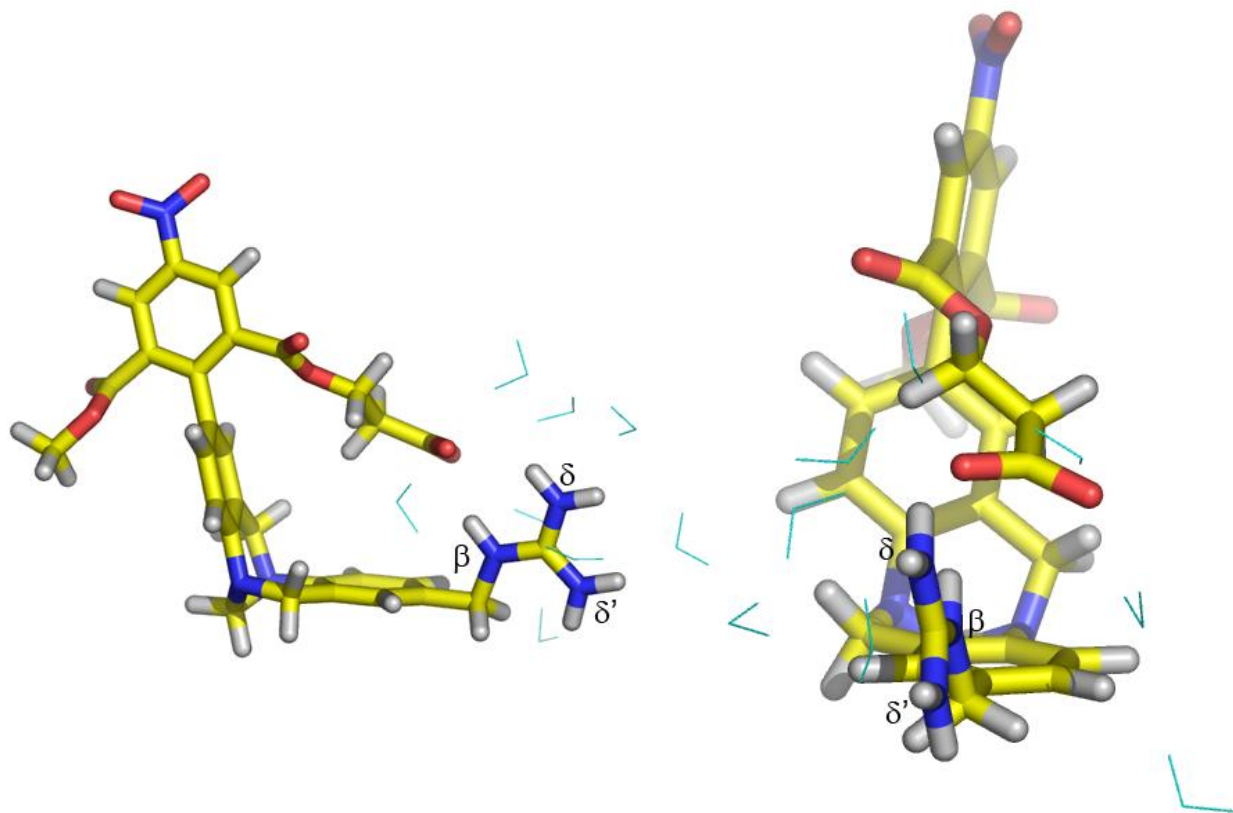


Figure 22. The lowest energy conformer of solvated 48b (front and side views)

Temperature has little effect on the folding energies of these torsion balances. The strength of the ion pair interaction remains constant over the 20 °C temperature range. Although the range is too small, other research groups have reached the same conclusion. The strength of salt bridges in hyperthermophilic protein Ssh10b were unchanged when the temperature was raised by 55 °C; Glu36/Lys68 was measured to be -1.4 kcal/mol and Glu54/Arg57 decreased slightly from -0.57 to -0.52 kcal/mol at 25 and 80 °C.¹³² Molecular dynamics also demonstrated the resilience of salt bridges at 25 and 100 °C.¹⁵⁷ Our data confirm that temperature does not adversely affect the strength of a salt bridge.

Most of the isopentyl esters are more prone to folding compared to their methyl analogs by approximately -0.1 kcal/mol. The difference between the folded and unfolded states for the chemical shift of the methine proton (f/f' , Figure 18) is minimal, suggesting that the isopentyl

group is not proximate to the dibenzodiazocine rings even when the isopentyl group is inside the cleft. Although, for the right size group, the hydrophobic effect will cause an alkyl group to remain inside,¹⁵⁶ steric effects discourage the isopentyl group from being inside the cleft.

To determine the degree to which the isopentyl group, which is similar in size to the carboxyethyl chain, affects folding, torsion balance **51** was synthesized. For convenience, we will refer to the convex side of the dibenzodiazocine as the *endo* position. In torsion balance **51**, the folded conformer in the following discussion is defined as the one in which the isopentyl group is *endo* to the cleft. The folding energies for **51** are shown in Table 9. The preference for the isopentyl group to stay outside the cleft of the dibenzodiazocine rings is about -0.06 kcal/mol. This small energetic difference explains the approximately 0.1 kcal/mol disparity between the methyl and isopentyl esters in Table 8 (**47**, **48**: **a** and **b** versus **c** and **d**). Although the isopentyl and carboxyethyl groups are isosteric, the energetic difference is due to the unfavorable fit of the isopentyl group in the *endo* position.

Table 9. Folding data for control 51.

	T	pD 3.1		pD 7.2		pD 10.0	
		%F ^{a,b}	-ΔG ^{oc,d}	%F ^{a,b}	-ΔG ^{oc,d}	%F ^{a,b}	-ΔG ^{oc,d}
51	5	48	-0.04	47	-0.06	46	-0.08
	15	48	-0.04	47	-0.06	49	-0.03
	25	49	-0.03	49	-0.03	49	-0.02

a) ‘%F’ represents percent folded, which were determined from line shape analyses of the ¹H NMR spectra acquired on a 700 MHz NMR. b) ±1.5% error in folding ratios. c) ±15% error for the free energy. d) kcal/mol.

5.4 THE EFFECTS OF IONIC STRENGTH ON SALT BRIDGE INTERACTIONS

The effect of ionic strength on the salt bridge interaction is under debate in the biophysics community. Salt bridges are electrostatic in nature. Theoretically, as the ionic strength of the

solution increases, the strength of the interaction should diminish.¹¹³ Experimental results however have led to contradictory conclusions. In human lysozyme, salt bridges with more than 50% exposure to solvent did not contribute to the stability of the protein in 0.2 M KCl,¹²⁵ and a loss of half or 0.57 kcal/mol in coupling energy between aspartic acid and arginine was measured in 0.5 M NaCl.¹³⁷ Meanwhile, in alanine-based model peptides with lysine or histidine interspersed with aspartic or glutamic acids at regular intervals^{139,140} salt bridges were only partially screened at salt concentrations up to 2.0 M, and the strength of salt bridges in haemoglobin (His HC3(146) β) were found to be independent from external salt concentrations in solution.¹⁴¹

Torsion balances **47a-b** were examined in phosphate buffers of two concentrations, 0.200 and 0.050 M. The phosphate buffers at pD 7.2 were composed of disodium hydrogen phosphate and sodium dihydrogen phosphate. The ionic strength, I , of a solution, which is the concentration of all the ions present in solution, is defined by the following equation:

$$I = \frac{1}{2} \sum_{i=1}^n c_i z_i^2 \quad (\text{Equation 3})$$

in which c_i is the molar concentration of ion i , and z_i is the charge number of ion i . According to equation 3, a 0.200 M phosphate buffer has an ionic strength of approximately 0.4 M, which a phosphate buffer of 0.050 M has an ionic strength of approximately 0.1 M.

The experimentally observed ¹H NMR spectra of torsion balances **47a** and **47b** were simulated using line shape analysis to determine the folding ratios and energies in the two phosphate buffers (Table 10). There is a small but experimentally significant difference in the folding energies between the two balances in 0.200 and 0.050 M buffers with a four-fold difference in ionic strengths.

Table 10. Ionic strength effect on folding energies.

	T	0.200 M phosphate		0.050 M phosphate		0.050 M + KCl	
		%F ^{a,b}	-ΔG ^{oc,d}	%F ^{a,b}	-ΔG ^{oc,d}	%F ^{a,b}	-ΔG ^{oc,d}
47a	5	70	0.48	74	0.58	72	0.53
	15	73	0.58	76	0.65	74	0.59
	25	72	0.56	75	0.64	71	0.54
47b	5	74	0.56	74	0.57	71	0.49
	15	75	0.62	78	0.71	74	0.59
	25	75	0.64	78	0.75	74	0.63

a) Percent folded was determined from line shape analyses of the ¹H NMR spectra acquired on a 700 MHz NMR. b) ±1.5% error in folding ratios. c) ±7% error for the free energy in this folding range (see Section 6.3). d) kcal/mol.

The 0.050 M phosphate buffer has an ionic strength of 0.1 M. The addition of potassium chloride to a concentration of 0.3 M in a 0.050 M phosphate buffer increases the ionic strength of the solution from 0.1 to 0.4 M. The torsion balances were studied in this adjusted solution to obtain their folding ratios (“0.050 M + KCl, Table 10). It is apparent from the data that ionic strength has a modest effect on the strength of the salt bridge interaction; the addition of 0.3 M potassium chloride to the 0.050 M phosphate buffers has an experimentally significant effect on the folding ratios.

Salt bridges are ion pairs, separated by short distances. The strength of the salt bridge is attributed partly to the hydrogen bond that forms between the two charged residues and partly to the Coulombic interaction. When salt bridges are immune to changes in ionic strength, this behavior has been justified by considering the salt bridge as more like a hydrogen bond than an electrostatic interaction.^{134,142} However, even clearly electrostatic interactions can still behave in this manner.^{139,143} There are multiple cases in which it appears that salt effects do not diminish salt bridges, but the results obtained from the torsion balances above suggest that the effects must be carefully considered on a case by case basis.

5.5 CONCLUSIONS

It is, for the most part, accepted that buried salt bridges stabilize the protein, but a significant number of these interactions occur on the surface or are partially solvent exposed. The biophysics community has not reached a consistent conclusion on whether or not these solvent exposed interactions are stabilizing. However, one limitation to the research conducted involves the use of proteins or peptides to determine the stabilization of the interaction. Quantification of the strength of one single interaction within this complex environment reduces the accuracy in the measurements and creates ambiguity in the interpretation of any observed effect. Our research sought to measure the energy of a salt bridge and its effect on folding by using a small molecule; the torsion balance is well-controlled, sensitive to weak interactions of less than 0.1 kcal/mol, and effectively reduces the number of interfering variables relative to a protein.

Surface or exposed salt bridges typically have maximum accessible contact surface areas (ASA) of 50% or greater, which compares the degree of solvation of residues in tertiary structures to that in the primary, unfolded state. An approximate ASA for the carboxyethyl group of **47a** was calculated to be 54%, indicating that the carboxyethyl group is to be considered exposed.

We found conclusively that the salt bridge was a stabilizing interaction when exposed to solvent. The stabilizing force varies between -0.3 to -0.5 kcal/mol for both the ammonium- and guanidinium-carboxylate interactions. This range is lower for the ammonium-carboxylate interaction compared here than reported results for solvent exposed ion pairs of proteins; an interaction between Asp23 and the N-terminus of ribosomal protein L9 gave coupling energies from -0.7 to -1.7 kcal/mol,¹³⁴ while the salt bridge between Glu36 and Lys68 was -1.4 kcal/mol

in hyperthermophilic protein Ssh10b.¹³² Measured salt bridge interactions between guanidinium and carboxylate groups were found to be considerably stronger in some proteins: the coupling energy of the salt bridge between Lys11 and Glu34 of ubiquitin was found to be -0.86 kcal/mol, using a double mutant cycle,¹³⁵ and in a cooperative network of two salt bridges between three residues, Asp8, Asp12, and Arg110, on the surface of barnase, the two salt bridges had coupling energies of -0.98 kcal/mol and -1.25 kcal/mol.¹³⁷ These latter values actually fall into our measured range when one salt bridge was removed from the network; strengths become -0.21 and -0.48 kcal/mol respectively. In future studies, it would be interesting to examine the effects of preorganization on salt bridge stability by restricting the number of positions and orientations that the ionic groups may occupy.

We found that the guanidinium and ammonium torsion balances gave similar folding energies, though this does not imply that the guanidinium-carboxylate interaction optimally is only as strong as the ammonium-carboxylate torsion balance. Molecular modeling using force field, MMFF94s, and a generalized Born solvation model suggest that water plays an integral role in increasing the distance between the guanidinium and carboxylate ions to form a pseudo-bidentate interaction.

Temperature seems negligible with regards to the strength of the salt bridge interaction. The temperature was varied within a 20 °C range, which is admittedly limited, and little difference was seen in the folding energies. Ionic strength was varied from 0.050 M to 0.200 M and this four-fold difference had a modest but experimentally significant effect on the strength of the salt bridge interaction in our torsion balances. A measurable change in the folding ratios also came from adjusting the pD of the buffer solutions. At pD 3.1 (and at 12 for the ammonium **47**), the folding ratios dropped from approximately 68% to no more than 59%, indicative of the

protonated state of the carboxylate and the breaking of the salt bridge interaction. The fact that the torsion balance still favors the folded state implies an interaction of some strength, approximately -0.2 kcal/mol, between the charged ammonium and the neutral carboxylic acid.

We found conclusively that a salt bridge is still a stabilizing force whether or not it is exposed to solvent. Solvent exposure has been shown to weaken the interaction, reducing the strength of the guanidinium-carboxylate to that measured for the ammonium-carboxylate interaction. The strength of the interaction was shown to be approximately -0.3 to -0.5 kcal/mol, independent of temperature and weakly dependent on ionic strength, and sensitive to pD changes.

6.0 EXPERIMENTAL

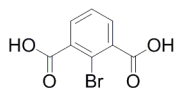
Melting points were determined using a Thomas Hoover capillary melting point apparatus and are uncorrected. Proton and carbon nuclear magnetic resonance spectra (^1H and ^{13}C NMR) were obtained using Bruker Avance 500 (halogen bonding torsion balances) and 700 MHz (salt bridge torsion balances) spectrometers. Chemical shifts are in parts per million (δ) using the residual solvent peak as the reference value. The values used for proton and carbon spectra, respectively, are 7.24 and 77.23 ppm for CDCl_3 , 3.34 and 49.17 ppm for MeOD, and 2.49 and 39.50 ppm for d_6 -DMSO. Abbreviations used in proton data are: s = singlet; d = doublet; t = triplet; q = quartet; dd = doublet of doublets; dt = doublet of triplets; m = multiplet. Also ^1H NMR chemical shifts are listed for all the possible conformations of a given molecule. For example, compound **45a** has protons with two possible environments due to different rotational isomers. Consequently these protons are exemplified as follows: 3.59/2.77. The ^1H NMR data of compounds **26a-c**, **27a-c**, **28a-d**, **29a-b**, **45a-d**, **47a-d**, and **48a-d** include the temperature at which the spectrum was taken. The ^{13}C NMR spectra were taken at room temperature unless otherwise indicated.

Thin layer chromatography (TLC) was performed on E. Merck 60F 254 (0.25 mm) analytical glass plates. The normal phase column chromatography was performed on SiliaFlash P60 silica gel (40-63 μm). Dry solvents were obtained by distilling the solvents from the appropriate drying agent under nitrogen atmosphere shortly before use. Dichloromethane

(CH₂Cl₂) was distilled from CaH₂, and diethyl ether and THF were distilled from sodium metal and benzophenone. Dry DMSO was purchased from Aldrich and used as supplied. References to “removal of volatile components under reduced pressure” refer to rotary evaporation of the sample at 25-65°C at a pressure of 18-25 mm Hg and then overnight under high vacuum (0.1 mm Hg) at room temperature. All percentage yields are for material of >95% purity as indicated by ¹H NMR spectra, unless stated otherwise.

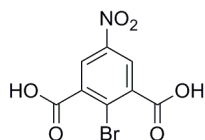
RP-HPLC purification was performed using a Hitachi HPLC system on a Jupiter 300 reverse phase column (C18, 300 Å, 250 × 21.2 mm, 10 μm) with a linear gradient of solvent polarity over the course of 20-30 minutes at a flow rate of 15 mL/min and detection at UV 220 nm. Solvents used for the HPLC elution were (A) H₂O containing 0.1% TFA and (B) acetonitrile containing 0.1% TFA. The solvent gradient is noted for each compound purified using RP-HPLC.

6.1 SYNTHESIS.

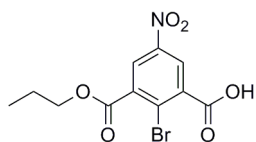


2-Bromoisophthalic acid (12): To a stirred solution of 100.3 g (0.63 mol) of potassium permanganate and 2.0 g (0.05 mol) of sodium hydroxide in 300 mL of water was added 25.0 g (0.135 mol) of 2-bromo-m-xylene. The reaction was refluxed for 24 hours, then cooled to room temperature and 40.0 g (0.38 mol) of NaHSO₃ were slowly added to the reaction. The mixture was filtered through a plug of Celite, which was then sonicated in 100 mL of water and filtered again. The combined filtrate was boiled to reduce the volume by 100 mL and then acidified with HCl (200 mL, 1 M). The solution was cooled slowly to room temperature over several hours and set aside for two days during which time solid precipitated.

Filtration afforded 18.57 g (56%) of the title compound as white crystals: ^1H NMR (CD_3OD , 300 MHz) δ 7.73 (d, 2H, $J = 7.6$ Hz), 7.48 (t, 1H, $J = 7.8$ Hz), 5.32 (s, 2H).¹⁵⁸



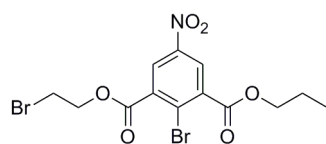
2-Bromo-5-nitroisophthalic acid (13): To a stirred solution of 0.56 mL of fuming nitric acid HNO_3 and 3.37 mL of fuming sulfuric acid at 0°C was added 0.50 g (2.04 mmol) of **12** portionwise over 10 minutes. The reaction was slowly warmed and stirred overnight. The solution was added dropwise to 20 mL of H_2O at 0°C , which was warmed to room temperature and extracted with EtOAc (4 x 20 mL). The organic extracts were washed with brine (20 mL), dried over MgSO_4 , and filtered, and volatile components of the filtrate were removed under reduced pressure to afford 0.5826 g (98%) of 2-bromo-5-nitroisophthalic acid as a white solid: IR (liquid) ν 3540-2500 (broad), 3084, 1717, 1349; ^1H NMR (MeOD-d_4 , 300 MHz) δ 8.55 (s, 2H); ^{13}C NMR (MeOD-d_4 , 300 MHz) δ 167.55, 166.52, 148.09, 139.22, 138.91, 127.29, 127.00, 126.22, 69.50, 23.09, 10.99; HRMS calculated for $\text{C}_8\text{H}_4\text{BrNO}_6$ 288.922198, found 288.921733.



2-Bromo-5-nitroisophthalic acid 1-propyl ester (14): To a stirred solution of 0.10 g (0.35 mmol) of 2-bromo-5-nitroisophthalic acid (**13**) in 3.4 mL of dimethyl sulfoxide was added 0.11 g (0.83 mmol) of potassium carbonate and then 0.03 mL (0.35 mmol) of 1-iodopropane. The mixture was stirred for six hours at 60°C temperature, after which the reaction mixture was treated with 20 mL of 1 M HCl and extracted with EtOAc (3 x 20 mL). The organic extracts were washed with brine (20 mL), dried over MgSO_4 , filtered and the volatile components of the filtrate were removed under reduced pressure. The residue was purified by column chromatography (hexanes: EtOAc, 1:1) to afford

0.84 g (73%) of the 2-bromo-5-nitroisophthalic acid monopropyl ester: IR (thin film) ν 3700-2400 (broad), 3089, 2971, 1711, 1347, 1292, 1242, 1148; ^1H NMR (MeOD, 700 MHz) δ 8.59 (d, 1H, $J = 2.8$ Hz), 8.52 (d, 1H, $J = 2.8$ Hz), 4.39 (t, 2H, $J = 6.3$ Hz), 1.85 (t, 2H, $J = 7$ Hz), 1.08 (t, 3H, $J = 7.7$ Hz); ^{13}C NMR (MeOD, 700 MHz) δ 166.02, 164.99, 146.56, 137.68, 137.38, 125.76, 125.47, 124.69, 67.08, 21.55, 9.46; HRMS calculated for $\text{C}_{11}\text{H}_{10}\text{BrNO}_6$ 330.969148, found 330.969002.

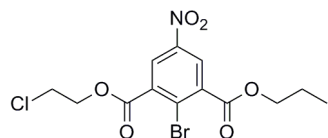
General Esterification Procedure: To a stirred solution of the alcohol in dry CH_2Cl_2 at 0°C was added 1,3-dicyclohexylcarbodiimide (DCC) and 4-dimethylaminopyridine (DMAP) in CH_2Cl_2 . After ten minutes, the carboxylic acid **13** was added in four portions over eight minutes. The reaction mixture was warmed to room temperature and then stirred for four hours. The precipitated urea was removed by filtration and washed with CH_2Cl_2 . Volatile components of the filtrate were removed under reduced pressure, and the residue was purified by column chromatography (hexanes, EtOAc, 20:1).



2-Bromo-5-nitroisophthalic acid 1-(2'-bromoethyl) ester 3-propyl

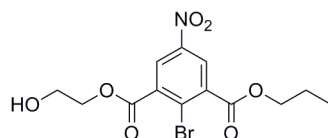
ester (15a): By the general esterification procedure, 0.12 mL (1.75 mmol) of 2-bromoethanol, 0.24 g (1.17 mmol) of DCC and 0.02 g (0.15 mmol) of DMAP in 3.0 mL of dry CH_2Cl_2 , treated with 0.19 g (0.58 mmol) of **13**, provided 0.19 g (74%) of the title compound as an oil: IR (thin film) ν 3083, 2968, 1739, 1535, 1232; ^1H NMR (CDCl_3 , 300 MHz) δ 8.52 (dd, 2H, $J = 15.6$ and 2.7 Hz), 4.68 (t, 2H, $J = 6.0$ Hz), 4.33 (t, 2H, $J = 6.9$ Hz), 3.64 (t, 2H, $J = 6$ Hz), 1.77 (sextet, 2H, $J = 6.9$ Hz), 0.989; ^{13}C NMR (CDCl_3 , 300 MHz) δ 164.58,

164.08, 146.39, 137.49, 136.14, 126.85, 126.78, 126.76, 68.64, 65.84, 28.11, 22.01, 10.64;
HRMS calculated for formula $C_{13}H_{13}BrNO_6$ 436.910960, found 436.910006.



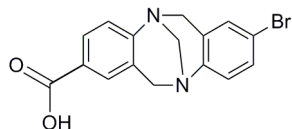
2-Bromo-5-nitroisophthalic acid 1-(2'-chloroethyl) ester 3-propyl

ester (15b): By the general esterification procedure, 0.06 mL (0.90 mmol) of 2-chloroethanol, 0.12 g (0.90 mmol) of DCC and 0.01 g (0.08 mmol) of DMAP in 1.5 mL of dry CH_2Cl_2 , treated with 0.10 (0.30 mmol) of **13**, provided 0.08 g (68%) of the title compound as an oil: IR (thin film) ν 3085, 2966, 2926, 1738, 1536, 1232, 1184; 1H NMR ($CDCl_3$, 300 MHz) δ 8.513 (dd, 2H, $J = 2.7$ and 12.0 Hz), 4.625 (t, 2H, $J = 5.4$ Hz), 4.332 (t, 2H, $J = 6.6$ Hz), 3.813 (t, 2H, $J = 5.7$ Hz), 1.789 (sextet, 2H, $J = 7.2$ Hz), 0.989 (t, 3H, 3.6 Hz); ^{13}C NMR ($CDCl_3$, 300 MHz) δ 164.71, 164.21, 146.39, 137.49, 136.17, 126.84, 126.74, 68.64, 66.1, 41.27, 22, 10.63; HRMS calculated for $C_{13}H_{13}BrClNO_6$ 392.961476, found 392.961003.



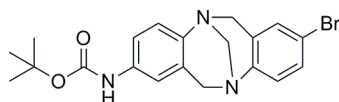
2-Bromo-5-nitroisophthalic acid 1-(2'-hydroxyethyl) ester 3-

propyl ester (15c): By the general esterification procedure, 0.10 mL (1.81 mmol) of ethylene glycol, 0.37 g (1.81 mmol) of DCC and 0.02 g (0.15 mmol) of DMAP in 3.0 mL of dry CH_2Cl_2 , treated with 0.20 g (0.60 mmol) of **13**, provided 0.11 g (49%) of the title compound as an oil: IR (thin film) ν 3431 (broad), 3085, 2967, 1738, 1536, 1351, 1238; 1H NMR ($CDCl_3$, 300 MHz) δ 8.517 (dd, 2H, $J = 2.7$ and 8.4 Hz), 4.518 (t, 2H, $J = 4.8$ Hz), 4.347 (t, 2H, $J = 6.6$ Hz) 3.970 (t, 2H, $J = 4.8$ Hz), 1.803 (sextet, 2H, $J = 6.9$ Hz), 1.018 (t, 3H, $J = 7.5$ Hz); ^{13}C NMR ($CDCl_3$, 300 MHz) δ 164.69, 164.57, 146.23, 137.16, 136.61, 126.53, 126.45, 126.37, 68.49, 68.02, 60.67, 21.83, 10.45; HRMS calculated for $C_{13}H_{14}BrNO_7$ 374.995363, found 374.994979.



2-Bromo-8-carboxy-6H,12H-5,11-methanodibenzo[*b,f*][1,5]

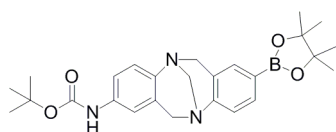
diazocine (17): To a stirred solution of 1.50 g (4.0 mmol) of 2,8-dibromo-6H,12H-5,11-methanodibenzo[*b,f*][1,5]diazocine (**16**) in 44 mL of dry THF:ether (8:3) at -78°C was added n-butyllithium (2.7 mL, 1.6 M in THF, 4.3 mmol) over two minutes. The solution was stirred for five minutes at -78°C and then carbon dioxide was bubbled through the reaction. The pink heterogeneous mixture was slowly warmed to room temperature over an hour, after which the volatile components were removed under reduced pressure. The residue was dissolved completely in methanol (10 mL) and then diluted with 50 mL of 1M HCl. The solution was extracted with EtOAc (5 x 50 mL), which in turn was washed with brine (100 mL). The organic extracts were dried over MgSO_4 , filtered, and volatile components of the filtrate were removed under reduced pressure. The residue was purified by column chromatography (hexanes: EtOAc, 2:1) to afford 0.84 g (61%) of the carboxylic acid as a pale yellow foam: ^1H NMR (MeOH- d_4 , 300 MHz) δ 7.90-7.95 (m, 1H), 7.78-7.79 (m, 1H), 7.34-7.51 (m, 4H), 4.81-5.05 (m, 4H), 4.43-4.55 (m, 2H).⁶⁹



2-Bromo-8-(*tert*-butoxycarbonylamino)-6H,12H-5,11-

methanodibenzo[*b,f*][1,5]diazocine (18): To a stirred solution of 1.24 g (3.6 mmol) of the carboxylic acid (**17**) and 0.75 mL (5.4 mmol) of triethylamine in 36 mL of *t*-butanol was added 1.2 mL (5.4 mmol) of diphenyl phosphoryl azide dropwise. The solution was refluxed for 24 hours, cooled to room temperature, and then diluted with 50 mL of EtOAc. The resulting mixture was washed successively with 25 mL of the following: 5% citric acid, water, saturated NaHCO_3 , and brine. The organic extract was dried over MgSO_4 , filtered, and volatile components of the filtrate were removed under reduced pressure. The residue was

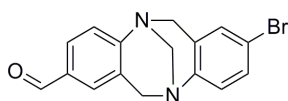
purified by column chromatography (hexanes: EtOAc, 4:1) to afford 0.87 g (58%) of the carbamate as a white foam: IR (thin film) ν 3307, 1718, 1529, 1496, 1477, 1160; ^1H NMR (CDCl_3 , 300 MHz) δ 6.96-7.22 (m, 6H), 6.33 (s, 1H), 4.61 (dd, 2H, $J = 7.5$ and 16.5 Hz), 4.25 (d, 2H, $J = 4.8$ Hz), 4.07 (dd, 2H, $J = 7.2$ and 16.8 Hz), 1.45 (s, 9H); ^{13}C NMR (CDCl_3 , 300 MHz) δ 153.1, 147.2, 142.9, 134.8, 130.7, 130.1, 129.9, 128.3, 126.9, 125.5, 118.7, 117.0, 116.8, 80.8, 67.1, 59.0, 58.5, 28.5; HRMS calculated for $\text{C}_{20}\text{H}_{22}^{79}\text{BrN}_3\text{O}_2$ 415.0895, found 415.0894.



2-(4,4,5,5-Tetramethyl-[1,3,2]dioxaborolan-2-yl)-8-(tert-butoxycarbonylamino)-6H,12H-5,11-methanodibenzo[*b,f*]

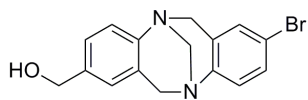
[1,5]diazocine (19): The carbamate (**18**) (0.25 g, 0.6 mmol), bis(pinacolato)diboron (0.31 g, 1.2 mmol), dichlorobis[methylene-bis(diphenylphosphine)]-dipalladium-dichloromethane adduct (9.0 mg, 0.009 mmol), and potassium acetate (0.08 g, 0.8 mmol) were combined in a flask, which was placed under vacuum for five to ten minutes and then filled with N_2 . Addition of 3.6 mL of anhydrous DMSO to this mixture provided an orange solution which was degassed twice by freeze pump thaw cycle and then heated at 80°C for 12 hours. The reaction was cooled to room temperature, diluted with 50 mL of CH_2Cl_2 , and the resultant mixture was washed with water (3 x 50 mL). The combined aqueous layers were extracted with CH_2Cl_2 (2 x 50 mL). The organic extracts were dried over MgSO_4 , filtered and the volatile components of the filtrate were removed under reduced pressure. The residue was purified by column chromatography (hexanes: EtOAc, 3:1) to afford 0.22 g (77%) of the title compound as a white foam: IR (thin film) ν 3327, 2977, 1723, 1609, 1361, 1160; ^1H NMR (CDCl_3 , 300 MHz) δ 7.57 (d, 1H, $J = 13.5$ Hz), 7.36 (s, 1H), 7.09 (d, 2H, $J = 13.5$ Hz), 7.01 (s, 1H), 6.95 (t, 1H, $J = 4.0$ Hz), 6.30 (s, 1H), 4.67 (s, 1H), 4.62 (s, 1H), 4.29 (s, 2H), 4.14 (t, 2H, $J = 27.5$ Hz), 1.45 (s, 9H), 1.27 (s, 12H); ^{13}C NMR

(CDCl₃, 300 MHz) δ 153.04, 151.17, 143.07, 134.53, 133.94, 130.62, 128.54, 127.17, 126.93, 125.52, 124.50, 118.55, 116.97, 83.88, 67.17, 66.06, 59.07, 58.75, 28.50, 24.99, 15.48; HRMS calculated for C₂₆H₃₄¹¹BN₃O₄ 463.2642, found 463.2658.



2-Bromo-8-formyl-6H,12H-5,11-methanodibenzo[*b,f*] [1,5]diazocine

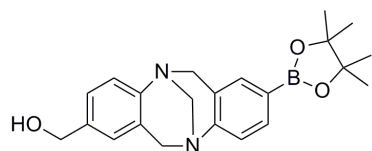
(20): To a stirred solution of 1.50 g (3.9 mmol) of 2,8- dibromo-6H,12H-5,11-methanodibenzo[*b,f*][1,5]diazocine (**16**) in 43 mL of dry THF:ether (8:3) at -78°C was added n-butyllithium (2.7 mL, 1.6 M in THF, 4.3 mmol) over two minutes. The solution was stirred for five minutes at -78°C , and dimethylformamide (mL, mmol) was added to the reaction. The heterogeneous mixture was slowly warmed to room temperature over an hour, after which 20 mL of H₂O was added to quench the reaction. The solution was extracted with EtOAc (3 x 30 mL), which in turn was washed with brine (100 mL). The organic extracts were dried over MgSO₄, filtered, and volatile components of the filtrate were removed under reduced pressure. The residue was purified by column chromatography (hexanes: EtOAc, 5:1) to afford 0.94 g (72%) of the aldehyde as a pale yellow foam: ¹H NMR (CDCl₃, 300 MHz) δ 9.82 (s, 1H), 7.67 (d, 1H, J = 6.0 Hz), 7.45 (s, 1H), 7.22-7.28 (m, 2H), 7.02 (t, 2H, J = 8.4 Hz), 4.70 (dd, 2H, J = 6.9 and 16.5 Hz), 4.28 (s, 2H), 4.19 (dd, 2H, J = 4.8 and 17.1 Hz).⁶⁹



2-Bromo-8-hydroxymethyl-6H,12H-5,11-methanodibenzo

[*b,f*][1,5]diazocine (21): To a stirred solution of 0.50 g (1.52 mmol) of the aldehyde (**20**) in 8.9 mL of methanol at 0 °C was added 0.07 g (1.84 mmol) of sodium borohydride. The heterogeneous solution was slowly warmed to room temperature over 10 minutes, stirred for an additional hour, and then diluted with 25 mL of H₂O. The resulting

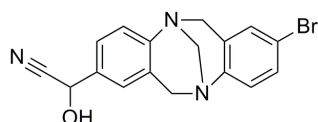
solution was extracted with EtOAc (4 x 25 mL). The organic extracts were dried over MgSO₄, filtered, and volatile components of the filtrate were removed under reduced pressure. The residue was purified by column chromatography (hexanes: EtOAc, 1:1) to afford 0.45 g (89%) of the Tröger's base analog as a white foam: IR (thin film) ν 3317 (broad), 2902, 2851, 1494, 1476, 1206, 833; ¹H NMR (CDCl₃, 300 MHz) δ 6.906 – 7.240 (m, 6H), 4.642 (dd, 2H, J = 9.3 and 16.8 Hz), 4.542 (d, 2H, J = 4.5 Hz), 4.255 (s, 2H), 4.105 (d, 2H, J = 17.1 Hz); ¹³C NMR (CDCl₃, 300 MHz) δ 147.33, 147.22, 137.01, 130.67, 130.12, 129.91, 127.78, 126.95, 126.72, 125.91, 125.35, 116.82, 66.94, 65.13, 58.90, 58.56; HRMS calculated for C₁₆H₁₆BrN₂O 331.0446, found 331.0435.



2-Hydroxymethyl-8-(4,4,5,5-tetramethyl-[1,3,2] dioxaborolan-2-yl)-6H,12H-5,11-methanodibenzo[*b,f*][1,5] diazocine (22):

The alcohol (**21**) (0.54 g, 1.6 mmol), bis(pinacolato)diboron (0.50 g, 2.0 mmol), dichlorobis[methylene-bis(diphenylphosphine)]-dipalladium-dichloromethane adduct (25 mg, 0.02 mmol), and potassium acetate (0.23 g, 2.3 mmol) were combined in a flask, which was placed under vacuum for five to ten minutes and then filled with N₂. Addition of 9.9 mL of anhydrous DMSO to this mixture provided an orange solution which was degassed twice by freeze pump thaw cycle and then heated at 80°C for 16 hours. The reaction was cooled to room temperature, diluted with 50 mL of CH₂Cl₂, and the resultant mixture was washed with water (3 x 50 mL). The combined aqueous layers were extracted with CH₂Cl₂ (2 x 50 mL). The organic extracts were dried over MgSO₄, filtered and the volatile components of the filtrate were removed under reduced pressure. The residue was purified by column chromatography (pentane: Et₂O, 1:1) to afford 0.59 g (95%) of the title compound as a white foam: IR (thin film) ν 3392

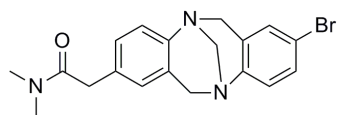
(broad), 2977, 1609, 1360, 1145; ^1H NMR (CDCl_3 , 300 MHz) δ 7.57 (d, 1H, $J = 7.8$ Hz), 7.35 (s, 1H), 7.00-7.09 (m, 3H), 6.80 (s, 1H), 4.58 (dd, 2H, $J = 5.7$ and 16.8 Hz), 4.46 (s, 2H), 4.20 (s, 2H), 4.10 (d, 2H, $J = 16.8$ Hz), 1.26 (s, 12H); ^{13}C NMR (CDCl_3 , 300 MHz) δ 151.01, 147.23, 136.94, 134.09, 133.90, 127.84, 127.14, 126.52, 125.78, 125.20, 124.45, 83.86, 66.86, 64.93, 58.81, 58.68, 24.93; HRMS calculated for $\text{C}_{22}\text{H}_{27}^{11}\text{BN}_2\text{O}_3$ 378.211473, found 378.21158.



2-Bromo-8-(cyano(hydroxy)methyl)-6H,12H-5,11-

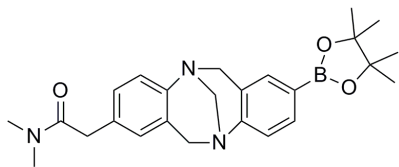
methanodibenzo [b,f][1,5]diazocine (23): To a stirred solution of

0.54 g (1.63 mmol) of the aldehyde (**20**) in 16.3 mL of dry CH_2Cl_2 was added 0.4 mL of trimethylsilyl cyanide (3.25 mmol) and then 0.18 g (0.81 mmol) of zinc bromide. The reaction was stirred for 45 minutes, after which the volatile components were removed under reduced pressure. To a solution of the residue in 12 mL of acetonitrile was then added 3 mL of 3M aqueous HCl. The solution was then diluted with 10 mL of H_2O and was extracted with CH_2Cl_2 (3 x 25 mL). The organic extracts were dried over MgSO_4 , filtered, and volatile components of the filtrate were removed under reduced pressure. The crude was taken directly to the next step residue to afford 0.36 g (82%) of the cyanohydrin as a white foam: IR (thin film) ν 3110, 2951, 2905, 1493, 1477, 1208, 837; ^1H NMR (CDCl_3 , 300 MHz) δ 7.25-7.31 (m, 2H), 7.12 (dd, 1H, $J = 3.6$ and 8.4 Hz), 7.01 (dd, 3H, $J = 8.7$ and 16.2 Hz), 5.38 (d, 1H, $J = 2.4$ Hz), 4.61 (dd, 2H, $J = 5.7$ and 16.8 Hz), 4.20 (s, 2H), 4.09 (d, 2H, $J = 17.1$ Hz); ^{13}C NMR (CDCl_3 , 300 MHz) δ 149.21, 146.69, 131.44, 130.94, 129.92, 129.68, 128.61, 126.95, 126.27, 125.77, 125.65, 118.93, 117.15, 66.69, 63.42, 58.63, 58.50; HRMS calculated for $\text{C}_{17}\text{H}_{15}\text{BrN}_3\text{O}$ 356.0398, found 356.0402.



2-Bromo-8-(2-(dimethylamino)-2-oxoethyl)-6H,12H-5,11-methanodibenzo[*b,f*] [1,5]diazocine (24): *Step 1 – Oxidation:* To

a solution of the cyanohydrin (0.68 g, 1.90 mmol) in 10.9 mL of hydroiodic acid was added red phosphorus (0.71 g, 22.78 mmol). The solution was heated to 80 °C for 6 hours and then cooled to room temperature, after which the phosphorus was removed by filtration. The filtrate was treated with 1 M NaHSO₃ (20 mL) and was extracted with EtOAc (3 x 30 mL). The organic extracts were washed with brine (40 mL), dried over MgSO₄, and the volatile components were removed under reduced pressure. The crude was taken directly to the next step. *Step 2 – Amidation:* To a stirred solution of dimethyl amine hydrochloride (0.11 g, 1.30 mmol) in 2.2 mL dry CH₂Cl₂ at 0°C was added 0.18 g (0.87 mmol) DCC and 0.01 g (0.11 mmol) of DMAP and then 0.12 mL (0.87 mmol) of triethylamine. After ten minutes, the crude carboxylic acid was added in four portions over eight minutes. The reaction mixture was warmed to room temperature and then stirred for five hours. The precipitated urea was removed by filtration and washed with CH₂Cl₂. Volatile components of the filtrate were removed under reduced pressure, and the residue was purified by column chromatography (EtOAc) to afford 0.15 g (58%) of the amide: IR (thin film) ν 2923, 2852, 1641, 1475, 1207; ¹H NMR (CDCl₃, 700 MHz) δ 7.24 (s, 1H), 7.02-7.05 (m, 3H), 6.98 (d, 1H, J = 8.4 Hz), 6.80 (s, 1H), 4.62 (t, 2H, J = 16.1 Hz), 4.24 (dq, 2H, J = 1.4 and 11.2 Hz), 4.09 (dd, 2H, J = 17.5 and 20.3 Hz), 3.55 (d, 2H, J = 2.1 Hz), 2.97 (s, 3H), 3.92 (s, 3H); ¹³C NMR (CDCl₃, 700 MHz) δ 171.00, 147.21, 146.34, 130.89, 130.41, 130.08, 129.72, 128.22, 127.67, 127.17, 126.84, 125.19, 116.51, 66.72, 58.61, 58.28, 40.13, 37.76, 35.65; HRMS calculated for C₁₉H₂₀BrNaN₃O 408.0687, found 408.0702;

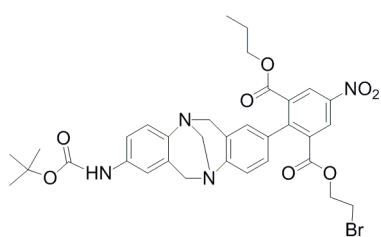


2-(2-(Dimethylamino)-2-oxoethyl)-8-(4,4,5,5-tetramethyl-[1,3,2]dioxaborolan-2-yl)-6H,12H-5,11-methanodibenzo[b,f][1,5]diazocine (25): The amide (0.06 g, 0.15 mmol),

bis(pinacolato)diboron (0.05 g, 0.19 mmol), dichlorobis[methylene-bis(diphenylphosphine)]-dipalladium-dichloromethane adduct (2 mg, 0.0002 mmol), and potassium acetate (0.02 g, 0.21 mmol) were combined in a flask, which was placed under vacuum for five to ten minutes and then filled with N₂. Addition of 0.9 mL of anhydrous DMSO to this mixture provided an orange solution which was degassed twice by freeze pump thaw cycle and then heated at 80°C for 16 hours. The reaction was cooled to room temperature, diluted with 10 mL of CH₂Cl₂, and the resultant mixture was washed with water (3 x 10 mL). The combined aqueous layers were extracted with CH₂Cl₂ (2 x 10 mL). The organic extracts were washed with brine (20 mL), dried over MgSO₄, filtered and the volatile components of the filtrate were removed under reduced pressure. The residue was purified by column chromatography (pentane: Et₂O, 1:4) to afford 0.05 g (75%) of title product as a white foam: IR (thin film) ν 2975, 2928, 1643, 1360, 1145; ¹H NMR (CDCl₃, 700 MHz) δ 7.57 (d, 1H, J = 7.7 Hz), 7.36 (s, 1H), 7.00-7.10 (m, 3H), 6.77 (s, 1H), 4.65 (d, 2H, J = 16.8 Hz), 4.27 (s, 2H), 4.14 (dd, 2H, J = 3.5 and 16.8 Hz), 3.53 (s, 2H), 2.94 (s, 3H), 2.90 (s, 3H), 1.27 (s, 12H); ¹³C NMR (CDCl₃, 700 MHz) δ 171.07, 151.17, 146.53, 133.91, 133.67, 130.58, 127.98, 127.97, 127.21, 127.05, 125.21, 124.43, 83.72, 66.80, 58.65, 58.51, 40.26, 37.79, 35.63, 24.82; HRMS calculated for C₂₅H₃₂B²³NaN₃O₃ 456.2434, found 456.2426.

General Suzuki Coupling Procedure: The isophthalate (**15a**, **15b**, or **15c**), dibenzodiazocine pinacolatoboronate (**19**, **22**, or **25**), and chloro(di-2-norbornylphosphino)(2'-dimethylamino-1,1'-

biphenyl-2-yl)palladium (II) were combined in a pressure reaction tube, which was placed under vacuum for five to ten minutes and then filled with N₂. The solids were dissolved in 1,2-dimethoxyethane (DME), and the solution was degassed twice by freeze pump thaw cycle. First water and then solid sodium bicarbonate were added to the pressure tube, and the contents were degassed two more times. The reaction was heated to 80°C for approximately 16 hours, cooled to room temperature, diluted with less than 1 mL of water. The subsequent mixture was extracted with CH₂Cl₂ or EtOAc (3 x 10-15 mL), the organic extracts were dried over MgSO₄, filtered and volatile components of the filtrate were removed under reduced pressure. The residue was purified by column chromatography and then by HPLC.

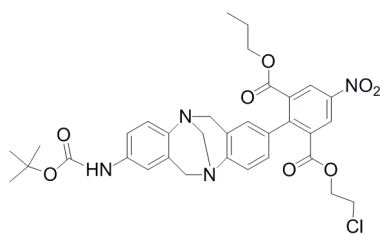


(2''-Bromoethyl) propyl 4'-nitro-2-phenyl-8-(tert-butoxy-carbonylamino)-6H,12H-5,11-methanodibenzo[b,f]

[1,5]diazocine-3',6'-dicarboxylate (26a): By the general Suzuki coupling procedure, 0.10 g (0.23 mmol) of isophthalate

15a, 0.12 g (0.25 mmol) of the pinacolatoboronate **19**, and 13.0 mg (0.023 mmol) of the palladium catalyst in 1.13 mL of DME were treated with 1.13 mL of water and 0.12 g (1.37 mmol) of sodium bicarbonate and purified by column chromatography (pentane: diethyl ether: CH₂Cl₂, 1:1:0.002) to provide 0.069 g (44%) of the title compound: IR (thin film) ν 3367, 2969, 1723, 1531, 1159; ¹H NMR (CDCl₃, 500 MHz, 25 °C) δ 8.63 (d, 2H, J = 11.5 Hz), 6.95-7.14 (m, 5H), 6.75 (s, 1H), 6.38 (s, 1H), 4.67 (d, 1H, J = 17.0 Hz), 4.63 (d, 1H, J = 17.0 Hz), 4.29 (s, 2H), 4.16 (d, 1H, J = 16.5 Hz), 4.11 (d, 1H, J = 17.5 Hz), 4.37/3.82 {s/d, (0.7/0.6+0.6) H, J = 68.0 Hz}, 4.03/3.53 {s/d, (1.2/0.4+0.4) H, J = 82 Hz}, 3.26/2.40 {d/d, (0.4+0.4/0.5+0.5) H, J = 39.5 and 16.5 Hz}, 1.46 (s, 12H), signal obscured at ~1.45/0.72 (s/s, {signal obscured/0.9) H}

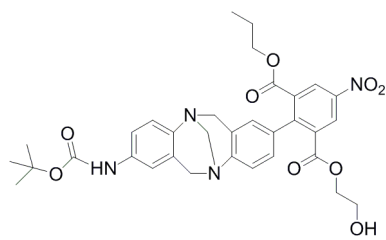
0.78/0.27 (s/s, (1.5/1.1) H); ^{13}C NMR (CDCl_3 , 500 MHz) δ 166.22, 166.13, 153.06, 152.86, 148.71, 148.65, 146.62, 146.46, 143.03, 134.68, 133.11, 133.00, 128.21, 127.78, 127.50, 126.74, 126.57, 125.70, 125.55, 124.85, 123.13, 118.87, 117.14, 116.58, 80.77, 67.93, 67.37, 65.25, 59.32, 58.87, 34.41, 30.51, 29.88, 28.49, 27.59, 21.82, 10.47; HRMS calculated for $\text{C}_{33}\text{H}_{35}\text{BrN}_4\text{O}_8$ 694.163826, found 694.162873.



(2''-Chloroethyl) propyl 4'-nitro-2-phenyl-8-(tert-butoxycarbonylamino)-6H,12H-5,11-methanodibenzo[b,f]

[1,5]diazocine-3',6'-dicarboxylate (26b): By the general Suzuki coupling procedure, 0.11 g (0.27 mmol) of isophthalate **15b**, 0.14

g (0.30 mmol) of the pinacolatoboronate **19**, and 15.0 mg (0.027 mmol) of the palladium catalyst in 1.4 mL of DME were treated with 1.4 mL of water and 0.14 g (1.64 mmol) of sodium bicarbonate and purified by column chromatography (pentane: diethyl ether: CH_2Cl_2 , 1:1:0.002) to provide 0.081 g (44%) of the title compound: IR (thin film) ν 3367, 2970, 1723, 1531, 1158; ^1H NMR (CDCl_3 , 500 MHz, 25 °C) δ 8.62 (d, 2H, $J = 28.0$ Hz), 6.95-7.13 (m, 5H), 6.75 (d, 1H, $J = 1.5$ Hz), 6.38 (s, 1H), 4.67 (d, 1H, $J = 17.0$ Hz), 4.63 (d, 1H, $J = 16.5$ Hz), 4.32/3.73 {s/d, (0.8/0.6+0.6) H, $J = 76.5$ Hz}, 4.29 (s, 2H), 4.15 (d, 1H, $J = 17.0$ Hz), 4.03/3.51 {s/d, (1.3/0.4+0.4) H, $J = \text{Hz}$ }, 4.10 (d, 1H, $J = 16.0$ Hz), 3.40/2.54 {s/d, (0.9/0.5+0.5) H, $J = 19.5$ Hz}, 1.45 (s, 12H), signal obscured at ~ 1.45 ppm/0.72 {signal obscured/s, (signal obscured/0.9)H}, 0.78/0.26 {s/s, (1.8/1.1) H}; ^{13}C NMR (CDCl_3 , 500 MHz) δ 153.04, 152.97, 148.77, 148.59, 146.62, 146.47, 143.04, 135.97, 134.66, 133.13, 128.26, 127.46, 126.73, 126.56, 125.70, 125.54, 124.82, 118.37, 117.09, 80.76, 67.94, 67.38, 65.36, 59.38, 58.90, 40.54, 34.41, 30.51, 28.48, 21.82, 21.37, 10.48; HRMS calculated for $\text{C}_{33}\text{H}_{35}\text{N}_4\text{O}_8\text{Cl}$ 650.214342, found 650.212944.

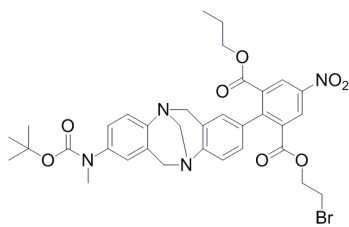


(2''-Hydroxyethyl) propyl 4'-nitro-2-phenyl-8-(tert-butoxycarbonylamino)-6H,12H-5,11-methanodibenzo[*b,f*]

[1,5]diazocine-3',6'-dicarboxylate (26c): By the general Suzuki coupling procedure, 0.025 g (0.07 mmol) of isophthalate

15c, 0.03 g (0.07 mmol) of the pinacolatoboronate **19**, and 4.0 mg (0.01 mmol) of the palladium catalyst in 0.3 mL of DME were treated with 0.3 mL of H₂O and 0.03 g (0.41 mmol) of sodium bicarbonate and purified by column chromatography (diethyl ether) to provide 0.017 g (40%) of the title compound: IR (thin film) ν 3360 (broad), 2926, 2754, 1721, 1531, 1159; ¹H NMR (CDCl₃, 500 MHz, 25 °C) δ 8.63 (s, 2H), 6.96-7.16 (m, 5H), 6.76 (s, 1H), 6.30 (s, 1H), 4.67 (t, 2H, J = 17.5 Hz), 4.32 (s, 2H), 4.19 (d, 1H, J = 15.5 Hz), 4.12 (s, 1H), 4.06/3.57 {d/d, (0.9+0.9/0.4+0.4) H, J = 25.0 and 60.0 Hz}, signal obscured/3.64 {signal obscured/d, (unknown/0.7+0.7) H, J = 85.0 Hz}, 3.55/2.58 {s/s, (0.4/1.0) H}, 1.46 (s, 12H), signal obscured/0.73 {signal obscured/s, (signal obscured/0.7) H}, 0.79/0.28 {s/s, (1.9/0.8) H}; ¹³C NMR (CDCl₃, 500 MHz) δ 166.83, 166.19, 153.60, 148.67, 146.67, 146.23, 143.65, 143.38, 135.46, 135.10, 134.48, 134.21, 133.43, 128.50, 127.42, 126.80, 126.56, 125.53, 124.78, 119.71, 118.39, 81.08, 67.91, 67.35, 66.89, 60.72, 59.56, 59.37, 59.00, 29.89, 28.49, 21.83, 21.18, 10.49;

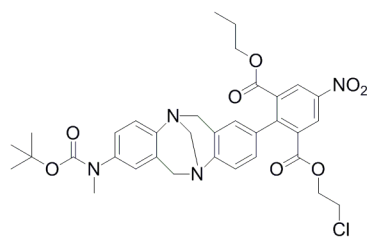
HRMS calculated for C₃₃H₃₇N₄O₉ 633.2561, found 633.2609.



(2''-Bromoethyl) propyl 4'-nitro-2-phenyl-8-(tert-butoxycarbonyl-(methyl)amino)-6H,12H-5,11-methanodibenzo[*b,f*][1,5]diazocine-3',6'-

dicarboxylate (29a): To a solution of 0.04 g (0.05 mol) of **26a** in 0.7 mL of dry THF at 0 °C

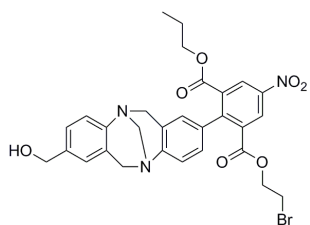
was added 6.0 mg (0.16 mmol) of 60% sodium hydride in mineral oil, which was stirred for 5 minutes. Methyl iodide (0.03 mL, 0.53 mmol) was added dropwise to the reaction mixture, which was warmed to room temperature and then stirred for an additional 30 minutes. The reaction was added to 10 mL of ice water and extracted with EtOAc (4 x 10 mL). The organic extracts were dried over MgSO₄, filtered and volatile components of the filtrate were removed under reduced pressure. The crude residue was purified by column chromatography (pentane: Et₂O, 2:1) to afford 0.02 g (58%) of the title compound: IR (thin film) ν 2969, 1723, 1698, 1532, 1496, 1351, 1309, 1243, 1151; ¹H NMR (CDCl₃, 700 MHz, 25 °C) δ 8.64 (d, 2H, J = 9.8 Hz), 7.14 (d, 1H, J = 7.7 Hz), 7.06 (s, 2H), 7.01 (d, 1H, J = 7.7 Hz), 6.82 (s, 1H), 6.78 (s, 1H), 4.67 (dd, 2H, J = 16.1 and 30.8 Hz), 4.38/3.84 {s/d, (0.7/0.6+0.5)H, J = 63.0 Hz}, 4.29 (s, 2H), 4.10-4.20 (m, 2H), 4.02/3.62 {s/d, (1.1/0.3+0.3)H, J = 77.7 Hz}, 3.26/2.43 {d/d, (0.3+0.3/0.4+0.5)H, J = 63.7 and 21.0 Hz}, 3.16 (s, 3H), 1.42 (s, 12H), signal obscured at ~1.45/~0.78 {signals obscured, (signal obscured/~0.5)H}, 0.78/0.22 {s/s, (2.0/1.0)H}; ¹³C NMR (CDCl₃, 700 MHz) δ 166.69, 166.19, 165.77, 154.87, 148.92, 148.59, 146.61, 145.01, 139.99, 135.81, 134.82, 134.45, 133.24, 133.02, 128.04, 127.68, 127.57, 126.70, 125.29, 124.98, 123.58, 123.36, 80.59, 67.94, 67.17, 65.37, 59.04, 58.72, 37.62, 28.54, 28.03, 21.82, 21.22, 10.50, 10.29; HRMS calculated for C₃₄H₃₇BrNaN₄O₈ 731.1692, found 731.1648.



(2''-Chloroethyl) propyl 4'-nitro-2-phenyl-8-(tert-butoxycarbonyl(methyl)amino)-6H,12H-5,11-methanodibenzo[*b,f*][1,5]diazocine-3',6'-dicarboxylate (29b): To a solution of 0.03 g (0.04 mol) of **26b** in 0.6 mL of dry THF at 0 °C was added 5.0 mg

(0.14 mmol) of 60% sodium hydride in mineral oil, which was stirred for 5 minutes. Methyl

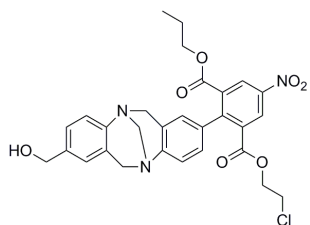
iodide (0.03 mL, 0.5 mmol) was added dropwise to the reaction mixture, which was warmed to room temperature and then stirred for an additional 30 minutes. The reaction was added to 10 mL of ice water and extracted with EtOAc (4 x 10 mL). The organic extracts were dried over MgSO₄, filtered and volatile components of the filtrate were removed under reduced pressure. The crude residue was purified by column chromatography (pentane: Et₂O: CH₂Cl₂, 1:1:0.1) to afford 0.01 g (34%) of the title compound: IR (thin film) ν 2969, 1724, 1698, 1496, 1351, 1312, 1238, 1151; ¹H NMR (CDCl₃, 700 MHz, 25 °C) δ 8.63 (s, 2H), 7.14 (d, 1H, J = 8.4 Hz), 7.02-0.10 (m, 2H), 7.00 (d, 1H, J = 7.7 Hz), 6.81 (s, 1H), 6.77 (s, 1H), 4.67 (dd, 2H, J = 16.8 and 30.8 Hz), 4.29 (s, 2H), ~4.29/3.80 {signal obscured/d, (~1.0/0.5+0.5)H, J = 68.6 Hz}, 4.08-4.19 (m, 2H), 4.02/3.62 {s/d, (1.1/0.3+0.3)H, J = 72.8 Hz}, 3.44/2.57 {d/s, (0.3+0.3/1.0)H, J = 59.5 Hz}, 3.15 (s, 3H), 1.41 (s, 12H), signal obscured at ~1.45/~0.78 {signals obscured, (signal obscured/~0.8)H}, 0.78/0.22 {s/s, (2.0/1.0)H}; ¹³C NMR (CDCl₃, 700 MHz) δ 166.67, 166.25, 165.87, 154.86, 148.90, 148.57, 146.60, 145.03, 139.98, 135.79, 135.27, 134.88, 134.46, 133.25, 133.01, 128.03, 127.70, 127.52, 126.68, 125.29, 124.93, 123.56, 123.37, 80.57, 67.93, 67.17, 65.55, 59.07, 58.73, 41.24, 40.80, 37.61, 30.49, 29.88, 28.52, 21.81, 21.22, 10.49; HRMS calculated for C₃₄H₃₇ClNaN₄O₈ 687.2198, found 687.2176.



(2''-Bromoethyl) propyl 4'-nitro-2-phenyl-8-hydroxymethyl-6H, 12H-5,11-methanodibenzo[*b,f*][1,5]diazocine-3',6'-dicarboxylate

(27a): By the general Suzuki coupling procedure, 0.03 g (0.08 mmol) of isophthalate **15a**, 0.05 g (0.12 mmol) of the pinacolatoboronate **22**, and 4.0 mg (0.008 mmol) of the palladium catalyst in 0.4 mL of DME were treated with 0.4 mL of water and 0.48 g (0.48 mmol) of sodium bicarbonate and purified by column chromatography (hexanes: EtOAc, 1:2) to

provide 0.013 g (28%) of the title compound: IR (thin film) ν 3372, 2924, 1719, 1531, 1494, 1349, 1309, 1243; ^1H NMR (CDCl_3 , 500 MHz, 25 °C) δ 8.63 (s, 2H), 7.13 (dd, 3H, $J = 8.0$ and 23.0 Hz), 7.01 (dd, 1H, $J = 14.0$ and 14.0 Hz), 6.94 (s, 1H), 6.77 (s, 1H), 4.72 (d, 1H, $J = 17.0$ Hz), 4.66 (d, 1H, $J = 16.0$ Hz), 4.56 (d, 2H, $J = 5.0$ Hz), 4.39/3.84 {s/d, (0.7/0.6+0.6) H, $J = 58.0$ Hz}, 4.32 (s, 2H), 4.19 (d, 1H, $J = 17.0$ Hz), 4.15 (d, 1H, $J = 18.0$ Hz), 4.03/3.56 {s/d, (0.9/0.5+0.5) H, $J = 75.0$ Hz}, 3.28/2.34 {d/s, (0.4+0.4/1.0) H, $J = 55.0$ Hz}, 1.48/0.72 {s/s, (0.7/0.6) H }, 0.79/0.24 {s/s, (1.5/0.8) H }; ^{13}C NMR (CDCl_3 , 600 MHz) δ 166.24, 148.72, 147.46, 146.62, 146.40, 136.87, 135.35, 134.79, 133.17, 130.67, 129.92, 127.83, 127.58, 127.18, 126.95, 126.62, 126.10, 125.73, 125.39, 124.97, 67.99, 67.24, 67.04, 65.14, 59.20, 58.59, 29.91, 28.08, 27.50, 22.91, 21.84, 21.16, 14.34, 10.49; HRMS calculated for $\text{C}_{29}\text{H}_{28}\text{BrN}_3\text{O}_7$ 609.111.062, found 609.110945.

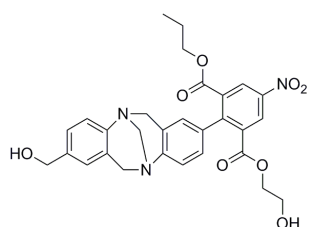


(2''-Chloroethyl) propyl 4'-nitro-2-phenyl-8-hydroxymethyl-6H, 12H-5,11-methanodibenzo[*b,f*][1,5]diazocine-3',6'-dicarboxylate

(27b): By the general Suzuki coupling procedure, 0.03 g (0.08 mmol) of isophthalate **15b**, 0.05 g (0.12 mmol) of the pinacolatoboronate **22**, and

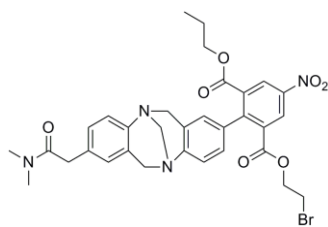
4.0 mg (0.008 mmol) of the palladium catalyst in 0.4 mL of DME were treated with 0.4 mL of water and 0.04 g (0.48 mmol) of sodium bicarbonate and purified by column chromatography (hexanes: EtOAc, 1:2) to provide 0.03 g (63%) of the title compound: IR (thin film) ν 3403, 3086, 2924, 1719, 916; ^1H NMR (CDCl_3 , 500 MHz, 25 °C) δ 8.63 (s, 2H), 7.13 (dd, 3H, $J = 8.5$ and 21.0 Hz), 7.01 (dd, 1H, $J = 2.0$ and 8.5 Hz), 6.94 (s, 1H), 6.76 (s, 1H), 4.72 (d, 1H, $J = 16.5$ Hz), 4.68 (d, 1H, $J = 17.5$ Hz), 4.55 (d, 2H, $J = 5.5$ Hz), 4.35/3.75 {s/d, (0.8/0.7+0.7) H, $J = 70.0$ Hz}, 4.32 (s, 2H), 4.19 (d, 1H, $J = 17.0$ Hz), 4.15 (d, 1H, $J = 17.0$ Hz), 4.03/3.57 {s/d,

(1.1/0.4+0.4) H, J = 65.0 Hz}, 3.46/2.49 {d/s, (0.5+0.5/1.1) H, J = 45.0 Hz}, 1.47/0.73 {s/s, (1.0/0.7) H}, 0.79/0.24 {s/s, (1.8/1.0) H}; ^{13}C NMR (CDCl_3 , 600 MHz) δ 166.32, 166.17, 148.68, 147.45, 146.62, 146.42, 136.87, 135.87, 135.30, 134.87, 133.17, 127.80, 127.54, 126.85, 126.67, 126.50, 126.02, 125.72, 125.37, 124.92, 67.98, 67.27, 65.57, 65.10, 59.24, 58.96, 41.24, 40.45, 29.90, 22.90, 21.83, 21.15, 14.34, 10.50; HRMS calculated for $\text{C}_{29}\text{H}_{28}\text{ClN}_3\text{O}_7$ 565.161578, found 565.160998.



(2''-Hydroxyethyl) propyl 4'-nitro-2-phenyl-8-hydroxymethyl-6H, 12H-5,11-methanodibenzo[*b,f*][1,5]diazocine-3',6'-dicarboxylate

(27c): By the general Suzuki coupling procedure, 0.01 g (0.03 mmol) of isophthalate **15c**, 0.02 g (0.05 mmol) of the pinacolatoboronate **22**, and 2.0 mg (0.003 mmol) of the palladium catalyst in 0.2 mL of DME were treated with 0.2 mL of H_2O and 0.02 g (0.19 mmol) of sodium bicarbonate and purified by column chromatography (ethyl acetate) to provide 0.01 g (45%) of the title compound: IR (thin film) ν 3390 (broad), 2925, 1721, 1530, 1349, 1307, 1243; ^1H NMR (CDCl_3 , 500 MHz, 25 °C) δ 8.63 (s, 1H), 8.61 (s, 1H), 6.97-7.17 (m, 5H), 6.75 (s, 1H), 4.70 (dd, 2H, J = 17.0 and 26.5 Hz), 4.54 (d, 2H, J = 4.5 Hz), 4.30-4.34 (m, 2H), 4.17 (dd, 2H, J = 16.0 and 28.5 Hz), signal obscured ~ 4.2/3.61 {signal obscured/d, (0.6/0.8+0.8) H, J = 75.0 Hz}, 4.03/3.58 {s/d, (1.3/0.3+0.3) H, J = 50.0 Hz}, 3.56/2.53 {s/s, (0.4/1.4) H}, 1.46/0.74 {s/s, (1.1/0.8) H}, 0.79/0.24 {s/s, (2.3/0.9) H}; ^{13}C NMR (CDCl_3 , 700 MHz) δ 166.82, 166.18, 148.66, 147.60, 147.55, 146.68, 146.11, 136.54, 135.32, 135.10, 133.38, 127.99, 127.42, 127.34, 126.80, 126.61, 126.50, 125.43, 125.24, 124.73, 67.98, 67.41, 66.52, 65.14, 59.51, 59.42, 59.27, 29.92, 21.85, 10.51; HRMS calculated for $\text{C}_{29}\text{H}_{29}\text{N}_3\text{O}_8$ 547.195465, found 547.194958.

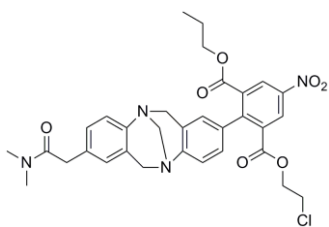


(2''-Bromoethyl) propyl 4'-nitro-2-phenyl-8-(2-(dimethylamino)-

2-oxoethyl)-6H,12H-5,11-methanodibenzo[*b,f*][1,5]diazocine-

3',6'-dicarboxylate (28a): By the general Suzuki coupling

procedure, 0.04 g (0.09 mmol) of isophthalate **15a**, 0.04 g (0.10 mmol) of the pinacolatoboronate **25**, and 5.0 mg (0.009 mmol) of the palladium catalyst in 0.5 mL of DME were treated with 0.5 mL of water and 0.05 g (0.55 mmol) of sodium bicarbonate and purified by column chromatography (EtOAc) to provide 0.026 g (42%) of the title compound: IR (thin film) ν 2925, 1723, 1643, 1308, 1143; ^1H NMR (CDCl_3 , 500 MHz, 25 °C) δ 8.64 (s, 2H), 7.14 (d, 1H, $J = 8.0$ Hz), 6.99-7.08 (m, 3H), 6.83 (s, 1H), 6.77 (d, 1H, $J = 2.0$ Hz), 4.70 (d, 1H, $J = 16.5$ Hz), 4.65 (s, 1H), 4.30 (s, 2H), 4.38/3.87 {s/d, (0.9/0.6+0.6) H, $J = 25.0$ Hz}, 4.17 (d, 2H, $J = 14.0$ Hz), 4.03/3.65+signal obscured {s/d, (1.24/0.6+signal obscured) H}, 3.56 (s, 2H), 3.27/2.36 {d/s, (0.5+0.5/1.2) H, $J = 40.0$ Hz}, 3.02 (broad s, 3H), 2.92 (s, 3H), 1.46/0.75 {s/s, (0.9/0.8) H}, 0.81/0.22 {s/s, (1.0/0.8) H}; ^{13}C NMR (CDCl_3 , 500 MHz) δ 171.05, 166.24, 146.67, 146.62, 133.23, 132.22, 128.76, 128.73, 127.74, 127.55, 127.27, 126.73, 126.60, 125.48, 125.44, 125.00, 68.01, 67.09, 65.41, 59.09, 58.80, 37.95, 35.85, 29.92, 28.04, 21.87, 14.35, 10.52; HRMS calculated for $\text{C}_{32}\text{H}_{33}\text{Br}^{23}\text{NaN}_4\text{O}_7$ 687.1430, found 687.1466.

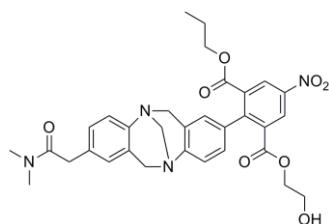


(2''-Chloroethyl) propyl 4'-nitro-2-phenyl-8-(2-(dimethylamino)-2-

oxoethyl)-6H,12H-5,11-methanodibenzo[*b,f*][1,5]diazocine-3',6'-

dicarboxylate (28b): By the general Suzuki coupling procedure, 0.03 g (0.06 mmol) of isophthalate **15b**, 0.03 g (0.07 mmol) of the pinacolatoboronate **25**, and 4.0 mg (0.006 mmol) of

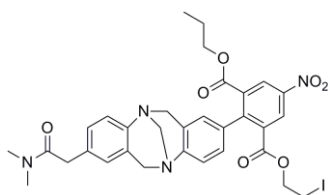
the palladium catalyst in 0.3 mL of DME were treated with 0.3 mL of water and 0.03 g (0.38 mmol) of sodium bicarbonate and purified by column chromatography (EtOAc) to provide 0.03 g (68%) of the title compound: IR (thin film) ν 2927, 1723, 1643, 1494, 1350, 1312, 1238; ^1H NMR (CDCl_3 , 500 MHz, 25 °C) δ 8.64 (s, 2H), 7.14 (d, 1H, $J = 8.5$ Hz), 6.99-7.08 (m, 3H), 6.83 (s, 1H), 6.77 (s, 1H), 4.70 (d, 1H, $J = 16.5$ Hz), 4.66 (d, 1H, $J = 16.5$ Hz), 4.33/3.79 {s/d, (0.6/0.5+0.5) H, $J = 30.0$ Hz}, 4.30 (s, 2H), 4.17 (d, 2H, $J = 16.0$ Hz), 4.03/3.65+signal obscured {s/d, (1.2/0.5+signal obscured) H}, 3.56 (s, 2H), 3.46/2.50 {d/s, (0.4+0.4/1.1) H, $J = 45.0$ Hz}, 3.01 (broad s, 3H), 2.92 (s, 3H), 1.46/0.75 {s/s, (1.2/0.9) H}, 0.80/0.22 {s/s, (1.3/0.8) H}; ^{13}C NMR (CDCl_3 , 600 MHz) δ 171.04, 166.24, 148.68, 146.63, 135.27, 134.92, 133.22, 131.17, 128.68, 128.19, 127.77, 127.60, 127.48, 127.36, 127.16, 126.69, 126.57, 126.31, 125.40, 124.94, 124.15, 67.94, 67.22, 66.97, 65.57, 59.10, 58.78, 41.23, 40.83, 40.31, 39.98, 37.92, 35.82, 29.90, 21.83, 21.21, 10.49; HRMS calculated for $\text{C}_{32}\text{H}_{33}\text{Cl}^{23}\text{NaN}_4\text{O}_7$ 632.1935, found 643.1975.



(2''-Hydroxyethyl) propyl 4'-nitro-2-phenyl-8-(2-(dimethylamino)-2-oxoethyl)-6H,12H-5,11-methanodibenzo[b,f]

[1,5]diazocine-3',6'-dicarboxylate (28c): By the general Suzuki coupling procedure, 0.02 g (0.03 mmol) of the pinacolatoboronate **25**, 0.02 g (0.05 mmol) of isophthalate **15c**, and 2.0 mg (0.003 mmol) of the palladium catalyst in 0.2 mL of DME were treated with 0.2 mL of H_2O and 0.02 g (0.21 mmol) of sodium bicarbonate and purified by column chromatography (EtOAc: MeOH, 40:1) to provide 0.01 g (69%) of the title compound: IR (thin film) ν 3400 (broad), 2927, 1722, 1632, 1530, 1494, 1349, 1307; ^1H NMR (CDCl_3 , 500 MHz, 25 °C) δ 8.62 (s, 2H), 7.14 (d, 1H, $J = 7.5$ Hz), 7.08 (d, 1H, $J = 8.5$ Hz), 6.97-7.04 (m, 2H), 6.79 (s, 1H), 6.75 (s, 1H), 4.68 (t, 2H, $J = 18.0$ Hz), 4.32 (s, 2H), 4.22 (t, 1H, $J = 17.0$ Hz), 4.16

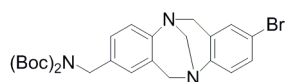
(d, 1H, J = 16.5 Hz), signal obscured ~4.2/3.65 {signal obscured/doublet of multiplets, (signal obscured/1.1+1.1) H, J = 48.0 Hz}, 3.99-4.06/signal obscured ~3.6 and 3.7 {m/d, (1.7/signal obscured) H}, 2.86/2.48 {s/d, (0.5/1.7) H, J = 5.5 Hz}, 3.55 (d, 2H, J = 8.5 Hz), 3.07 (s, 3H), 2.92 (s, 3H), 1.46/0.73 {q/s, (1.3/0.3) H, J = 7.0 Hz}, 0.78/0.22 {t/s, (2.3/0.5) H, J = 7.0 Hz}; ¹³C NMR (CDCl₃, 600 MHz) δ 171.56, 166.82, 166.19, 148.50, 146.47, 146.42, 145.91, 135.39, 134.89, 133.19, 132.31, 130.75, 128.76, 127.97, 127.75, 127.58, 127.20, 126.51, 126.41, 126.13, 125.19, 124.99, 124.69, 114.94, 112.73, 67.72, 67.04, 66.76, 58.96, 58.74, 58.55, 40.15, 39.18, 37.64, 35.85, 35.65, 21.64, 10.30; HRMS calculated for C₃₂H₃₅N₄O₈ 603.2455, found 603.2447.



(2''-Iodoethyl) propyl 4'-nitro-2-phenyl-8-(2-(dimethylamino)-2-oxoethyl)-6H,12H-5,11-methanodibenzo[*b,f*][1,5]diazocine-3',6'-dicarboxylate (28d): To a solution of 0.01 g (0.01 mmol) of **28a** in

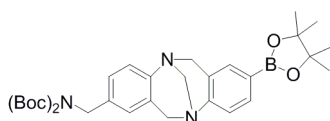
0.3 mL of dry acetone was added 0.1 g (0.38 mmol) of sodium iodide, which was heated to reflux for 16 hours. The solution was cooled to room temperature, the salt removed by filtration, and the reaction mixture diluted with 10 mL H₂O. The aqueous layer was extracted with CH₂Cl₂ (3 x 10 mL). The organic extracts were dried over MgSO₄, filtered and volatile components of the filtrate were removed under reduced pressure. The crude residue was purified by column chromatography (pentane: EtOAc, 1:8) to afford 0.01 g (quantitative yield) of the title compound: IR (thin film) ν 2924, 2854, 1823, 1640, 1530, 1494, 1306; ¹H NMR (CDCl₃, 500 MHz, 25 °C) δ 8.64 (s, 2H), 7.15 (d, 1H, J = 8.0 Hz), 7.00-7.08 (m, 3H), 6.84 (s, 1H), 6.78 (s, 1H), 4.70 (d, 1H, J = 16.5 Hz), 4.66 (d, 1H, J = 15.0 Hz), 4.30 (s, 2H), 4.17 (d, 2H, J = 15.5 Hz), 4.33/3.87 {s/s, (0.6/1.33) H}, 4.02/3.58 {s/d, (1.1/0.4+0.4) H, J = 50.0 Hz}, 3.57 (s, 2H), 3.01 (s, 3H), 2.92 (s, 3H), signal obscured at ~3.0/2.20 {signal obscured/s, (signal obscured/1.1) H},

1.46/0.75 {s/s, (0.8/0.5) H}, 0.79/0.22 {s/s, (1.7/0.9) H}; ^{13}C NMR (CDCl_3 , 700 MHz) δ 171.06, 146.76, 146.62, 146.55, 146.49, 131.37, 131.22, 127.80, 127.73, 127.72, 127.67, 127.59, 127.23, 126.71, 126.65, 126.61, 126.58, 125.47, 125.07, 124.98, 67.97, 66.09, 58.99, 58.76, 38.00, 35.88, 32.15, 29.92, 29.54, 22.91, 14.35; HRMS calculated for $\text{C}_{32}\text{H}_{34}^{127}\text{IN}_4\text{O}_7$ 713.1472, found 713.1509.



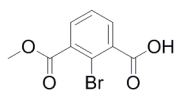
2-Bromo-8-((di-tert-butoxycarbonylamino)methyl)-6H,12H-5,11-methanodibenzo[*b,f*] [1,5]diazocine (35): To a stirred solution of 0.50

g (1.5 mmol) of **21** and 0.6 mL (4.5 mmol) of triethylamine in 3.4 mL of THF at 0 °C was added 0.99 g (3.8 mmol) of triphenylphosphine and 1.31 g (6.0 mmol) of di-*tert*-butyl iminodicarboxylate in 13.4 mL of THF. Di-*tert*-butyl azodicarboxylate (0.70 g, 3.0 mmol) was added portionwise to the reaction mixture at 0 °C. The solution was heated to 60 °C for 2 hours, volatile components were removed under reduced pressure, and the crude material was purified by column chromatography (hexanes: EtOAc, 8:1) to afford 0.52 g (65%) of the carbamate: IR (KBr) ν 2978, 1744, 1697, 1477, 1367, 1348, 1323; ^1H NMR (CDCl_3 , 300 MHz) δ 7.21 (d, 1H, J = 2.1 Hz), 6.96-7.10 (m, 5H), 6.81 (s, 1H), 4.55-4.67 (m, 4H), 4.26 (dd, 2H, J = 12.9 and 18.3 Hz), 4.07 (dd, 2H, J = 9.3 and 16.8 Hz), 1.38 (s, 18H); ^{13}C NMR (CDCl_3 , 300 MHz) δ 152.78, 147.28, 146.80, 134.60, 130.59, 130.19, 129.85, 127.44, 127.07, 126.89, 126.29, 125.01, 116.68, 82.71, 67.06, 59.06, 58.69, 49.17, 28.16; HRMS calculated for $\text{C}_{26}\text{H}_{32}\text{BrNaN}_3\text{O}_4$ 552.1474, found 552.1491.



2-(Di-tert-butoxycarbonylamino)methyl-8-4,4,5,5-tetramethyl-[1,3,2]dioxaborolan-2-yl-6H,12H-5,11-methanodibenzo[*b,f*]

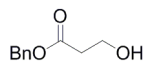
[1,5]diazocine (34): The carbamate (0.82 g, 1.6 mmol), bis(pinacolato)diboron (0.79 g, 3.1 mmol), dichloro[1,1]-bis(diphenylphosphine)ferrocene] palladium dichloromethane adduct (0.11 g, 0.2 mmol), and potassium acetate (0.30 g, 3.1 mmol) were combined in a flask, which was placed under vacuum for five to ten minutes and then filled with N₂. Addition of 9.3 mL of anhydrous DMSO to this mixture provided an orange solution which was degassed twice by freeze pump thaw cycle and then heated at 80°C for 16 hours. The reaction was cooled to room temperature, diluted with 50 mL of CH₂Cl₂, and the resultant mixture was washed with water (3 x 50 mL). The combined aqueous layers were extracted with CH₂Cl₂ (2 x 50 mL). The organic extracts were dried over MgSO₄, filtered and the volatile components of the filtrate were removed under reduced pressure. The residue was purified by column chromatography (pentane: Et₂O, 6:1) to afford 0.83 g (93%) of the title compound as a white foam: IR (thin film) ν 2977, 1746, 1598, 1361, 1143, 1113; ¹H NMR (CDCl₃, 300 MHz) δ 7.56 (dd, 1H, J = 1.2 and 8.1 Hz), 7.35 (s, 1H), 7.00-7.10 (m, 3H), 6.80 (s, 1H), 4.53-4.67 (m, 4H), 4.29 (s, 2H), 4.14 (d, 2H, J = 16.8 Hz), 1.37 (s, 18H), 1.26 (s, 12H); ¹³C NMR (CDCl₃, 300 MHz) δ 152.79, 151.33, 147.10, 140.39, 134.32, 134.11, 133.9, 127.72, 127.35, 126.98, 126.37, 125.03, 124.48, 83.87, 82.66, 67.17, 59.12, 58.93, 49.20, 28.19, 25.00; HRMS calculated for C₃₂H₄₄B²³NaN₃O₆ 600.3221, found 600.3274.



2-Bromoisophthalic acid 1-methyl ester (36): *Step 1 - Esterification:* To a

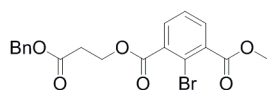
stirred solution of 18.58 g (75.8 mmol) of **12** in 330 mL of methanol at 0°C was added 80 mL (1441 mmol) of concentrated H₂SO₄ over an hour. The reaction was slowly warmed and then refluxed for two days. The solution was cooled to room temperature and methanol was removed under reduced pressure. The residue was diluted with 1000 mL EtOAc

and washed with saturated K_2CO_3 (3 x 500 mL). The organic extract was dried over $MgSO_4$, filtered, and volatile components of the filtrate were removed under reduced pressure. The residue was purified by column chromatography (hexanes: EtOAc, 20:1) to afford 13.24 g (64%) of 2-bromoisophthalic acid dimethyl ester as an amber liquid: IR (liquid) ν 2953, 1736, 1587, 1433, 1417; 1H NMR ($CDCl_3$, 300 MHz) δ 7.68 (d, 2H, $J = 7.4$ Hz), 7.40 (t, 1H, $J = 7.8$ Hz), 3.94 (s, 6H). **Step 2 – Selective Hydrolysis:** To a stirred solution of 1.64 g (6.0 mmol) of 2-bromoisophthalic acid dimethyl ester in 15 mL of methanol:acetone (1:4) was added 0.26 g (6.6 mmol) of sodium hydroxide. The mixture was stirred for two days at room temperature, after which the acetone and methanol were removed under reduced pressure. The residue was treated with 50 mL of 1 M HCl and extracted with EtOAc (3 x 75 mL). The organic extracts were washed with brine (100 mL), dried over $MgSO_4$, filtered and the volatile components of the filtrate were removed under reduced pressure. The residue was purified by column chromatography (hexanes: EtOAc, 3:1) to afford 1.34 g (86%) of the 2-bromoisophthalic acid monomethyl ester: IR (thin film) ν 2954 (broad), 1731, 1586, 1556, 1421, 1288, 1256, 1207; 1H NMR (MeOD, 300 MHz) δ 7.71-7.81 (m, 2H), 7.51-7.57 (m, 1H), 3.96 (s, 3H).²³



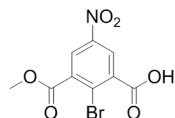
Benzyl 3-hydroxypropionate (38): To a stirred solution of 0.72 g (8.0 mmol) of 3-hydroxypropionic acid¹⁵⁹ in 20.0 mL of dimethylsulfoxide was added 1.20 g (8.0 mmol) of sodium iodide, 1.33 g (9.6 mmol) of potassium carbonate at 10 °C. The reaction was stirred for five minutes, after which 1.2 mL (9.6 mmol) of benzyl bromide was added. The reaction was heated to 55 °C and stirred for 6 hours. The reaction was added to water and EtOAc (50 mL each). The layers were separated and the organic layer was washed with water (2 x 50 mL). The combined aqueous layers were extracted with EtOAc (5 x 50 mL). The organic extracts were

dried over MgSO₄, filtered, and volatile components of the filtrate were removed under reduced pressure. The residue was purified by column chromatography (hexanes: EtOAc, 5:1) to afford 0.84 g (58%) of the title compound as an oil: IR (KBr) ν 3436 (broad), 2920, 2850, 1731, 1163, 1041, 737; ¹H NMR (CDCl₃, 300 MHz) δ 7.32-7.36 (m, 5H), 5.14 (s, 2H), 3.87 (q, 2H, J = 6.0 Hz), 2.61 (t, 2H, J = 5.7 Hz), 2.42 (t, 1H, J = 6.6 Hz); ¹³C NMR (CDCl₃, 300 MHz) δ 172.72, 135.63, 128.65, 128.41, 128.28, 66.55, 58.27, 36.84; HRMS calculated for C₁₀H₁₂O₃ 180.078644, found 180.078368.



2-Bromoisophthalic acid 1-(3'-(benzyloxy)-3'-oxopropyl) ester 3-methyl ester (37): By the general esterification procedure, 0.09 g (0.5

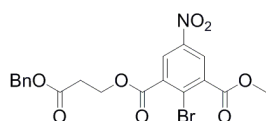
mmol) of benzyl 3-hydroxypropionate (**38**), 0.10 g (0.4 mmol) of DCC and 0.01 g (0.1 mmol) of DMAP in 2.0 mL of dry CH₂Cl₂ treated with 0.10 g (0.4 mmol) of the carboxylic acid **36**, provided 0.14 g (82%) of the title compound: IR (thin film) ν 3066, 3032, 2953, 1735, 1586, 1455, 1283, 1254, 1202, 1148; ¹H NMR (CDCl₃, 300 MHz) δ 7.68 (dd, 1H, J = 1.8 and 7.8 Hz), 7.59 (dd, 1H, J = 1.8 and 7.8 Hz), 7.30-7.37 (m, 5H), 5.15 (s, 2H), 4.62 (t, 2H, J = 6.3 Hz), 3.93 (s, 3H), 2.83 (t, 2H, J = 6.3 Hz); ¹³C NMR (CDCl₃, 300 MHz) δ 170.45, 167.10, 166.31, 135.79, 135.64, 135.32, 132.59, 132.53, 128.81, 128.59, 128.54, 127.32, 119.34, 66.94, 61.43, 52.95, 34.04; HRMS calculated for C₁₉H₁₇BrO₆ 420.020850, found 420.020498.



2-Bromo-5-nitroisophthalic acid 1-methyl ester (39): To a stirred solution of 1.5 mL of fuming nitric acid and 8.9 mL of concentrated sulfuric acid at 0°C was

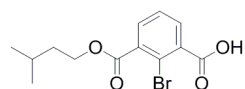
added 1.34 g (5.2 mmol) of 2-bromoisophthalic acid monomethyl ester (**36**). The reaction was slowly warmed to room temperature and stirred for 16 hours. The reaction was added dropwise

to a stirring mixture of 100 mL of EtOAc and 100 mL of ice water. The layers were separated and the organic layer was washed with water (2 x 100 mL). The combined aqueous layers were extracted with EtOAc (2 x 100 mL). The organic extracts were dried over MgSO₄, filtered, and volatile components of the filtrate were removed under reduced pressure to yield 1.41 g (89%) of the title compound as a crude yellow solid: IR (KBr) ν 3093 (broad), 1741, 1713, 1607, 1531, 1352, 1297, 1201; ¹H NMR (MeOD, 300 MHz) δ 8.58 (dd, 2H, J = 2.7 and 11.4 Hz), 4.02 (s, 3H); ¹³C NMR (MeOD, 300 MHz) δ 167.64, 165.92, 147.19, 138.32, 137.64, 126.64, 126.39, 126.21, 52.97.²³



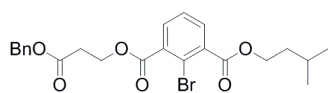
2-Bromo-5-nitroisophthalic acid 1-(3'-(benzyloxy)-3'-oxopropyl) ester

3-methyl ester (40): By the general esterification procedure, 0.39 g (2.1 mmol) of benzyl 3-hydroxypropionate (**38**), 0.68 g (3.3 mmol) of DCC and 0.05 g (0.4 mmol) of DMAP in 8.3 mL of dry CH₂Cl₂ treated with 0.50 g (1.6 mmol) of the carboxylic acid **39**, provided 0.45 g (59%) of the title compound: IR (thin film) ν 3084, 2954, 2854, 1739, 1535, 1352, 1239, 1174; ¹H NMR (CDCl₃, 300 MHz) δ 8.52 (d, 1H, J = 2.7 Hz), 8.44 (d, 1H, J = 2.7 Hz), 7.29-7.31 (m, 5H), 5.16 (s, 2H), 4.68 (t, 2H, J = 6.0 Hz), 3.99 (s, 3H), 2.85 (t, 2H, J = 6.0 Hz); ¹³C NMR (CDCl₃, 300 MHz) δ 170.21, 165.04, 164.40, 146.46, 136.85, 136.80, 135.63, 128.82, 128.66, 128.63, 126.89, 126.86, 67.11, 62.17, 53.61, 33.89; HRMS calculated for C₁₉H₁₇BrNO₈ 466.013753, found 466.013582.



2-Bromoisophthalic acid 1-isoamyl ester (41): To a stirred solution of 1.00 g (3.9 mmol) of 2-bromoisophthalic acid (**12**) in 38.6 mL of dimethylsulfoxide was added 0.58 g (3.9 mmol) of sodium iodide, 0.64 g (4.6 mmol) of potassium carbonate at 10 °C. The

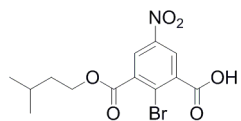
reaction was stirred for five minutes, after which 0.5 mL (3.9 mmol) of 1-bromo-3-methylbutane was added. The reaction was heated to 40 °C, stirred overnight, and cooled to room temperature. The reaction was treated with aqueous HCl (20 mL, 1M) and was extracted with EtOAc (3 × 50 mL). The combined organic layers were washed with water and brine (50 mL each), dried over MgSO₄, and filtered, and volatile components of the filtrate were removed under reduced pressure. The residue was purified by column chromatography (hexanes: EtOAc, 8:1) to afford 0.65 g (54%) of the title compound as a solid: IR (KBr) ν 3500-2800 (broad), 2959, 1732, 1586, 1289, 1256, 1204, 1150; ¹H NMR (CDCl₃, 700 MHz) δ 7.91 (dd, 1H, J = 2.1 and 7.7 Hz), 7.69 (dd, 1H, J = 2.1 and 7.7 Hz), 7.44 (t, 1H, J = 7.7 Hz), 4.38 (t, 2H, J = 7.0 Hz), 1.78 (quintet, 1H, J = 7.0 Hz), 1.65 (q, 2H, J = 7.0 Hz), 0.95 (d, 6H, J = 6.3 Hz); ¹³C NMR (CDCl₃, 700 MHz) δ 170.64, 167.03, 136.96, 133.37, 133.31, 133.13, 127.44, 119.87, 65.03, 37.38, 25.26, 22.65; HRMS calculated for C₁₃H₁₅BrO₄ 314.015370, found 314.015298.



2-Bromoisophthalic acid 1-(3'-(benzyloxy)-3'-oxopropyl) ester 3-isopentyl ester (42): By the general esterification procedure, 0.14 g

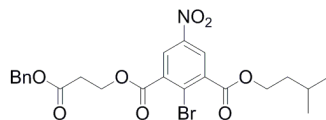
(0.8 mmol) of benzyl 3-hydroxypropionate (**38**), 0.26 g (1.3 mmol) of DCC and 0.02 g (0.2 mmol) of DMAP in 3.2 mL of dry CH₂Cl₂ treated with 0.20 g (0.6 mmol) of the carboxylic acid **41**, provided 0.26 g (84%) of the title compound as an oil: IR (thin film) ν 2959, 1737, 1253, 1197, 1149; ¹H NMR (CDCl₃, 300 MHz) δ 7.64 (dd, 1H, J = 1.8 and 7.8 Hz), 7.57 (dd, 1H, J = 1.8 and 7.8 Hz), 7.29-7.36 (m, 5H), 5.14 (s, 2H), 4.62 (t, 2H, J = 6.3 Hz), 4.36 (t, 2H, J = 6.6 Hz), 2.82 (t, 2H, J = 6.3 Hz), 1.76 (sextet, 1H, J = 6.6 Hz), 1.63 (q, 2H, J = 6.9 Hz), 0.94 (d, 6H, J = 6.6 Hz); ¹³C NMR (CDCl₃, 300 MHz) δ 170.38, 166.73, 166.23, 136.00, 135.69, 135.08,

132.33, 132.30, 128.71, 128.49, 128.45, 127.25, 119.06, 66.82, 64.80, 61.33, 37.30, 33.92, 25.17, 22.56; HRMS calculated for $C_{23}H_{25}BrNaO_6$ 499.0732, found 499.0694.



2-Bromo-5-nitroisophthalic acid 1-isoamyl ester (43): To a stirred

solution of 1.00 g (3.4 mmol) of 2-bromo-5-nitroisophthalic acid (**13**) in 34.5 mL of dimethylsulfoxide was added 0.52 g (3.4 mmol) of sodium iodide, 0.72 g (5.2 mmol) of potassium carbonate at 10 °C. The reaction was stirred for five minutes, after which 0.4 mL (3.4 mmol) of 1-bromo-3-methylbutane was added. The reaction was heated to 40 °C, stirred overnight, and cooled to room temperature. The reaction was treated with aqueous HCl (20 mL, 1M) and was extracted with EtOAc (3 × 50 mL). The combined organic layers were washed with water and brine (50 mL each), dried over $MgSO_4$, and filtered, and volatile components of the filtrate were removed under reduced pressure. The residue was purified by column chromatography (hexanes: EtOAc, 8:1) to afford 0.68 g (55%) of the title compound as a solid: IR (KBr) ν 3300-2500 (broad), 3091, 2961, 1741, 1705, 1609, 1534, 1354, 1298, 1252; 1H NMR ($CDCl_3$, 700 MHz) δ 8.74 (d, 1H, $J = 2.8$ Hz), 8.52 (d, 1H, $J = 2.8$ Hz), 4.44 (t, 2H, $J = 3.0$ Hz), 1.78 (quintet, 1H, $J = 7.0$ Hz), 1.68 (q, 2H, $J = 7.0$ Hz), 0.96 (d, 6H, $J = 6.3$ Hz); ^{13}C NMR ($CDCl_3$, 700 MHz) δ 168.98, 164.99, 146.51, 138.36, 134.64, 127.65, 127.40, 127.39, 65.97, 37.28, 25.28, 22.62; HRMS calculated for $C_{13}H_{15}BrNO_6$ 360.008274, found 360.007537.



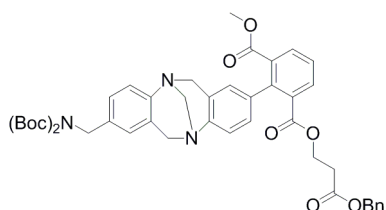
2-Bromo-5-nitroisophthalic acid 1-(3'-(benzyloxy)-3'-oxopropyl)

ester 3-isopentyl ester (44): To a stirred solution of 0.15 g (0.4 mmol) of **43** and 0.03 mL (0.4 mmol) of DMF in 10.4 mL of CH_2Cl_2 at 0 °C was added oxalyl chloride dropwise (1.2 mL, 2 M in CH_2Cl_2 , 2.3 mmol). The reaction was stirred for one hour at

room temperature and volatile components were removed under reduced pressure. The residue was diluted with 10.4 mL of CH₂Cl₂ and added dropwise to a stirred solution of 0.15 g (0.8 mmol) of benzyl 3-hydroxypropionate (**38**), and 0.4 mL (2.8 mmol) of triethylamine in 10.4 mL of CH₂Cl₂ at 0 °C. The solution was stirred for two hours at room temperature. The reaction was treated with saturated NaHCO₃ (50 mL) and was extracted with EtOAc (3 × 50 mL). The combined organic layers were washed with brine (50 mL), dried over MgSO₄, and filtered, and volatile components of the filtrate were removed under reduced pressure. The residue was purified by column chromatography (hexanes: EtOAc, 15:1) to afford 0.13 g (60%) of the title compound as an oil: IR (KBr) ν 30.86, 2960, 1740, 1536, 1608, 1536, 1352, 1237, 1183; ¹H NMR (CDCl₃, 300 MHz) δ 8.47 (d, 1H, J = 2.7 Hz), 8.43 (d, 1H, J = 2.7 Hz), 7.26-7.33 (m, 5H), 5.15 (s, 2H), 4.67 (t, 2H, J = 6.0 Hz), 4.42 (t, 2H, J = 6.6 Hz), 2.85 (t, 2H, J = 6.3 Hz), 1.76 (sextet, 1H, J = 6.3 Hz), 1.67 (q, 2H, J = 6.6 Hz), 0.96 (d, 6H, J = 6.3 Hz); ¹³C NMR (CDCl₃, 300 MHz) δ 170.20, 164.78, 164.36, 146.42, 137.41, 136.57, 135.58, 128.77, 128.61, 128.58, 126.65, 126.62, 67.05, 65.75, 62.11, 37.26, 33.83, 25.24, 22.59; HRMS calculated for C₂₃H₂₄BrNaNO₈ 544.0583, found 544.0562.

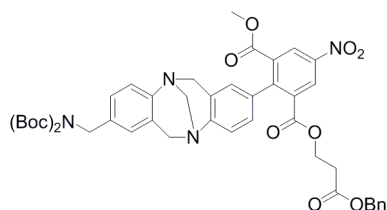
General Suzuki coupling procedure: The isophthalate (**37**, **40**, **42**, or **44**) benzodiazocine pinacolatoboronate (**34**), and 1,1'-bis(diphenylphosphino)ferrocene]dichloropalladium (II) were combined in a pressure reaction tube, which was placed under vacuum for five to ten minutes and then filled with N₂. The solids were dissolved in 1,2-dimethoxyethane (DME), and the solution was degassed twice by freeze pump thaw cycle. Saturated sodium bicarbonate was added to the pressure tube, and the contents were degassed two more times. The reaction was heated to 80°C for approximately 12 hours, cooled to room temperature, diluted with less than 1

mL of water. The subsequent mixture was extracted with CH₂Cl₂ (3 x 5 mL), the organic extracts were dried over MgSO₄, filtered and volatile components of the filtrate were removed under reduced pressure. The residue was purified by column chromatography and then by HPLC.



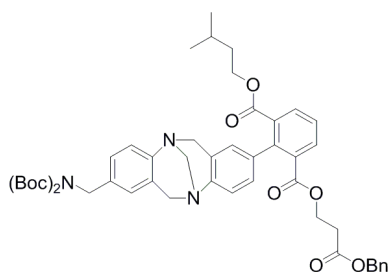
(3'-(benzyloxy)-3'-oxopropyl) methyl 2-phenyl-8-((di-tert-butoxycarbonylamino)methyl)-6H,12H-5,11-methanodibenzo[*b,f*] [1,5]diazocine-3',6'-dicarboxylate (45a):

By the general Suzuki coupling procedure, 0.07 g (0.16 mmol) of isophthalate **37**, 0.06 g (0.10 mmol) of the pinacolatoboronate **34**, and 6 mg (0.01 mmol) of the palladium catalyst in 0.5 mL of DME were treated with 0.05 g (0.62 mmol) of sodium bicarbonate in 0.5 mL of water and purified by column chromatography (pentane: Et₂O, 1:4) to provide 0.05 g (57%) of the title compound: IR (thin film) ν 2978, 1737, 1495, 1367, 1174, 1144, 1115; ¹H NMR (CDCl₃, 600 MHz, 25 °C) δ 7.73-7.82 (m, 2H), 7.39 (s, 1H), 7.29 (s, 5H), 6.77-7.07 (m, 6H), 6.61 (s, 1H), 5.10/5.00 {s/s, (1.0/1.0)H}, 4.54-4.63 (m, 4H), ~4.3/3.67 {signal obscured/d, (~0.7/0.9)H, J = 112.4 Hz}, 4.26-4.33 (m, 2H), 4.06-4.11 (m, 2H), 3.59/2.77 {s/s, (1.5/1.3) H}, 2.42/1.21 {d/signal obscured, 0.9/signal obscured, J = 19.2 Hz}, 1.47 (s, 18H); ¹³C NMR (CDCl₃, 600 MHz, 25 °C) δ 170.40, 169.08, 168.39, 167.66, 152.95, 147.33, 147.06, 140.89, 135.85, 135.23, 134.16, 133.61, 132.79, 132.12, 131.95, 128.75, 128.61, 127.80, 127.39, 127.14, 126.81, 126.13, 126.06, 124.99, 124.41, 124.20, 82.77, 67.11, 66.73, 66.54, 60.62, 58.80, 49.01, 33.61, 32.27, 28.44, 28.29, 28.15, 28.00; HRMS calculated for C₄₅H₄₉N₃O₁₀ 791.341795, found 791.343319.



(3'-(benzyloxy)-3'-oxopropyl) methyl 4'-nitro-2-phenyl-8-((di-tert-butoxycarbonylamino)methyl)-6H,12H-5,11-

methanodibenzo[*b,f*][1,5]diazocine-3',6'-dicarboxylate (45b): By the general Suzuki coupling procedure, 0.04 g (0.09 mmol) of isophthalate **40**, 0.04 g (0.06 mmol) of the pinacolatoboronate **34**, and 3 mg (0.006 mmol) of the palladium catalyst in 0.3 mL of DME were treated with 0.03 g (0.36 mmol) of sodium bicarbonate in 0.3 mL of water and purified by column chromatography (pentane: Et₂O, 1:4) to provide 0.04 g (72%) of the title compound: IR (thin film) ν 2978, 1738, 1531, 1495, 1350, 1231, 1171, 1143; ¹H NMR (CDCl₃, 300 MHz, 25 °C) δ 8.57 (s, 2H), 7.29 (s, 5H), 7.02 (s, 3H), 6.81 (s, 2H), 6.61 (d, 1H, *J* = 1.8 Hz), 5.02/5.01 {s/s, (1.0/1.0)H}, 4.52-4.65 (m, 4H), 4.25-4.35 (m, 2H), 4.09 (dd, 2H, *J* = 4.5 and 16.5 Hz), ~4.29/3.71 {signal obscured/d, (~1.2/1.0)H, *J* = 63.3 Hz}, 3.67/2.85 {s/s, (1.5/1.2)H}, 2.48/~1.25 {s/signal obscured, (0.6/signal obscured)H}, 1.43 (s, 18H); ¹³C NMR (CDCl₃, 300 MHz, 25 °C) δ 170.08, 166.15, 152.98, 148.59, 146.93, 146.82, 146.52, 135.74, 135.39, 134.32, 133.92, 132.89, 128.74, 128.66, 127.84, 128.66, 127.84, 127.66, 127.36, 126.54, 126.41, 126.04, 125.03, 124.70, 82.80, 67.21, 66.76, 61.32, 59.07, 52.97, 52.15, 49.00, 33.42, 32.36, 28.22; HRMS calculated for C₄₅H₄₈NaN₄O₁₂ 859.3166, found 859.3113.

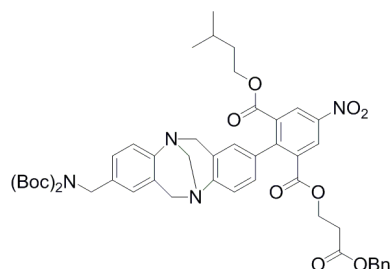


(3'-(benzyloxy)-3'-oxopropyl) isopentyl 2-phenyl-8-((di-tert-butoxycarbonylamino)methyl)-6H,12H-5,11-

methanodibenzo[*b,f*][1,5]diazocine-3',6'-dicarboxylate (45c):

By the general Suzuki coupling procedure, 0.06 g (0.13 mmol) of isophthalate **42**, 0.05 g (0.09 mmol) of the pinacolatoboronate **34**, and 5 mg (0.005 mmol) of the palladium catalyst in 0.4 mL of DME were treated with 0.04 g (0.52 mmol) of sodium bicarbonate in 0.4 mL of water and purified by column chromatography (pentane: Et₂O, 1:2) to provide 0.04 g (55%) of the title compound: IR (thin film) ν 2958, 1738, 1495, 1302, 1259,

1173, 1144; ¹H NMR (CDCl₃, 300 MHz, 25 °C) δ 7.79 (s, 1H), 7.73 (dd, 1H, J = 1.2 and 7.8 Hz), 7.39 (t, 1H, J = 8.5 Hz), 7.28 (s, 5H), 6.78-6.99 (m, 5H), 6.62 (s, 1H), 5.09/4.99 {s/s, (0.7/1.3)H}, 4.59 (m, 4H), ~4.3/3.69 {signal obscured/d, (0.7/1.2)H, J 51.3 Hz}, 4.27 (s, 2H), 4.08 (d, 2H, J = 17.4 Hz), 2.37/~1.3 {s/signal obscured, (0.4/signal obscured)H}, 1.43 (s, 18H), ~1.2/~0.7 {signals obscured}, 0.80/0.60 {s/s, (4.3/1.6)H}; ¹³C NMR (CDCl₃, 500 MHz, 25 °C) δ 170.38, 168.40, 152.95, 147.39, 147.22, 147.05, 140.53, 135.85, 135.39, 134.15, 133.48, 133.41, 131.85, 128.72, 128.63, 128.59, 127.77, 127.33, 127.11, 126.73, 126.39, 126.09, 125.70, 125.07, 124.51, 82.72, 67.18, 66.51, 63.97, 60.51, 58.81, 49.04, 37.12, 32.21, 30.48, 28.21, 24.85, 22.55; HRMS calculated for C₄₉H₅₇N₃O₁₀Na 870.3942, found 870.3964.

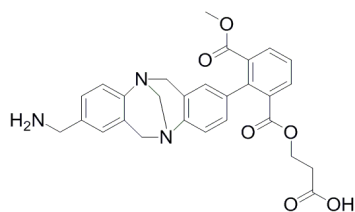


(3'-(benzyloxy)-3'-oxopropyl) isopentyl 4'-nitro-2-phenyl-8-((di-tert-butoxycarbonylamino)methyl)-6H,12H-5,11-methanodibenzo[*b,f*][1,5]diazocine-3',6'-dicarboxylate (45d):

By the general Suzuki coupling procedure, 0.7 g (0.13 mmol) of isophthalate **44**, 0.5 g (0.09 mmol) of the pinacolatoboronate **34**, and 5 mg (0.01 mmol) of the palladium catalyst in 0.4 mL of DME were treated with 0.04 g (0.52 mmol) of sodium bicarbonate in 0.4 mL of water and purified by column chromatography (pentane: Et₂O, 2:1) to provide 0.06 g of the title compound: IR (thin film) ν 2959, 1738, 1532, 1495, 1387, 1366, 1350, 1173, 1145; ¹H NMR (CDCl₃, 700 MHz, 5 °C) δ 8.62/6.56 {s/s, (0.5/0.5)H}, 8.55 (s, 1H), 7.29 (s, 5H), 7.00-7.09 (m, 2H), 6.93 (d, 1H, J = 7.0 Hz), 6.80 (d, 1H, J = 7.0 Hz), 6.77 (s, 1H), 6.62 (d, 1H, J = 13.3 Hz), 5.10/4.98 {s/dd, (0.5/1.2)H, J = 11.9 and 20.3 Hz}, 4.52-4.68 (m, 4H), 4.33/3.72 {d/d, (0.4/1.0)H, J = 35 and 147 Hz}, 4.26 (s, 2H), 4.06/3.60 {d/d, (signal obscured/0.2)H, J = 41.0 and 155.4 Hz}, 4.02-4.15 (m, 2H) 2.45/1.29 {d/d, (0.3/signal

obscured)H, J = 35 and 210.7 Hz}, 1.42 (s, 18H), 1.27/0.71 {d/d, (1.6/0.6)H, J = 6.3 and 32.9 Hz}, 1.37/1.18 {s/s, (0.9/0.7)H}, 0.81/0.59 {t/s, (4.4/1.9)H, J = 6.3 Hz}; ¹³C NMR (CDCl₃, 500 MHz, 25 °C) δ 170.06, 166.22, 165.95, 152.97, 148.61, 147.1, 146.87, 146.53, 146.43, 135.76, 135.69, 135.18, 135.08, 134.32, 133.19, 128.72, 128.67, 127.77, 127.6, 127.31, 126.5, 126.26, 126.01, 125.68, 125.09, 124.87, 82.76, 67.13, 66.63, 64.81, 61.28, 58.90, 58.66, 49.02, 37.06, 32.25, 28.21, 24.87, 22.51; HRMS calculated for C₄₉H₅₆N₄O₁₂Na 915.3792, found 915.3837.

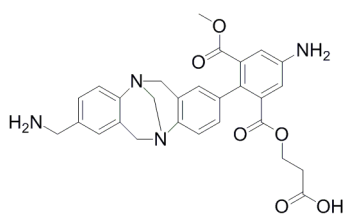
General deprotection procedure (aminomethyl torsion balances, 47a-d): *Step 1* – To the torsion balance (**45a-d**) in CH₂Cl₂ was added trifluoroacetic acid dropwise at 0 °C. The solution was stirred for 30 minutes at room temperature and added to NH₄OH (1 M). The solution was extracted with EtOAc three times, which in turn was washed with brine. The organic extracts were dried over MgSO₄ and filtered, and volatile components of the filtrate were removed under reduced pressure. *Step 2* – To a two-dram vial was added the crude material in methanol and a suspension of 10% palladium/carbon in water. The vial was placed in a Parr shaker bottle and the debenzylation was carried out at 40 psi H₂ for 48 hours. The solution was filtered through a plug of Celite, the volatile components of the filtrate were concentrated under reduced pressure, and the residue was then purified by reverse phase HPLC.



2-Carboxyethyl methyl 2-phenyl-8-aminomethyl-6H,12H-5,11-methanodibenzo[*b,f*][1,5]diazocine-3',6'-dicarboxylate (47a): By

the general deprotection procedure, 0.05 g (0.06 mmol) of the torsion balance **45a** in 0.4 mL of dichloromethane was treated with 0.2 mL (2.73 mmol) of trifluoroacetic acid. Following the workup, to the crude material in 6.2 mL of methanol was then added 0.03 g (10%, 0.03 mmol) of

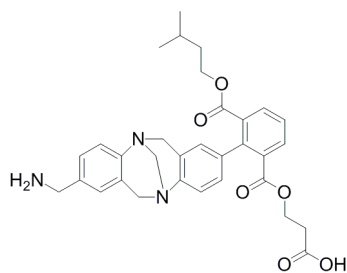
palladium/carbon in 0.7 mL of water and purified by reverse phase HPLC (linear gradient of 80% solvent A to 69% A in solvent B) to provide 24 mg (81% over two steps) of the title compound: IR (KBr pellet) ν 3433, 3700-2500 (broad), 1684, 1435, 1262, 1205, 1136; ^1H NMR (D_2O , 700 MHz) δ 7.89 (dd, 1H, $J = 7.7$ and 18.2 Hz), 7.78 (dd, 1H, $J = 7.7$ and 34.3 Hz), 7.48 (t, 1H, $J = 7.7$ Hz), 7.40 (dd, 2H, $J = 8.4$ and 13.3 Hz), 7.35 (dd, 1H, $J = 8.4$ and 20.3 Hz), 7.20 (d, 1H, $J = 14.7$ Hz), 7.04 (dd, 1H, $J = 8.4$ and 13.3 Hz), 6.86/6.797 {s/s, (0.5/0.4)H}, 4.96 (dd, 1H, $J = 16.8$ and 21.7 Hz), 4.83-4.88 (m, 2H), 4.52 (dd, 1H, $J = 16.8$ and 41.3 Hz), 4.40 (dd, 1H, $J = 16.8$ and 25.2 Hz), 4.23-4.26/3.73 {m/dm, (0.8/1.0)H, $J = 72.1$ Hz}, 3.61/2.90 {s/s, (1.7/1.2)H}, 2.38/1.38-1.43 {dm/m, (0.7/1.1)H, $J = 53.2$ Hz}; ^{13}C NMR (MeOD, 700 MHz, 25 °C) δ 175.99, 171.30, 171.00, 170.56, 164.26, 164.06, 146.12, 144.41, 140.84, 137.76, 134.00, 133.49, 133.42, 133.31, 133.05, 131.13, 129.81, 129.37, 129.32, 128.34, 128.20, 128.07, 127.62, 126.43, 125.27, 118.32, 116.67, 66.75, 62.28, 58.76, 58.48, 54.00, 53.13, 43.65, 33.85, 33.34; HRMS calculated for $\text{C}_{28}\text{H}_{27}\text{NaN}_3\text{O}_6$ 524.1798, found 524.1852.



2-Carboxyethyl methyl 4'-amino-2-phenyl-8-aminomethyl-6H, 12H-5,11-methanodibenzo[*b,f*][1,5]diazocine-3',6'-dicarboxylate (47b): By the general deprotection procedure, 0.05 g (0.06 mmol)

of the torsion balance **45b** in 0.4 mL of dichloromethane was treated with 0.2 mL (2.89 mmol) of trifluoroacetic acid. Following the workup, to the crude material in 6.6 mL of methanol was then added 0.03 g (10%, 0.03 mmol) of palladium/carbon in 0.7 mL of water and purified by reverse phase HPLC (linear gradient of 90% solvent A to 78% A in solvent B) to provide 23 mg (71% over two steps) of the title compound: IR (KBr pellet) ν 3373, 3700-2300 (broad), 1678, 1464, 1263, 1203, 1132; ^1H NMR (D_2O , 700 MHz) δ 7.67 (dd, 1H, $J = 2.1$ and 11.2 Hz), 7.57 (dd, 1H,

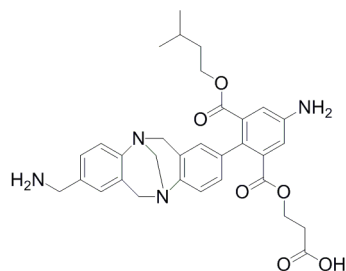
J = 2.8 and 34.3 Hz), 7.39 (dd, 2H, J = 8.4 and 23.8 Hz), 7.19 (d, 1H, J = 16.8 Hz), 7.12 (d, 1H, J = 8.4 Hz), 6.94/6.88 {s/s, (0.5/0.4)H}, 4.95 (dd, 1H, J = 16.8 and 22.4 Hz), 4.87 (t, 2H, J = 16.8 Hz), 4.53 (dd, 1H, J = 16.8 and 35.7 Hz), 4.43 (t, 1H, J = 17.5 Hz), 4.23-4.29/3.74 {m/dm, (0.8/1.0)H, J = 58.1 Hz}, 4.05 (s, 2H), 3.63/2.94 {s/s, (1.7/1.2)H}, 2.38/1.37 {dm/dm, (0.6/1.0)H, J = 58.1 and 11.9 Hz); ¹³C NMR (D₂O, 700 MHz, 25 °C) δ 174.51, 169.40, 169.02, 168.59, 168.27, 163.05, 162.85, 142.33, 139.98, 137.81, 135.22, 134.08, 133.30, 132.46, 131.30, 129.23, 128.28, 127.37, 125.55, 125.43, 126.56, 126.36, 125.16, 124.66, 124.60, 124.33, 120.14, 118.48, 116.83, 67.52, 62.51, 58.35, 58.12, 54.36, 53.50, 43.63, 33.95, 33.29; HRMS calculated for C₂₈H₂₈NaN₄O₆ 539.1907, found 539.1902.



2-Carboxyethyl isopentyl 2-phenyl-8-aminomethyl-6H,12H-5,11-methanodibenzo[b,f][1,5]diazocine-3',6'-dicarboxylate (47c):

By the general deprotection procedure, 0.04 g (0.05 mmol) of the torsion balance **45c** in 0.3 mL of dichloromethane was treated with 0.2 mL (2.10 mmol) of trifluoroacetic acid. Following the workup, to the crude material in 4.9 mL of methanol was then added 0.03 g (10%, 0.02 mmol) of palladium/carbon in 0.5 mL of water and purified by reverse phase HPLC (linear gradient of 70% solvent A to 58% A in solvent B) to provide 13 mg (51% over two steps) of the title compound: IR (KBr pellet) ν 3431, 2959, 3500-2500 (broad), 1717, 1499, 1307, 1280, 1203, 1139; ¹H NMR (D₂O, 700 MHz) δ 7.80 (dd, 1H, J = 7.7 and 48.3 Hz), 7.73 (dd, 1H, J = 9.1 and 28.0 Hz), 7.44-7.46 (m, 1H), 7.31 (d, 2H, J = 9.8 Hz), 7.25 (dd, 1H, J = 8.4 and 28.0 Hz), 7.14 (d, 1H, J = 21.7 Hz), 7.00 (dd, 1H, J = 7.7 and 23.1 Hz), 6.79 (d, 1H, J = 13.3 Hz), 4.68-4.87 (m, 1H), 4.61 (dd, 1H, J = 11.9 and 39.2 Hz), 4.52 (dd, 1H, J = 12.6 and 39.2 Hz), 4.38 (d, 1H, J = 16.8 Hz), 4.29 (t, 1H, J = 15.4 Hz), 4.18-

4.24/3.66 {m/dm, (0.9/1.2)H, J = 86.0 Hz}, 4.02 (s, 2H), 3.96-4.00/3.48 {m/dm, (1.4/0.8)H, J = 77.7 Hz}, 2.33/1.32 {dm/t, (0.6/1.1)H, J = 70.0 Hz and 6.3 Hz}, 1.10/0.50 {s/dd, (1.3/0.9)H, J = 6.3 and 12.6 Hz}, 1.1/0.96-0.99 {signal obscured/m, (0.5/0.3)H}, 0.66-0.69/0.42 {m/dd, (3.9/2.7)H, J = 6.3 and 14.0 Hz}; ^{13}C NMR (MeOD, 700 MHz, 25 °C) δ 175.65, 171.49, 170.82, 170.61, 164.18, 163.98, 145.76, 145.52, 144.40, 140.25, 138.20, 137.97, 134.05, 133.76, 133.44, 133.18, 132.94, 131.35, 130.12, 129.88, 129.40, 128.40, 128.25, 128.14, 127.41, 126.40, 125.44, 125.21, 118.32, 116.67, 67.00, 66.20, 65.83, 62.39, 62.16, 58.58, 58.43, 43.64, 37.41, 36.73, 33.21, 25.29, 25.11, 22.73, 22.59, 22.26; HRMS calculated for $\text{C}_{32}\text{H}_{35}\text{NaN}_3\text{O}_6$ 580.2424, found 580.2431.



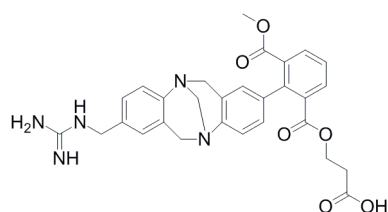
2-Carboxyethyl isopentyl 4'-amino-2-phenyl-8-aminomethyl-6H,12H-5,11-methanodibenzo[b,f][1,5]diazocine-3',6'-dicarboxylate (47d): By the general deprotection procedure, 0.05 g (0.06 mmol) of the torsion balance **45d** in 0.4 mL of

dichloromethane was treated with 0.2 mL (2.10 mmol) of trifluoroacetic acid. Following the workup, to the crude material in 3.7 mL of methanol was then added 0.02 g (10%, 0.02 mmol) of palladium/carbon in 0.4 mL of water and purified by reverse phase HPLC (linear gradient of 80% solvent A to 50% A in solvent B) to provide 10 mg (29% over two steps) of the title compound: IR (KBr pellet) ν 3449.58, 3700-2700 (broad), 1686, 1463, 1204, 1128; ^1H NMR (MeOD, 700 MHz) δ 7.48 (d, 1H, J = 39.9 Hz), 7.41 (dd, 1H, J = 2.1 and 27.3 Hz), 7.34 (d, 2H, J = 23.1 Hz), 7.29 (dd, 1H, J = 8.4 and 27.3 Hz), 7.17 (d, 1H, J = 23.8 Hz), 7.06 (dd, 1H, J = 7.7 and 22.4 Hz), 6.86 (s, 1H), 4.74-4.90 (m, 1H), 4.66 (dd, 1H, J = 12.6 and 42.7 Hz), 4.58 (dd, 1H, J = 13.3 and 34.3 Hz), 4.43 (d, 1H, J = 16.8 Hz), 4.35 (t, 1H, J = 16.1 Hz), 4.22-4.25/3.69

{m/dm, (0.6/0.5)H, J = 81.9 Hz}, 4.03 (s, 2H), 4.01-4.03/3.51 {m/dm, (signal obscured/0.2)H, J = 87.5 Hz}, 2.35/1.34 {dm/dd, (0.4/1.0)H, J = 77.0/6.3 and 13.3 Hz}, 1.13-1.16/0.52-0.54 {m/m, (1.4/0.9)H}, 1.11-1.12/0.99-1.01 {m/m, (signal obscured/0.2)H}, 0.71/0.44 {t/dd, (4.0/3.0)H, J = 7.0/7.0 and 13.3 Hz}; ¹³C NMR (MeOD, 700 MHz, 25 °C) δ 174.47, 174.18, 170.36, 170.31, 170.04, 163.06, 148.89, 148.00, 146.03, 138.40, 135.64, 135.36, 130.90, 130.20, 130.06, 129.32, 128.87, 128.75, 127.98, 127.05, 126.89, 118.88, 68.00, 67.65, 59.44, 59.31, 44.06, 38.20, 26.12, 26.00, 22.97, 22.90; HRMS calculated for C₃₂H₃₆NaN₄O₆ 595.2533, found 595.2559.

General guanylation and deprotection procedure (guanidinomethyl torsion balances, 48a-

d): Step 1 – To torsion balance **45a-d** in CH₂Cl₂ was added trifluoroacetic acid dropwise at 0 °C. The solution was stirred for 30 minutes at room temperature and added to NH₄OH (1 M). The solution was extracted with EtOAc, which in turn was washed with brine. The organic extracts were dried over MgSO₄ and filtered, and volatile components of the filtrate were removed under reduced pressure. **Step 2** – To the crude material in DMF was added Hünig's base (DIPEA) and pyrazole-1-carboxamide hydrochloride. The reaction was stirred at room temperature for 8 hours. The reaction was diluted with water and extracted with EtOAc. The organic extracts were dried over MgSO₄ and filtered, and volatile components of the filtrate were removed under reduced pressure. **Step 3** – To a two-dram vial was added the crude guanylated torsion balances in methanol and 10% palladium/carbon suspended in water. The vial was placed in a Parr shaker bottle and the debenzoylation was carried out at 40 psi H₂ for 48 hours. The solution was filtered through a plug of Celite, the volatile components of the filtrate were concentrated under reduced pressure, and the residue was then purified by reverse phase HPLC.

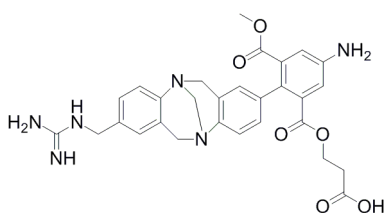


2-Carboxyethyl methyl 2-phenyl-8-guanidinomethyl-6H,12H-

5,11-methanodibenzo[*b,f*][1,5]diazocine-3',6'-dicarboxylate

(48a): By the general guanylation and deprotection procedure,

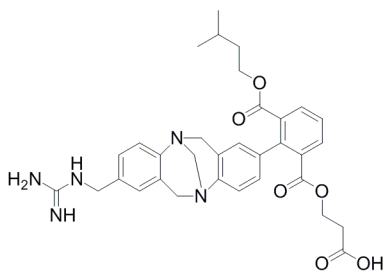
0.03 g (0.04 mmol) of the torsion balance **45a** in 0.3 mL of dichloromethane was treated with 0.1 mL (1.93 mmol) of trifluoroacetic acid. The crude material was dissolved in 0.04 mL of anhydrous DMF and reacted with 0.02 mL of DIPEA and 0.01 g of pyrazole-1-carboxamide hydrochloride. Following the workup, to the crude material in 4.4 mL of methanol was then added 0.02 g (10%, 0.02 mmol) of palladium/carbon in 0.5 mL of water and purified by reverse phase HPLC (linear gradient of 90% solvent A to 78% A in solvent B) to provide 15 mg (66% over three steps) of the title compound: IR (KBr pellet) ν 3433, 3600-2700 (broad), 1685, 1205; ^1H NMR (MeOD, 700 MHz, 25 °C) δ 8.00 (t, 1H, $J = 8.4$ Hz), 7.89 (dd, 1H, $J = 7$ and 32.9 Hz), 7.614 (s, 1H), 7.41-7.46 (m, 2H), 7.37 (s, 1H), 7.17 (s, 2H), 6.94 (d, 1H, $J = 42.7$ Hz), 4.88-5.01 (m, 4H), 4.52 (dd, 1H, $J = 16.8$ and 80.5 Hz), 4.51 (d, 1H, $J = 16.1$ Hz), 4.38 (s, 2H), 4.31/3.78 {s/dm, (0.8/0.9)H, $J = 78.4$ Hz}, 3.68/2.92 {s/s, (1.6/1.1)H}, 2.46/1.42 {dm/dm, (0.5/0.9)H, $J = 64.4$ and 20.3 Hz}; ^{13}C NMR (MeOD, 700 MHz, 25 °C) δ 175.61, 175.27, 171.27, 170.78, 170.44, 170.04, 163.99, 163.79, 158.00, 141.50, 141.34, 140.62, 139.45, 137.04, 133.81, 133.69, 133.60, 133.20, 133.06, 130.04, 129.60, 128.73, 128.42, 128.31, 127.27, 126.83, 126.83, 126.83, 125.05, 118.39, 116.73, 67.80, 67.60, 62.34, 62.05, 58.49, 58.20, 53.87, 52.86, 44.81, 33.87, 33.14; HRMS calculated for $\text{C}_{29}\text{H}_{29}\text{NaN}_5\text{O}_6$ 566.2016, found 566.2009.



2-Carboxyethyl methyl 4'-amino-2-phenyl-8-guanidinomethyl-

6H,12H-5,11-methanodibenzo[*b,f*][1,5]diazocine-3',6'-

dicarboxylate (48b): By the general guanylation and deprotection procedure, 0.04 g (0.04 mmol) of the torsion balance **45b** in 0.3 mL of dichloromethane was treated with 0.1 mL (1.91 mmol) of trifluoroacetic acid. The crude material was dissolved in 0.04 mL of anhydrous DMF and reacted with 0.02 mL of DIPEA and 0.01 g of pyrazole-1-carboxamide hydrochloride. Following the workup, to the crude material in 4.4 mL of methanol was then added 0.02 g (10%, 0.02 mmol) of palladium/carbon in 0.5 mL of water and purified by reverse phase HPLC (linear gradient of 90% solvent A to 78% A in solvent B) to provide 12 mg (51% over three steps) of the title compound: IR (KBr pellet) ν 3449, 3700-2700 (broad), 1686, 1464, 1351, 1264, 1205; ^1H NMR (D_2O , 700 MHz, 5 °C) δ 7.37/7.27 {d/d, (0.3/0.5)H, J = 2.1/2.8 Hz}, 7.35/7.21 {d/d, (0.8/0.3)H, J = 1.4/2.1 Hz}, 7.14 (t, 1H, J = 8.4 Hz), 7.10-7.12 (m, 1H), 7.07 (d, 1H, J = 7.7 Hz), 6.90 (s, 1H), 6.87 (d, 1H, J = 16.1 Hz), 6.71/6.63 {s/s, (0.5/0.3)H}, 4.67 (dd, 1H, J = 16.1 and 24.5 Hz), 4.58-4.65 (m, 1H), 4.56 (s, 1H), 4.27 (dd, 1H, J = 16.8 and 48.3 Hz), 4.20 (d, 1H, J = 17.5 Hz), 4.11 (d, 2H, J = 9.1 Hz), 4.01-4.08/3.51 {m/dm, (0.5/1.0)H, J = 76.3}, 3.44/2.67 {s/s, (1.8/0.9)H}, 2.16/0.98 {dm/dm (0.4/0.9)H, J = 87.5/93.1 Hz}; ^{13}C NMR (MeOD, 700 MHz, 25 °C) δ 174.22, 170.21, 158.74, 148.89, 148.41, 146.90, 137.73, 135.25, 133.88, 129.91, 129.84, 129.57, 128.80, 128.19, 127.77, 127.32, 126.70, 125.20, 118.35, 118.27, 67.95, 67.40, 64.85, 64.05, 61.81, 59.74, 45.60; HRMS calculated for $\text{C}_{29}\text{H}_{31}\text{N}_6\text{O}_6$ 559.2305, found 559.2290.

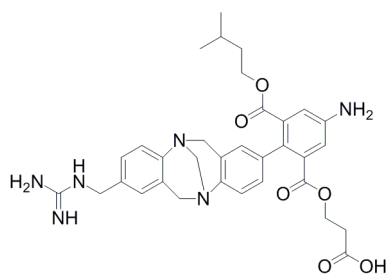


**2-Carboxyethyl isopentyl 2-phenyl-8-guanidinomethyl-6H,
12H-5,11-methanodibenzo[b,f][1,5]diazocine-3',6'-**

dicarboxylate (48c): By the general guanylation and deprotection procedure, 0.05 g (0.05 mmol) of the torsion balance **45c** in 0.4

mL of dichloromethane was treated with 0.2 mL (2.44 mmol) of trifluoroacetic acid. The crude

material was dissolved in 0.05 mL of anhydrous DMF and reacted with 0.02 mL of DIPEA and 0.02 g of pyrazole-1-carboxamide hydrochloride. Following the workup, to the crude material in 2.8 mL of methanol was then added 0.01 g (10%, 0.01 mmol) of palladium/carbon in 0.3 mL of water and purified by reverse phase HPLC (linear gradient of 70% solvent A to 58% A in solvent B) to provide 21.6 mg (68% over three steps) of the title compound: IR (KBr pellet) ν 2411, 2959, 3700-2700 (broad), 1686, 1309, 1204, 1137; ^1H NMR (MeOD, 600 MHz, 25 °C) δ 7.81 (d, 2H, $J = 14.4$ Hz), 7.52 (t, 1H, $J = 7.8$ Hz), 7.19 (dd, 3H, $J = 8.4$ and 22.8 Hz), 6.98 (d, 2H, $J = 7.8$ Hz), 6.77 (d, 1H, $J = 1.8$ Hz), 4.72 (dd, 2H, $J = 16.8$ and 31.2 Hz), 4.39 (s, 2H), 4.30 (s, 4H), 4.22/3.75 {s/d, (0.9/1.4)H, $J = 108.6$ Hz}, 4.04/3.68 {s/d, (1.2/0.8)H, $J = 81.6$ Hz}, 2.33/1.61 {d/s, (0.3/1.0)H, $J = 49.8$ Hz}, 1.39/~1.3 {s/signal obscured, (0.6/signal obscured)H}, 1.26/~0.9 {s/signal obscured, (1.3/signal obscured)H}, 0.85/0.69 {s/s, (4.2/2.2)H}; ^{13}C NMR (MeOD, 600 MHz, 25 °C) δ 174.73, 170.56, 170.23, 163.79, 163.57, 159.29, 149.22, 148.84, 141.94, 137.46, 135.66, 135.39, 134.29, 133.26, 130.22, 129.80, 129.30, 129.12, 128.86, 127.96, 127.88, 127.35, 126.23, 68.60, 65.62, 62.38, 60.21, 60.13, 46.25, 38.91, 34.30, 26.59, 23.47; HRMS calculated for $\text{C}_{31}\text{H}_{37}\text{NaN}_5\text{O}_6$ 622.2642, found 622.2620.

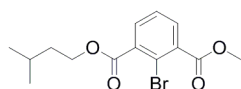


2-Carboxyethyl isopentyl 4'-amino-2-phenyl-8-guanidino-methyl-6H,12H-5,11-methanodibenzo[*b,f*][1,5]diazocine-

3',6'-dicarboxylate (48d):

By the general guanylation and deprotection procedure, 0.09 g (0.10 mmol) of the torsion balance **45d** in 0.7 mL of dichloromethane was treated with 0.3 mL (4.48 mmol) of trifluoroacetic acid. The crude material was dissolved in 0.10 mL of anhydrous DMF and reacted with 0.03 mL of DIPEA and 0.03 g of pyrazole-1-carboxamide hydrochloride. Following the

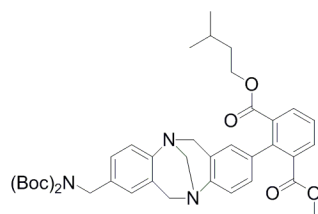
workup, to the crude material in 2.6 mL of methanol was then added 0.01 g (10%, 0.01 mmol) of palladium/carbon in 0.3 mL of water and purified by reverse phase HPLC (linear gradient of 80% solvent A to 66% A in solvent B) to provide 25.2 mg (42% over three steps) of the title compound: IR (KBr pellet) ν 3368, 2961, 3800-2800 (broad), 1675, 1465, 1349, 1260, 1199, 1134; ^1H NMR (MeOD, 700 MHz, 5 °C) δ 7.34 (d, 1H, J = 8.4 Hz), 7.28 (dd, 2H, J = 11.9 and 21.0 Hz), 7.21 (d, 2H, J = 25.2 Hz), 7.03-7.11 (m, 2H), 6.83 (s, 1H), 4.90 (td, 2H, J = 16.1 and 46.6 Hz), 4.70 (s, 2H), 4.45 (dd, 2H, J = 17.5 and 44.1 Hz), 4.40 (s, 2H), 4.19/3.75 {s/d, (1.0/1.4)H, J = 125.3 Hz}, 4.03/3.69 {d/d, (1.4/0.8)H, J = 5.6 and 74.9 Hz}, 2.34/1.62 {d/d, (0.9/1.4)H, J = 69.3 and 5.6 Hz}, 1.44/1.33 {s/s, (0.8/0.6)H}, 1.30/0.92 {s/s, (1.8/1.1)H}, 0.87/0.70 {d/s, (3.8/2.2)H, J = 5.6 Hz}; ^{13}C NMR (MeOD, 700 MHz, 25 °C) δ 174.11, 170.06, 169.82, 162.58, 162.36, 158.81, 147.67, 146.15, 144.65, 139.09, 135.55, 135.32, 130.37, 128.95, 128.42, 128.32, 127.48, 126.64, 125.15, 119.14, 118.78, 117.13, 68.13, 64.87, 64.81, 61.80, 59.08, 45.52, 38.34, 33.77, 26.06, 22.90; HRMS calculated for $\text{C}_{33}\text{H}_{39}\text{N}_6\text{O}_6$ 615.2931, found 615.2948.



2-Bromoisophthalic acid 1-isopentyl ester 3-methyl ester (49): By the general esterification procedure, 0.05 mL (0.5 mmol) of isoamyl alcohol,

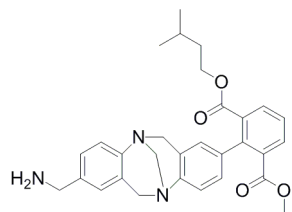
0.16 g (0.8 mmol) of DCC and 0.01 g (0.1 mmol) of DMAP in 2.0 mL of dry CH_2Cl_2 treated with 0.10 g (0.4 mmol) of the carboxylic acid **36**, provided 0.10 g (81%) of the title compound as an oil: IR (thin film) ν 2957, 1734, 1307, 1283, 1254, 1202, 1150; ^1H NMR (CDCl_3 , 300 MHz) δ 7.66 (dd, 1H, J = 1.8 and 5.1 Hz), 7.63 (dd, 1H, J = 1.8 and 5.4 Hz), 7.36 (t, 1H, J = 7.5 Hz), 1.73 (sextet, 1H, J = 6.6 Hz), 1.61 (q, 2H, J = 6.9 Hz), 0.91 (d, 6H, J = 6.6 Hz); ^{13}C NMR (CDCl_3 , 300

MHz) δ 167.04, 166.76, 135.98, 135.36, 132.24, 132.22, 127.25, 119.02, 64.78, 52.88, 37.27, 25.13, 22.54; HRMS calculated for $C_{14}H_{17}BrNaO_4$ 351.0208, found 351.0199.



Isopentyl methyl 2-phenyl-8-((di-tert-butoxycarbonylamino)-methyl)-6H,12H-5,11-methanodibenzo[*b,f*][1,5]diazocine-3',6'-

dicarboxylate (50): By the general Suzuki coupling procedure, 0.04 g (0.13 mmol) of isophthalate **49**, 0.05 g (0.08 mmol) of the pinacolatoboronate **34**, and 5 mg (0.008 mmol) of the palladium catalyst in 0.4 mL of DME were treated with 0.04 g (0.50 mmol) of sodium bicarbonate in 0.4 mL of water and purified by column chromatography (pentane: Et₂O, 2:1) to provide 0.03 g (44%) of the title compound: IR (thin film) ν 2956, 1721, 1367, 1304, 1144; ¹H NMR (CDCl₃, 300 MHz, 25 °C) δ 7.76 (d, 2H, J = 17.1 Hz), 7.39 (t, 1H, J = 7.8 Hz), 7.06 (dd, 3H, J = 8.4 and 12.4 Hz), 6.97 (d, 1H, J = 8.7 Hz), 6.85 (s, 1H), 6.70 (s, 1H), 4.66 (d, 2H, J = 16.5 Hz), 4.59 (s, 2H), 4.33 (s, 2H), 4.12 (dd, 2H, J = 8.1 and 16.8 Hz), 4.04/3.41 {s/s, (0.9/0.4)H}, 3.58/2.75 {s/s, (0.9/1.5)}, 1.42 (s, 18H), 1.23 (broad m, 3H), 0.80/0.65 {s/s, (4.6/1.5)H}; ¹³C NMR (CDCl₃, 300 MHz, 25 °C) δ 169.16, 168.50, 152.89, 147.44, 147.13, 140.51, 135.17, 134.25, 133.11, 133.00, 131.81, 131.62, 127.94, 127.78, 127.33, 127.28, 126.97, 126.19, 124.97, 124.35, 82.73, 77.44, 67.49, 63.97, 59.27, 51.49, 49.04, 37.14, 29.89, 28.23, 24.84, 22.55; HRMS calculated for $C_{40}H_{49}NaN_3O_8$ 722.3417, found 722.3401.



Isopentyl methyl 2-phenyl-8-aminomethyl-6H,12H-5,11-methanodibenzo[*b,f*][1,5]diazocine-3',6'-dicarboxylate (51):

By the general deprotection procedure, 0.05 g (0.05 mmol) of the torsion balance **50** in 0.4 mL of dichloromethane was treated with 0.2 mL (2.10 mmol) of trifluoroacetic acid to

provide the title compound in quantitative yield: IR (thin film) ν 2955, 2925, 1718, 1496, 1307, 1280, 1203, 1136; ^1H NMR (CDCl_3 , 300 MHz, 25 °C) δ 7.76 (d, 2H, $J = 15.3$ Hz), 7.40 (t, 1H, $J = 8.1$ Hz), 7.04 (s, 3H), 6.95 (d, 1H, $J = 7.5$ Hz), 6.84 (s, 1H), 6.65 (s, 1H), 4.59 (t, 2H, $J = 17.1$ Hz), 4.26 (s, 2H), 4.05 (d, 2H, $J = 16.2$ Hz), $\sim 4.1/3.59$ {signal obscured/s, ($\sim 1.0/1.2$)H}, 3.64/2.93 {s/s, (1.8/1.4)H}, 1.2-1.3 (m, 3H), 0.80/0.64 {s/s, (4.4/1.5)H}; ^{13}C NMR (CDCl_3 , 300 MHz, 25 °C) δ 169.15, 168.47, 162.09, 148.38, 147.40, 140.50, 134.96, 133.60, 133.48, 131.91, 131.69, 128.57, 128.04, 127.71, 127.41, 127.36, 127.02, 125.53, 124.50, 124.37, 67.21, 64.05, 58.85, 51.72, 44.15, 38.11, 29.92, 24.91, 22.55; HRMS calculated for $\text{C}_{30}\text{H}_{33}\text{NaN}_3\text{O}_4$ 522.2369, found 522.2390.

6.2 PREPARATION OF BUFFER SOLUTIONS

Preparation of Stock Solutions

Deuterium chloride (35% wt in D_2O) was purchased from Aldrich. To a 5 mL volumetric flask was added 0.043 mL of the DCl solution, which was diluted to 5 mL with D_2O . This stock solution was 0.10 M in DCl and was used to adjust the pD of the buffer solutions.

Sodium deuterioxide (40% wt in D_2O) was purchased from Cambridge Isotopes. To a 5 mL volumetric flask was added 0.035 mL of the concentrated NaOD solution, which was diluted to 5 mL with D_2O . This stock solution was 0.10 M in NaOD and used to adjust the pD of the buffer solutions.

Preparation of the 0.050 M Potassium Deuterium Phthalate Buffers

A solution of 2.0 g of potassium hydrogen phthalate (KHP) in 20 mL of D₂O was dried by lyophilization. The solid was redissolved in another 20 mL portion of D₂O, and the solvent was again removed by lyophilization.

A solution of 0.1026 g of the deuterated potassium salt and 2.2 mL of the 0.10 M DCl stock solution was diluted to 10 mL with D₂O in a 10 mL volumetric flask. The solution was 0.050 M in phthalate and was used as an NMR solvent for the torsion balances. The pD of the solution was calculated as 3.1, which was determined by adding 0.4 to a reading taken from a glass electrode pH meter.¹⁶⁰

A solution of 0.1026 g of the deuterated potassium salt and 2.2 mL of the 0.10 M NaOD stock solution was diluted to 10 mL with D₂O in a 10 mL volumetric flask. The solution was 0.050 M in phthalate and was used as an NMR solvent for the torsion balances. The pD of the solution was calculated as 5.5.

Preparation of the 0.050 M Deuterated Phosphate Buffer

A solution of 1.4196 g (0.0100 mol) of Na₂HPO₄ and 1.3609 g (0.0100 mol) of KH₂PO₄ in 10 mL of D₂O was dried by lyophilization. The solid mixture was redissolved in another portion of D₂O, and the solvent again was removed by lyophilization. The deuterated solid was transferred to a 100 mL volumetric flask and diluted to 100 mL with D₂O. This stock solution was 0.200 M in phosphate and diluted to 0.050 M by standard methods. The 0.050 M solution was used as an NMR solvent for the torsion balances. The pD of the solution was calculated as 7.2.

Preparation of the 0.050 M Deuterated Borate Buffer

A solution of 0.0478 g of sodium tetraborate and 0.4 mL of the 0.10 M DCl stock solution was diluted to 10 mL with D₂O in a 10 mL volumetric flask. The solution was 0.050 M in borate and was used as an NMR solvent for the torsion balances. The pD of the solution was calculated as 10.0.

6.3 ERROR ANALYSIS

For torsion balances **26a-c**, **27a-c**, **28a-d**, and **29a-b**, NMR simulations were conducted on three sets of protons: the inner methylene, and outer methyl of the propyl group, and the bromoethyl group. NMR simulations were conducted on the methyl ester or the methyl of the isoamyl group for torsion balances **47a-d** and **48a-d**. In Figure 23, a simulation of a bromoethyl group (blue) was overlaid with the experimental spectrum of **26a** (red). The simulated spectrum was similar to the experimental one and was sensitive to changes in the folding ratio. Changes as little as 1.5% to the overall folding percent led to distinct discrepancies between observed and calculated spectra. The error in the percent of the folded conformer was minimized in Figure 23, whereas a 1.5% decrease and increase in the folding ratios were featured in Figures 24 and 25 respectively. Therefore, a $\pm 1.5\%$ error was estimated for the folding ratios for the torsion balances.

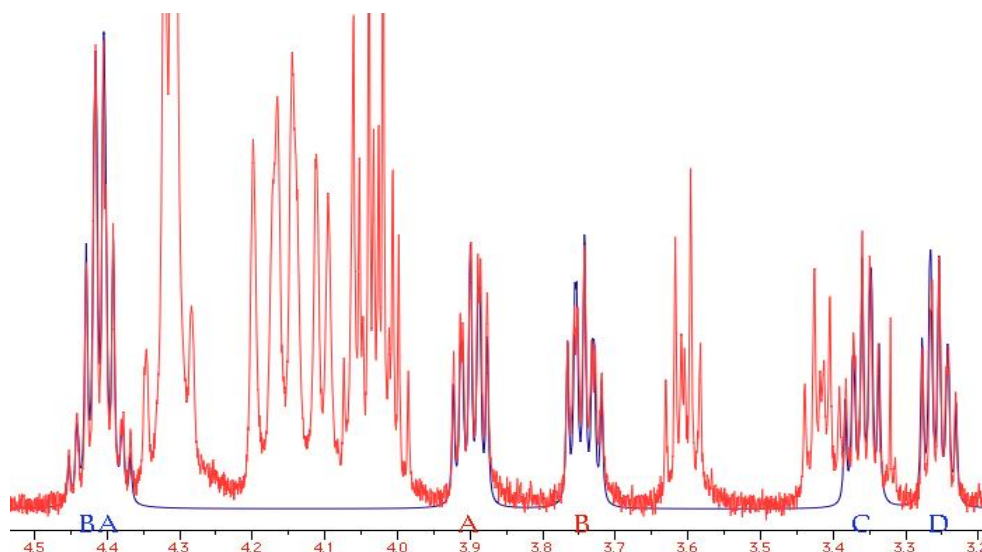


Figure 23. A simulation of the bromoethyl protons (blue) overlaid with the experimental spectrum (red) of 26a at -5 °C.

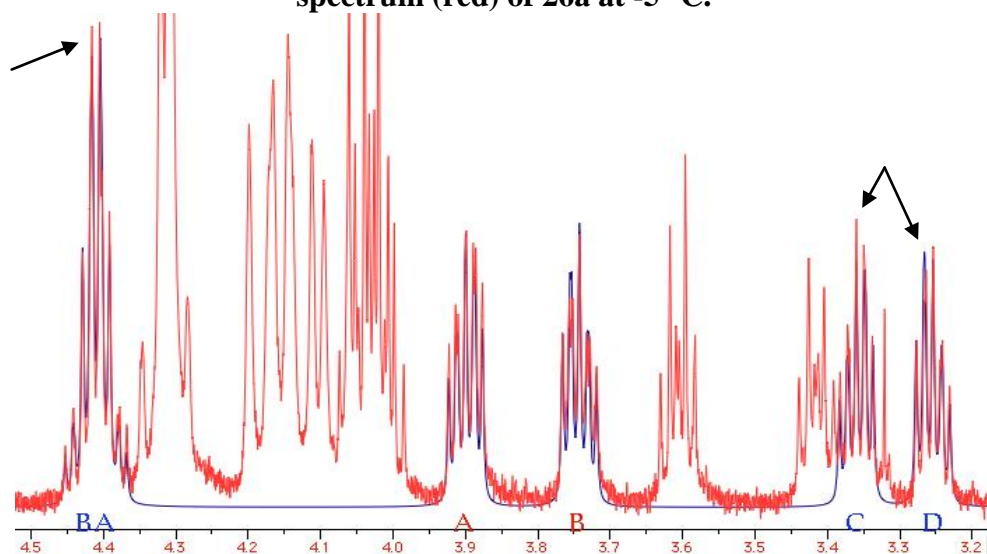


Figure 24. A simulation of the bromoethyl group with a 1.5% reduction in the folding ratio.

The error for the folding energies can be determined by multiplying the derivative of the energy equation by the error in the folding percentages ($\pm 1.5\%$). The Gibbs free energy equation (Equation 2) was redefined in terms of the folding energy. The equilibrium constant was written in terms of folding percentage, x (Equation 3), which was plugged into Equation 2.

$$\Delta G^\circ = -RT \ln K_{eq} \quad (\text{Equation 2})$$

$$K_{eq} = \frac{x}{100-x} \quad (\text{Equation 3})$$

$$\Delta G^\circ = -RT \ln \frac{x}{100-x} \quad (\text{Equation 4})$$

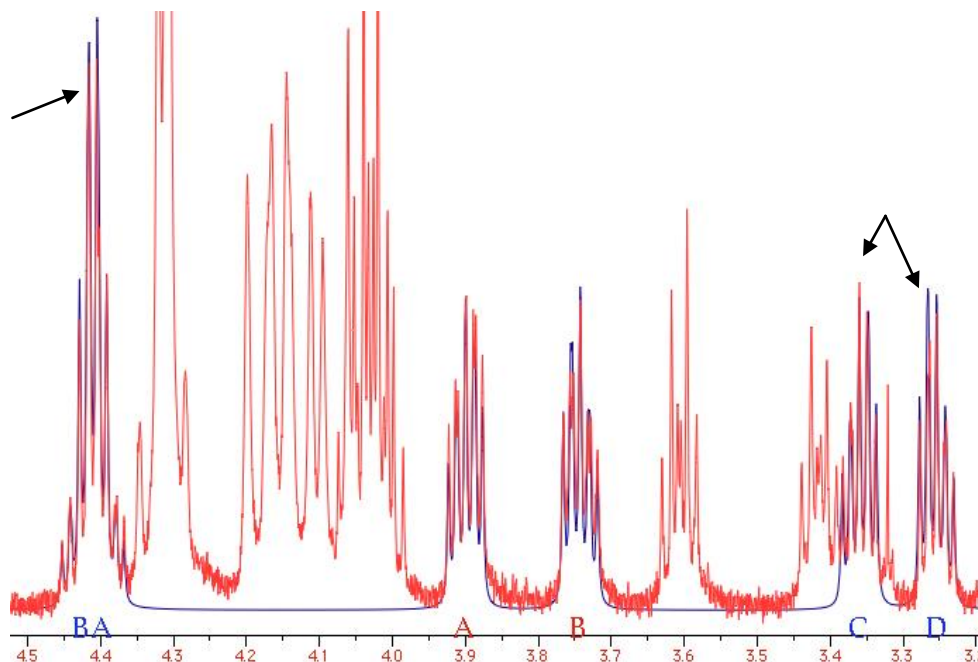


Figure 25. A simulation of the bromoethyl group with a 1.5% increase in the folding ratio.

The derivative of Equation 4 is

$$\frac{d(\Delta G^\circ)}{dx} = -RT \frac{100}{x(100-x)} \quad (\text{Equation 5})$$

in which x is the folding percentage. The error for the folding energies is the product of Equation 5 multiplied by Δx (1.5%, Equation 6) and the relative error is given by Equation 7.

$$\Delta(\Delta G^\circ) = \left(\frac{d(\Delta G^\circ)}{dx} \right) \Delta x = -\frac{100RT}{x(100-x)} \Delta x \quad (\text{Equation 6})$$

$$\frac{\Delta \Delta G^\circ}{\Delta G^\circ} = \frac{\frac{100RT}{x(100-x)} \Delta x}{-RT \ln \left(\frac{x}{100-x} \right)} = \frac{\Delta x}{\ln \left(\frac{x}{100-x} \right) \frac{100-x}{100} \frac{x}{100}} \quad (\text{Equation 7})$$

At 55% folding with a temperature of 268 K, the folding energy is -0.107 kcal/mol with an absolute error of ± 0.03 kcal/mol and a relative error of $\pm 30\%$. At 65% folding, the folding energy is -0.329 kcal/mol with an absolute error of ± 0.035 kcal/mol. The relative error is $\pm 11\%$. At 75% folding, the folding energy is -0.585 kcal/mol, the absolute error is 0.43, and the relative error is 7%. A graph that depicts the relative error in the folding energies with relation to the folding ratios, assuming a $\pm 1.5\%$ error in the folding ratios, is shown in Figure 26. Therefore, we estimated the relative error in the range of 55% to 75% folding to be $\pm 15\%$ in folding energy.

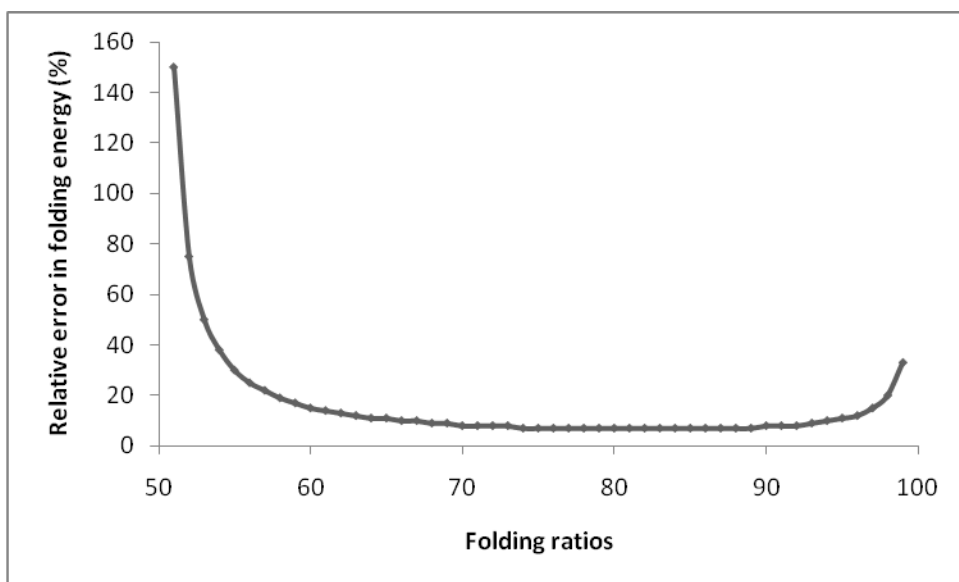


Figure 26. Relative error in folding energies versus folding ratios for a $\pm 1.5\%$ error in folding ratios.

7.0 BIBLIOGRAPHY

- (1) Troeger, J. J. *Prakt. Chem.* **1887**, *36*, 225-245.
- (2) Spielman, M. A. *J. Am. Chem. Soc.* **1935**, *57*, 583-585.
- (3) Wilcox, C. S.; Cowart, M. D. *Tetrahedron Lett.* **1986**, *27*, 5563-5566.
- (4) Cowart, M. D.; Sucholeiki, I.; Bukownik, R. R.; Wilcox, C. S. *J. Am. Chem. Soc.* **1988**, *110*, 6204-6210.
- (5) Adrian, J. C., Jr.; Wilcox, C. S. *J. Am. Chem. Soc.* **1991**, *113*, 678-680.
- (6) Adrian, J. C., Jr.; Wilcox, C. S. *J. Am. Chem. Soc.* **1992**, *114*, 1398-1403.
- (7) Wilcox, C. S.; Adrian, J. C., Jr.; Webb, T. H.; Zawacki, F. J. *J. Am. Chem. Soc.* **1992**, *114*, 10189-10197.
- (8) Goswami, S.; Ghosh, K.; Dasgupta, S. *J. Org. Chem.* **2000**, *65*, 1907-1914.
- (9) Paliwal, S.; Geib, S.; Wilcox, C. S. *J. Am. Chem. Soc.* **1994**, *116*, 4497-4498.
- (10) Cox, E. G.; Cruickshank, D. W. J.; Smith, J. A. S. *Proc. R. Soc. London, Ser. A* **1958**, *247*, 1-21.
- (11) Singh, J.; Thornton, J. M. *FEBS Lett.* **1985**, *191*, 1-6.
- (12) Burley, S. K.; Petsko, G. A. *J. Am. Chem. Soc.* **1986**, *108*, 7995-8001.
- (13) Burley, S. K.; Petsko, G. A. *Science*. **1985**, *229*, 23-28.
- (14) Jorgensen, W. L.; Severance, D. L. *J. Am. Chem. Soc.* **1990**, *112*, 4768-4774.

- (15) Hobza, P.; Selzle, H. L.; Schlag, E. W. *J. Am. Chem. Soc.* **1994**, *116*, 3500-3506.
- (16) Kim, E.-i.; Paliwal, S.; Wilcox, C. S. *J. Am. Chem. Soc.* **1998**, *120*, 11192-11193.
- (17) Gouverneur, V. *Science*. **2009**, *325*, 1630-1631.
- (18) Mueller, K.; Faeh, C.; Diederich, F. *Science*. **2007**, *317*, 1881-1886.
- (19) Olsen, J. A.; Banner, D. W.; Seiler, P.; Wagner, B.; Tschopp, T.; Obst-Sander, U.; Kansy, M.; Mueller, K.; Diederich, F. *ChemBioChem*. **2004**, *5*, 666-675.
- (20) Hof, F.; Scofield, D. M.; Schweizer, W. B.; Diederich, F. *Angew. Chem., Int. Ed.* **2004**, *43*, 5056-5059.
- (21) Adams, H.; Carver, F. J.; Hunter, C. A.; Morales, J. C.; Seward, E. M. *Angew. Chem., Int. Ed. Engl.* **1996**, *35*, 1542-1544.
- (22) Fischer, F. R.; Schweizer, W. B.; Diederich, F. *Angew. Chem., Int. Ed.* **2007**, *46*, 8270-8273.
- (23) Bhayana, B.; Wilcox, C. S. *Angew. Chem., Int. Ed.* **2007**, *46*, 6833-6836.
- (24) Ramasubbu, N.; Parthasarathy, R.; Murray-Rust, P. *J. Am. Chem. Soc.* **1986**, *108*, 4308-4314.
- (25) Auffinger, P.; Hays, F. A.; Westhof, E.; Ho, P. S. *Proc. Natl. Acad. Sci. U. S. A.* **2004**, *101*, 16789-16794.
- (26) Legon, A. C. *Struct. Bonding*. **2008**, *126*, 17-64.
- (27) Cody, V.; Murray-Rust, P. *J. Mol. Struct.* **1984**, *112*, 189-199.
- (28) Lommerse, J. P. M.; Stone, A. J.; Taylor, R.; Allen, F. H. *J. Am. Chem. Soc.* **1996**, *118*, 3108-3116.
- (29) Metrangolo, P.; Neukirch, H.; Pilati, T.; Resnati, G. *Acc. Chem. Res.* **2005**, *38*, 386-395.
- (30) Xu, K.; Ho, D. M.; Pascal, R. A., Jr. *J. Am. Chem. Soc.* **1994**, *116*, 105-110.

- (31) Valerio, G.; Raos, G.; Meille, S. V.; Metrangolo, P.; Resnati, G. *J. Phys. Chem. A* **2000**, *104*, 1617-1620.
- (32) Corradi, E.; Meille, S. V.; Messina, M. T.; Metrangolo, P.; Resnati, G. *Angew. Chem., Int. Ed.* **2000**, *39*, 1782-1786.
- (33) Martinez Amezaga, N. J.; Pamies, S. C.; Peruchena, N. M.; Sosa, G. L. *J. Phys. Chem. A* **2010**, *114*, 552-562.
- (34) Price, S. L.; Stone, A. J.; Lucas, J.; Rowland, R. S.; Thornley, A. E. *J. Am. Chem. Soc.* **1994**, *116*, 4910-4918.
- (35) Nyburg, S. C.; Wong-Ng, W. *Proc. R. Soc. London, Ser. A* **1979**, *367*, 29-45.
- (36) Clark, T.; Hennemann, M.; Murray, J. S.; Politzer, P. *J. Mol. Model.* **2007**, *13*, 291-296.
- (37) Riley, K. E.; Merz, K. M., Jr. *J. Phys. Chem. A* **2007**, *111*, 1688-1694.
- (38) Lu, Y.-X.; Zou, J.-W.; Wang, Y.-H.; Jiang, Y.-J.; Yu, Q.-S. *J. Phys. Chem. A* **2007**, *111*, 10781-10788.
- (39) Guthrie, F. *J. Chem. Soc., Trans.* **1863**, *16*, 239-244.
- (40) Hassel, O.; Hvoslef, J. *Acta Chem. Scand.* **1954**, *8*, 873.
- (41) Bent, H. A. *Chem. Rev.* **1968**, *68*, 587-648.
- (42) Dumas, J. M.; Gomel, M.; Guerin, M. In *The Chemistry of Functional Groups, Supplement D*; Patai, S., Rappoport, Z., Eds.; John Wiley & Sons, Ltd.: New York, 1983, p 985-1020.
- (43) Muzet, N.; Guillot, B.; Jelsch, C.; Howard, E.; Lecomte, C. *Proc. Natl. Acad. Sci. U. S. A.* **2003**, *100*, 8742-8747.

- (44) Howard, E. I.; Sanishvili, R.; Cachau, R. E.; Mitschler, A.; Chevrier, B.; Barth, P.; Lamour, V.; Van Zandt, M.; Sibley, E.; Bon, C.; Moras, D.; Schneider, T. R.; Joachimiak, A.; Podjarny, A. *Proteins: Struct., Funct., Bioinf.* **2004**, *55*, 792-804.
- (45) Hays, F. A.; Vargason, J. M.; Ho, P. S. *Biochemistry.* **2003**, *42*, 9586-9597.
- (46) Holliday, R. *Genet. Res.* **1964**, *5*, 282-304.
- (47) Voth, A. R.; Hays, F. A.; Ho, P. S. *Proc. Natl. Acad. Sci. U. S. A.* **2007**, *104*, 6188-6193.
- (48) Bouchmella, K.; Boury, B.; Dutremez, S. G.; van der Lee, A. *Chem.--Eur. J.* **2007**, *13*, 6130-6138.
- (49) Aakeroey, C. B.; Schultheiss, N. C.; Rajbanshi, A.; Desper, J.; Moore, C. *Cryst. Growth Des.* **2009**, *9*, 432-441.
- (50) Aakeroey, C. B.; Fasulo, M.; Schultheiss, N.; Desper, J.; Moore, C. *J. Am. Chem. Soc.* **2007**, *129*, 13772-13773.
- (51) Tawarada, R.; Seio, K.; Sekine, M. *J. Org. Chem.* **2008**, *73*, 383-390.
- (52) Kraut, D. A.; Churchill, M. J.; Dawson, P. E.; Herschlag, D. *ACS Chem. Biol.* **2009**, *4*, 269-273.
- (53) Groth, P.; Hassel, O. *Acta Chem. Scand.* **1964**, *18*, 402-408.
- (54) Di Paolo, T.; Sandorfy, C. *Can. J. Chem.* **1974**, *52*, 3612-3622.
- (55) Di Paolo, T.; Sandorfy, C. *Chem. Phys. Lett.* **1974**, *26*, 466-469.
- (56) Abraham, M. H.; Platts, J. A. *J. Org. Chem.* **2001**, *66*, 3484-3491.
- (57) Wash, P. L.; Ma, S.; Obst, U.; Rebek, J., Jr. *J. Am. Chem. Soc.* **1999**, *121*, 7973-7974.
- (58) Xu, K.; Ho, D. M.; Pascal, R. A., Jr. *J. Org. Chem.* **1995**, *60*, 7186-7191.
- (59) Blackstock, S. C.; Kochi, J. K. *J. Am. Chem. Soc.* **1987**, *109*, 2484-2496.
- (60) Cabot, R.; Hunter, C. A. *Chem. Commun.* **2009**, 2005-2007.

- (61) Sarwar, M. G.; Dragisic, B.; Salsberg, L. J.; Gouliaras, C.; Taylor, M. S. *J. Am. Chem. Soc.* **2010**, *132*, 1646-1653.
- (62) Bailey, W. J.; Economy, J. *J. Org. Chem.* **1958**, *23*, 1002-1004.
- (63) Guo, W.; Li, J.; Fan, N.; Wu, W.; Zhou, P.; Xia, C. *Synth. Commun.* **2005**, *35*, 145-152.
- (64) Debdab, M.; Mongin, F.; Bazureau, J. P. *Synthesis*. **2006**, 4046-4052.
- (65) Ariafard, A.; Lin, Z. *Organometallics*. **2006**, *25*, 4030-4033.
- (66) Ishiyama, T.; Abe, S.; Miyaura, N.; Suzuki, A. *Chem. Lett.* **1992**, 691-694.
- (67) Netherton, M. R.; Dai, C.; Neuschuetz, K.; Fu, G. C. *J. Am. Chem. Soc.* **2001**, *123*, 10099-10100.
- (68) Jensen, J.; Strozyk, M.; Warnmark, K. *J. Heterocycl. Chem.* **2003**, *40*, 373-375.
- (69) Jensen, J.; Tejler, J.; Waernmark, K. *J. Org. Chem.* **2002**, *67*, 6008-6014.
- (70) Ninomiya, K.; Shioiri, T.; Yamada, S. *Chem. Pharm. Bull.* **1974**, *22*, 1795-1799.
- (71) Norris, T.; Lambert, J. F.; Hnatow, M. E. EP 1081143, 2001.
- (72) Ishiyama, T.; Murata, M.; Miyaura, N. *J. Org. Chem.* **1995**, *60*, 7508-7510.
- (73) Paizs, C.; Tahtinen, P.; Lundell, K.; Poppe, L.; Irimie, F.-D.; Kanerva, L. T. *Tetrahedron Asymmetry*. **2003**, *14*, 1895-1904.
- (74) Shaw, K. N. F.; Armstrong, M. D.; McMillan, A. *J. Org. Chem.* **1956**, *21*, 1149-1151.
- (75) Shibata, N.; Das, B. K.; Honjo, H.; Takeuchi, Y. *J. Chem. Soc., Perkin Trans. 1.* **2001**, 1605-1611.
- (76) Schnyder, A.; Indolese, A. F.; Studer, M.; Blaser, H.-U. *Angew. Chem., Int. Ed.* **2002**, *41*, 3668-3671.
- (77) Cousaert, N.; Toto, P.; Willand, N.; Deprez, B. *Tetrahedron Lett.* **2005**, *46*, 6529-6532.

- (78) Deetz, M. J.; Forbes, C. C.; Jonas, M.; Malerich, J. P.; Smith, B. D.; Wiest, O. *J. Org. Chem.* **2002**, *67*, 3949-3952.
- (79) Saito, S.; Toriumi, Y.; Tomioka, N.; Itai, A. *J. Org. Chem.* **1995**, *60*, 4715-4720.
- (80) Balacco, G., iNMR, version 3, Nucleomatica, Molfetta, Italy, **2008**.
- (81) Cox, C.; Lectka, T. *J. Org. Chem.* **1998**, *63*, 2426-2427.
- (82) Anet, F. A. L.; Ghiaci, M. *J. Am. Chem. Soc.* **1979**, *101*, 6857-6860.
- (83) Mackenzie, R. K.; MacNicol, D. D. *J. Chem. Soc. D* **1970**, 1299-1300.
- (84) Pedersen, B. F.; Pedersen, B. *Tetrahedron Lett.* **1965**, 2995-3001.
- (85) Brown, C. J.; Corbridge, D. E. C. *Acta Crystallogr.* **1954**, *7*, 711-715.
- (86) Bitencourt, M.; Freitas, M. P.; Rittner, R. *J. Mol. Struct.* **2007**, *840*, 133-136.
- (87) Freitas, M. P.; Rittner, R. *J. Phys. Chem. A* **2007**, *111*, 7233-7236.
- (88) Durig, J. R.; Zhou, L.; Gounev, T. K.; Klæboe, P.; Guirgis, G. A.; Wang, L.-F. *J. Mol. Struct.* **1996**, *385*, 7-21.
- (89) Thomassen, H.; Samdal, S.; Hedberg, K. *J. Phys. Chem.* **1993**, *97*, 4004-4010.
- (90) Durig, J. R.; Shen, S.; Guirgis, G. A. *J. Mol. Struct.* **2001**, *560*, 295-314.
- (91) Souza, F. R.; Freitas, M. P.; Rittner, R. *Theochem* **2008**, *863*, 137-140.
- (92) Nomura, S.; Itoh, T.; Nakasho, H.; Uno, T.; Kubo, M.; Sada, K.; Inoue, K.; Miyata, M. *J. Am. Chem. Soc.* **2004**, *126*, 2035-2041.
- (93) Momose, Y.; Maekawa, T.; Yamano, T.; Kawada, M.; Odaka, H.; Ikeda, H.; Sohda, T. *J. Med. Chem.* **2002**, *45*, 1518-1534.
- (94) Matsumoto, A.; Tanaka, T.; Tsubouchi, T.; Tashiro, K.; Saragai, S.; Nakamoto, S. *J. Am. Chem. Soc.* **2002**, *124*, 8891-8902.

- (95) Itoh, T.; Tachino, K.; Uno, T.; Kubo, M.; Tohnai, N.; Miyata, M. *Chem. Lett.* **2006**, *35*, 918-919.
- (96) Neiger, M.; Hupfer, H.; Lehmann, J.; Diewald, D., *Private communication*, 2002.
- (97) Clive, D. L. J.; Zhang, J.; Subedi, R.; Bouetard, V.; Hiebert, S.; Ewanuk, R. *J. Org. Chem.* **2001**, *66*, 1233-1241.
- (98) Ogawa, T.; Matsumoto, K.; Yokoo, C.; Hatayama, K.; Kitamura, K. *J. Chem. Soc., Perkin Trans. 1* **1993**, 525-528.
- (99) Wiberg, K. B.; Keith, T. A.; Frisch, M. J.; Murcko, M. *J. Phys. Chem.* **1995**, *99*, 9072-9079.
- (100) Ramasami, P. *J. Solution Chem.* **2007**, *36*, 901-911.
- (101) Sreeruttun, R. K.; Ramasami, P. *Phys. Chem. Liq.* **2006**, *44*, 315-328.
- (102) Cappelli, C.; Corni, S.; Tomasi, J. *J. Phys. Chem. A* **2001**, *105*, 10807-10815.
- (103) Bondi, A. *J. Phys. Chem.* **1964**, *68*, 441-451.
- (104) Charton, M. *J. Am. Chem. Soc.* **1969**, *91*, 615-618.
- (105) Kamlet, M. J.; Abboud, J. L. M.; Abraham, M. H.; Taft, R. W. *J. Org. Chem.* **1983**, *48*, 2877-2887.
- (106) Reichardt, C. *Solvents and Solvent Effects in Organic Chemistry*; 3rd ed.; Wiley-VCH: Weinheim, 2003; pp 417-424.
- (107) Creighton, T. E. *Curr. Opin. Struct. Biol.* **1991**, *1*, 5-16.
- (108) Barlow, D. J.; Thornton, J. M. *J. Mol. Biol.* **1983**, *168*, 867-885.
- (109) Kumar, S.; Nussinov, R. *J. Mol. Biol.* **1999**, *293*, 1241-1255.
- (110) Marqusee, S.; Baldwin, R. L. *Proc. Natl. Acad. Sci. USA.* **1987**, *84*, 8898-8902.
- (111) Tissot, A. C.; Vuilleumier, S.; Fersht, A. R. *Biochemistry.* **1996**, *35*, 6786-6794.

- (112) Luo, R.; David, L.; Hung, H.; Devaney, J.; Gilson, M. K. *J. Phys. Chem. B.* **1999**, *103*, 727-736.
- (113) Hendsch, Z. S.; Tidor, B. *Prot. Sci.* **1994**, *3*, 211-226.
- (114) Waldburger, C. D.; Schildbach, J. F.; Sauer, R. T. *Nat. Struct. Biol.* **1995**, *2*, 122-128.
- (115) Torrado, M.; Revuelta, J.; Gonzalez, C.; Corzana, F.; Bastida, A.; Asensio, J. L. *J. Biol. Chem.* **2009**, *284*, 23765-23779.
- (116) Wimley, W. C.; Gawrisch, K.; Creamer, T. P.; White, S. H. *Proc. Natl. Acad. Sci. USA* **1996**, *93*, 2985-2990.
- (117) Elcock, A. H. *J. Mol. Biol.* **1998**, *284*, 489-502.
- (118) Vijayakumar, M.; Zhou, H.-X. *J. Phys. Chem. B* **2001**, *105*, 7334-7340.
- (119) Dong, F.; Zhou, H.-X. *Biophys. J.* **2002**, *83*, 1341-1347.
- (120) Sigler, P. B.; Blow, D. M.; Matthews, B. W.; Henderson, R. *J. Mol. Biol.* **1968**, *35*, 143-164.
- (121) Fersht, A. R. *J. Mol. Biol.* **1972**, *64*, 497-509.
- (122) Pervushin, K.; Billeter, M.; Siegal, G.; Wuethrich, K. *J. Mol. Biol.* **1996**, *264*, 1002-1012.
- (123) Matthews, B. W. *Curr. Opin. Struct. Biol.* **1993**, *3*, 589-593.
- (124) Serrano, L.; Horovitz, A.; Avron, B.; Bycroft, M.; Fersht, A. R. *Biochemistry.* **1990**, *29*, 9343-9352.
- (125) Takano, K.; Tsuchimori, K.; Yamagata, Y.; Yutani, K. *Biochemistry.* **2000**, *39*, 12375-12381.
- (126) Tomlinson, J. H.; Ullah, S.; Hansen, P. E.; Williamson, M. P. *J. Am. Chem. Soc.* **2009**, *131*, 4674-4684.
- (127) Sali, D.; Bycroft, M.; Fersht, A. R. *J. Mol. Biol.* **1991**, *220*, 779-788.

- (128) Spek, E. J.; Bui, A. H.; Lu, M.; Kallenbach, N. R. *Protein Sci.* **1998**, *7*, 2431-2437.
- (129) Dao-Pin, S.; Sauer, U.; Nicholson, H.; Matthews, B. W. *Biochemistry.* **1991**, *30*, 7142-7153.
- (130) Strop, P.; Mayo, S. L. *Biochemistry.* **2000**, *39*, 1251-1255.
- (131) Loladze, V. V.; Makhataдзе, G. I. *Protein Sci.* **2002**, *11*, 174-177.
- (132) Ge, M.; Xia, X.-Y.; Pan, X.-M. *J. Biol. Chem.* **2008**, *283*, 31690-31696.
- (133) Sanz-Aparicio, J.; Hermoso, J. A.; Martinez-Ripoll, M.; Gonzalez, B.; Lopez-Camacho, C.; Polaina, J. *Proteins: Struct., Funct., Genet.* **1998**, *33*, 567-576.
- (134) Luisi, D. L.; Snow, C. D.; Lin, J.-J.; Hendsch, Z. S.; Tidor, B.; Raleigh, D. P. *Biochemistry.* **2003**, *42*, 7050-7060.
- (135) Makhataдзе, G. I.; Loladze, V. V.; Ermolenko, D. N.; Chen, X.; Thomas, S. T. *J. Mol. Biol.* **2003**, *327*, 1135-1148.
- (136) Anderson, D. E.; Becktel, W. J.; Dahlquist, F. W. *Biochemistry.* **1990**, *29*, 2403-2408.
- (137) Horovitz, A.; Serrano, L.; Avron, B.; Bycroft, M.; Fersht, A. R. *J. Mol. Biol.* **1990**, *216*, 1031-1044.
- (138) Kammerer, R. A.; Jaravine, V. A.; Frank, S.; Schulthess, T.; Landwehr, R.; Lustig, A.; Garcia-Echeverria, C.; Alexandrescu, A. T.; Engel, J.; Steinmetz, M. O. *J. Biol. Chem.* **2001**, *276*, 13685-13688.
- (139) Smith, J. S.; Scholtz, J. M. *Biochemistry.* **1998**, *37*, 33-40.
- (140) Scholtz, J. M.; Qian, H.; Robbins, V. H.; Baldwin, R. L. *Biochemistry.* **1993**, *32*, 9668-9676.
- (141) Perutz, M. F.; Gronenborn, A. M.; Clore, G. M.; Fogg, J. H.; Shih, D. T. B. *J. Mol. Biol.* **1985**, *183*, 491-498.

- (142) Meeker, A. K.; Garcia-Moreno, B.; Shortle, D. *Biochemistry*. **1996**, *35*, 6443-6449.
- (143) Kao, Y.-H.; Fitch, C. A.; Bhattacharya, S.; Sarkisian, C. J.; Lecomte, J. T. J.; Garcia-Moreno E, B. *Biophys. J.* **2000**, *79*, 1637-1654.
- (144) Sindelar, C. V.; Hendsch, Z. S.; Tidor, B. *Prot. Sci.* **1998**, *7*, 1898-1914.
- (145) Bosshard, H. R.; Marti, D. N.; Jelesarov, I. *J. Mol. Recognit.* **2004**, *17*, 1-16.
- (146) Hughes, D. L.; Reamer, R. A.; Bergan, J. J.; Grabowski, E. J. J. *J. Am. Chem. Soc.* **1988**, *110*, 6487-6491.
- (147) But, T. Y. S.; Toy, P. H. *Chem.-Asian J.* **2007**, *2*, 1340-1355.
- (148) Davidson, M. H.; McDonald, F. E. *Org. Lett.* **2004**, *6*, 1601-1603.
- (149) Chen, M. H.; Davidson, J. G.; Freisler, J. T.; Iakovleva, E.; Magano, J. *Org. Prep. Proced. Int.* **2000**, *32*, 381-384.
- (150) Inoue, M.; Yokota, W.; Katoh, T. *Synthesis*. **2007**, 622-637.
- (151) Xie, W.; Ding, D.; Li, G.; Ma, D. *Angew. Chem., Int. Ed.* **2008**, *47*, 2844-2848.
- (152) Levy, S. G.; Jacques, V.; Zhou, K. L.; Kalogeropoulos, S.; Schumacher, K.; Amedio, J. C.; Scherer, J. E.; Witowski, S. R.; Lombardy, R.; Koppetsch, K. *Org. Process Res. Dev.* **2009**, *13*, 535-542.
- (153) Bernatowicz, M. S.; Wu, Y.; Matsueda, G. R. *J. Org. Chem.* **1992**, *57*, 2497-2502.
- (154) Halgren, T. A. *J. Comput. Chem.* **1999**, *20*, 730-748.
- (155) Halgren, T. A. *J. Comput. Chem.* **1999**, *20*, 720-729.
- (156) Bhayana, B. Ph.D dissertation, University of Pittsburgh, 2007.
- (157) Thomas, A. S.; Elcock, A. H. *J. Am. Chem. Soc.* **2004**, *126*, 2208-2214.
- (158) Courchay, F. C.; Sworen, J. C.; Ghiviriga, I.; Abboud, K. A.; Wagener, K. B. *Organometallics* **2006**, *25*, 6074-6086.

(159) Read, R. R. *Org. Syn.* **1927**, 7, 54.

(160) Glasoe, P. K.; Long, F. A. *J. Phys. Chem.* **1960**, 64, 188-90.